Effects of DHCR24 Depletion *in vivo* and *in vitro*

Dissertation

zur

Erlangung der naturwissenschaftlichen Doktorwürde

(Dr. sc. nat)

vorgelegt der

Mathematisch-naturwissenschaftlichen Fakultät

der

Universität Zürich

von

Katrin Kuehnle

aus Deutschland

Promotionskommitee

Prof. Esther Stöckli (Vorsitz)

PD Dr. M. Hasan Mohajeri (Leitung der Dissertation)

Prof. Alex Hajnal

Zürich, 2006

It is almost precisely 100 years ago that Auguste D. reported to a German psychiatrist in Frankfurt with the words: 'I lost myself'. The psychiatrist was none other than Alois Alzheimer, and this day should mark the beginning of Alzheimer's disease research.

Christian Haass, 2004

SUMMARY

Accumulation of the β-amyloid peptide (Aβ) in the central nervous system (CNS) is an invariant feature of the pathophysiology of Alzheimer's disease (AD), the most common form of dementia in the elderly. The amyloidogenesis occurring in AD represents a fundamental membrane-related pathology involving a transmembrane substrate, the amyloid precursor protein (APP), that is metabolized by integral membrane proteases, the β-secretase (BACE) cleaving at the N-terminus, and the γ-secretase complex cleaving within the transmembrane domain at the C-terminus of the Aβ peptide (Selkoe, 2001). The alternative pathway involves the α-secretase that cleaves APP within the Aβ sequence and therefore prevents Aβ formation. Since α- and β-cleavages directly compete for their substrate APP, the key in understanding Aβ generation is to find out how access of these enzymes to APP is regulated.

There is growing evidence that cholesterol plays an important role in AD pathology and particularly in the regulation of Aβ production. Cholesterol determines and modulates the structural characteristics of membranes and is an important constituent of lipid rafts, dynamic entities enriched in sphingolipids, which can only be detected in living cells. Their *in vitro* counterparts are detergent resistant membrane domains (DRMs), which can be isolated by cellular fractionation procedures. DRMs were shown to be critically involved in the regulation of APP processing, and it was demonstrated that changes in cholesterol levels exert their effects by altering the distribution of APP-cleaving enzymes within the membrane.

Given the fundamental role of cholesterol in membrane organization and function we studied the consequences of cholesterol depletion on DRM formation, APP processing and Aβ generation in the murine brain. Mice with a targeted disruption in the *dhcr24* gene (DHCR24$^{-/-}$ mice) are entirely devoid of cholesterol, while heterozygous mice (DHCR24$^{+/-}$) depleted of only one *dhcr24* allele show moderately reduced brain cholesterol levels by about 25%. These two mouse models allow the analyses of cholesterol concentration-dependent changes in DRM composition and their functional consequences *in vivo*.

Here we show that cholesterol depletion in a dose-dependent manner resulted in disorganized DRMs in brains of DHCR24$^{+/-}$ and DHCR24$^{-/-}$ mice. This was associated with inefficient plasminogen binding and plasmin activation and the displacement of β-secretase (BACE) from DRMs to APP-containing membrane fractions. In DHCR24$^{+/-}$ mice the moderate cholesterol depletion resulted in increased β-cleavage of APP and high levels of Aβ peptides. In contrast, DHCR24$^{-/-}$ mice exhibited a clear shift towards the non-amyloidogenic pathway, with reduced β-cleavage and diminished Aβ formation. These results show that membrane cholesterol regulates APP processing by altering the subcellular distribution of involved

proteins, but they clearly demonstrate that the steady state of Aβ is not maintained in membranes completely devoid of cholesterol, possibly due to reduced proteolytic activity of involved secretases.

DHCR24$^{-/-}$ mice gradually accumulate the direct precursor of cholesterol, desmosterol, that was shown to account for 99% of all sterols in these mice. In adult knock-out mice the concentration of desmosterol was comparable to that of cholesterol in aged-matched wildtype mice. In contrast to young DHCR24$^{-/-}$ mice, age-related desmosterol accumulation and integration in membranes of adult DHCR24$^{-/-}$ mice resulted in formation of functional membranes, DRM formation and sustained APP metabolism. These observations suggest that desmosterol is capable of substituting cholesterol in biological membranes, insofar it is abundant enough, ensuring proper DRM formation and physiological APP processing *in vivo*.

ZUSAMMENFASSUNG

Die Alzheimer Krankheit ist die häufigste Form der Altersdemenz und betrifft bis zu 10% der über 65-jährigen. Obgleich die Ursache und der zugrunde liegende Mechanismus der Krankheit noch immer nicht genau bekannt sind, scheint die Anhäufung und krankhafte Ablagerung von Amyloid-β-Peptiden (Aβ) im Gehirn von Alzheimer-Patienten ein wichtiger Auslöser für den massiven Verlust von Nervenzellen zu sein. Daher ist die Entstehung von Aβ für die Forschung von besonderem Interesse. Das Amyloid-Vorläuferprotein APP ist ein Membranprotein und wird von unterschiedlichen Enzymen geschnitten, wobei es bei der so genannten amyloiden Prozessierung zur Entstehung von Aβ kommt, bei der harmlosen nicht-amyloiden Prozessierung allerdings kein Aβ gebildet wird. Diese Tatsache macht sich die Wissenschaft zunutze, indem sie Faktoren erforscht, welche den harmlosen Prozessierungsweg ankurbeln.

Cholesterin ist ein wichtiger Bestandteil zellulärer Membranen und es wurde gezeigt, dass die Veränderung des Cholesteringehaltes in einer Zelle sich auf die Bildung von Aβ auswirkt. Da es allerdings keine effiziente Möglichkeit gibt, Cholesterin aus dem Gehirn von Versuchtieren zu entfernen, konnte man bislang nicht untersuchen, wie sich ein veränderter Cholesteringehalt auf die Aβ Bildung im lebenden Organismus auswirkt.

In der vorliegenden Arbeit wurde ein Mausmodell untersucht, dem im homozygoten Fall beide Allele des *dhcr24* genes fehlen, welches für ein Protein kodiert, das eine zentrale Rolle in der Cholesterinbiosynthese spielt. Diese DHCR24$^{-/-}$ Mäuse sind nicht in der Lage Cholesterin herzustellen, akkumulieren allerdings im Alter ein Vorläufer des Cholesterins, das Desmosterin. Wir konnten zeigen, dass heterozygote DHCR24 Mäuse (DHCR24$^{+/-}$), denen nur ein *dhcr24* Allel fehlt, bis zu 25% weniger Cholesterin aufweisen, was ein gutes Modell für eine partielle Cholesterin Verminderung darstellt. In beiden Genotypen wurden massive Veränderungen der Membranbeschaffenheit nachgewiesen, die ganz klar mit dem Cholesteringehalt korrelierten. Die Untersuchungen dieser Veränderungen auf die Bildung von Aβ haben gezeigt, dass im Falle der partiellen Cholesterin Verminderung eine deutliche Erhöhung von Aβ im Gehirn der heterozygoten Tiere zu verzeichnen war, wohingegen eine gänzliche Verarmung an Cholesterin zu einer Verminderung von Aβ führte. Diese Ergebnisse lassen sich am besten dadurch erklären, dass durch die Cholesterin Verminderung die relative Verteilung von APP und den es schneidenden Enzymen innerhalb der Membran derart verändert ist, dass es zu einer Erhöhung der Schnittfrequenz zwischen Substrat und Enzymen kommt. Ist die Membranbeschaffenheit durch vollständige Cholesterin Verarmung jedoch so sehr gestört, dass Aktivität und Funktion von ansässigen Membranproteinen geschmälert sind,

bleibt die amyloide Prozessierung von APP weitgehend aus, wie im Gehirn von jungen DHCR24$^{-/-}$ Tiere nachgewiesen werden konnte. Weiterhin wurde untersucht, ob Desmosterin, welches in erwachsenen DHCR24$^{-/-}$ Mäusen in genauso grossen Mengen vorhanden ist wie Cholesterin in den Kontrollmäusen, die Rolle von Cholesterin übernehmen kann. Membrananalysen und Funktionsuntersuchungen haben ergeben, dass Desmosterin ein guter Ersatz für Cholesterin ist, und dass die in den jungen DHCR24$^{-/-}$ Mäusen detektierten Veränderungen durch die Akkumulation und Integration von Desmosterin in die Zellmembranen erwachsener Mäuse rückgängig gemacht werden konnten.

1. INTRODUCTION

1.1 ALZHEIMER'S DISEASE

Alzheimer's disease (AD) is a devastating neurodegenerative disease and the most common cause of dementia today. It is estimated that more than 10% of people over the age of 65 are affected and, with this sector of the population increasing more rapidly than any other, it is easy to see why determining the cause of the disease with a view to developing therapies is the focus of much current research.

One of the first clinically recognized symptoms of AD is diminished performance on tests assessing declarative memory function. Apathy defined by loss of drive, motivation or lack of feeling or emotion is the most common neuropsychiatric symptom in AD, and increases with disease progression. The destructive neurodegenerative disorder slowly corrodes the brain until memories, moods and many other cognitive traits are permanently lost (Mega et al., 1996). On external examination the brains of AD patients often show some degree of atrophy (Figure 1A) and dilatation of the lateral ventricles due to loss of brain tissue (Fox et al., 1996; Juottonen et al., 1998). The two most prominent neuropathological hallmarks of AD are extracellular deposition of the amyloid β-peptide (Aβ) in senile plaques (SPs) and the appearance of intracellular neurofibrillary tangles (NFTs) (Figure 1B). SPs are spherical lesions in the cerebral cortex, measuring up to 100 microns. In their fully developed stage - the neuritic plaque - SPs have a central core of Aβ in a fibrillary fine structure surrounded by dystrophic neuronal processes with neurofibrillary degeneration.

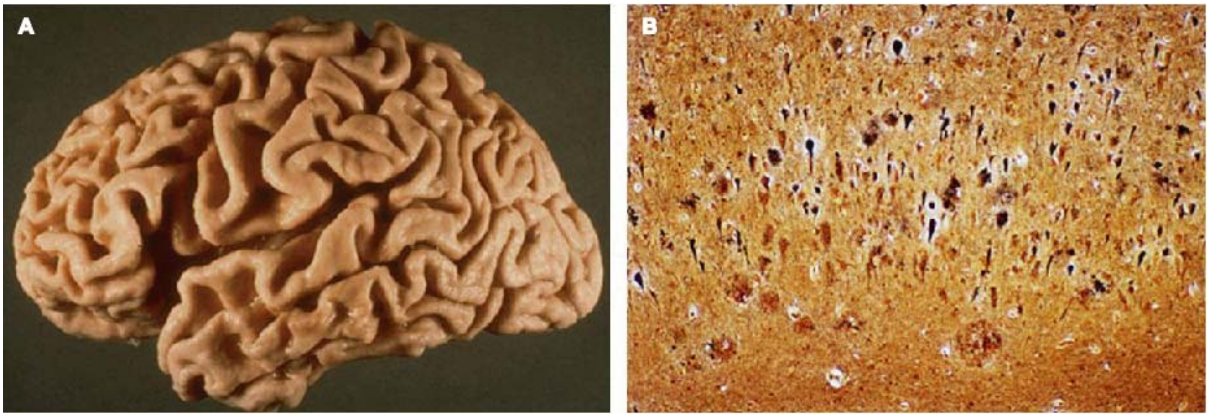

Figure 1 Brain atrophy due to neurodegeneration (A) and the concomitance of senile plaques, consisting of β-amyloid, and neurofibrillary tangels, consisting of hyperphosphorylated tau (B) are major neuropathological hallmarks of AD.

The zone around the amyloid core also contains reactive astrocytes and microglia. In addition to neuritic plaques, Aβ is also found in diffuse, non-fibrillar deposits (diffuse plaques). Diffuse plaques do not disrupt the neuropil. They are sometimes seen in large numbers in old, non-demented people and are not associated with dementia (Ogeng'o et al., 1996).

NFTs are deposits of hyperphosphorylated tau filaments in the neuronal body. Similar deposits are present in the dystrophic processes that surround the amyloid core of SPs and in dendrites (neuropil threads). In severe AD, the hippocampus often contains extracellular NFTs embedded in the neuropil, like fossilized skeletons of neurons. The mechanism of accumulation of tau in NFTs is unclear.

1.1.1 The Disease Hypotheses

AD is regarded as an age-related but not an age-dependent disease (Braak and Braak, 1995). Several hypotheses have been proposed in order to explain this age-relationship, including systemic metabolic changes (Mattson et al., 1999), altered calcium homeostasis (Begley et al., 1999), neurotransmitter dependency (Religa and Winblad, 2003), and neuronal oxidative stress (Mattson et al., 1999). However, none of these have provided a conclusive explanation for the molecular hallmarks of the disease, which combined result in selective neuronal loss. Given the molecular pathology of AD, two major hypotheses have been proposed: the 'amyloid cascade' hypothesis (Hardy and Higgins, 1992) and the 'neuronal cytoskeletal degeneration' hypothesis (Braak and Braak, 1995; Terry, 1998). The 'amyloid cascade' hypothesis basically states that the neurodegenerative process observed in AD brains is best explained as a series of events triggered by the abnormal processing of the amyloid-β precursor protein (APP), the consequences of which are the production, aggregation, deposition and toxicity of its Aβ derivative. On the other hand, since the observation that neurofibrillary changes may precede the deposition of amyloid plaques (Arriagada et al., 1992a; Arriagada et al., 1992b), the staging hypothesis proposed by Braak and Braak accounts for the view that cytoskeletal changes are the main events leading to neuronal degeneration in AD brains. Although until recently both lines of research were somehow in dispute, the two hypotheses were reconciled to some extent by showing that an age-dependent process is required in order to render the brain vulnerable to Aβ-dependent toxicity (Geula et al., 1998). Even though toxic effects of Aβ on cells have been demonstrated *in vitro* and *in vivo*, the mechanism leading to Aβ-induced neuronal damage, as well as the true nature of the neurotoxic Aβ species, have not yet been resolved. Moreover, recent studies suggest that Aβ may not be toxic when deposited in amyloid plaques; instead its neurotoxic properties might

be attributed to the prefibrillar Aβ aggregates (McLean et al., 1999). This notion was supported by the observation that synaptic dysfunction could be observed even before the formation of amyloid plaques in transgenic animals (Terry et al., 1991). A revision of the amyloid cascade hypothesis is required in the light of increasing evidence that neurons secrete small, readily diffusible Aβ oligomers that are highly neurotoxic (Lambert et al., 1998). Moreover, insoluble pools of intracellular Aβ accumulate with time in neurons and may cause the onset of early AD-related cognitive deficits (Skovronsky et al., 1998). Given the important role of non-fibrillar Aβ aggregates in the pathogenesis of AD, the development of strategies to prevent their formation is of great importance.

1.1.2 APP processing

APP is part of a larger gene family that includes APP-like proteins (APLPs) 1 and 2. This family of proteins has a membrane-associated receptor-like structure composed of a large extracellular, a single transmembrane, and a short cytoplasmic domain. APP homologs are also found in Caenorhabditis elegans (Apl-1) (Daigle and Li, 1993) and Drosophila (APPL) (Martin-Morris and White, 1990). In mammals, APP is ubiquitously expressed as different isoforms in neuronal and non-neuronal tissues.

Processing of APP, including Aβ production, represents a fundamental membrane-related pathology involving a membrane-bound substrate metabolized by integral membrane proteases (secretases) (Figure 2). Aβ is cleaved out of APP sequentially by β- and γ-secretase. The β-site APP cleavage enzyme BACE1 has recently been identified as a novel membrane-bound aspartyl-protease (De Strooper and Annaert, 2000; Esler and Wolfe, 2001) and cleaves APP in its luminal domain to generate a secreted ectodomain (sAPPβ). The remaining 10 kD β-cleaved C-terminal fragment of APP (β-CTF) fragment is subsequently the substrate for γ-secretase complex cleaving within the transmembrane domain at the C-terminus of the Aβ peptide (Selkoe, 2001), which leads to the release of Aβ (amyloidogenic pathway). The γ-secretase is a protein complex composed of presenilin (PS), nicastrin (NCT), APH-1 and PEN-2. PS 1 and PS 2 are required for intramembrane cleavage of an increasing number of type I membrane proteins, including the Notch receptor, which signals during differentiation and development. While PS1 and PS2 function as catalytic subunit, all four proteins are necessary for proteolytic activity of the complex (De Strooper, 2003). γ-secretase cleavage can take place at position 40 as well as position 42 of Aβ. Under physiological conditions,

$A\beta_{40}$ levels are approximately 10 fold higher than those of $A\beta_{42}$, while the latter is more prone to aggregate (Davis-Salinas and Van Nostrand, 1995).

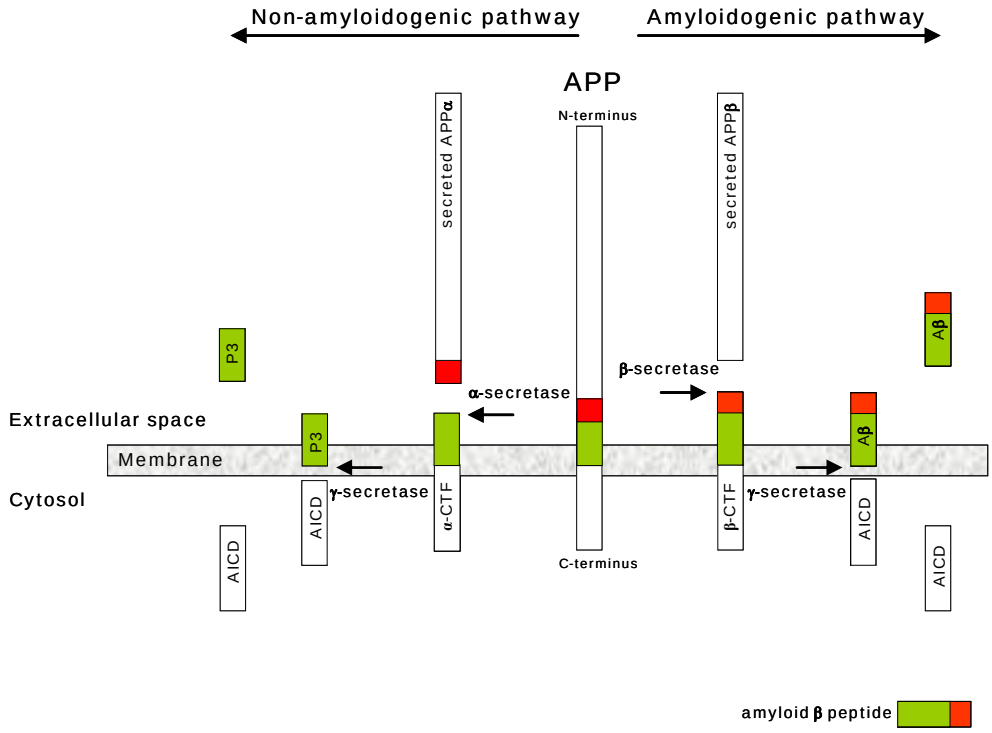

Figure 2 APP processing and Aβ generation. Aβ is derived by sequential proteolytic cleavage of APP. The non-amyloidogenic pathway is initiated by α-secretase cleavage of APP within the Aβ sequence thus precluding Aβ formation, generating a secreted ectodomain (sAPPα) and a shorter α-cleaved C-terminal fragment of APP (α-CTF) that is subsequently cleaved within the transmembrane domain by the γ-secretase complex producing the small P3 peptide. Amyloidogenic APP processing involves the β-secretase cleavage at the N-terminus, and the γ-secretase complex at the C-terminus. β-secretase cleavage releases a secreted ectodomain (sAPPβ) and generates a C-terminal fragment of APP (β-CTF), which is subsequently cleaved by the γ-secretase leading to the secretion of Aβ.

The alternative pathway (non-amyloidogenic pathway) involves the α-secretase, a member of the ADAM family of disintegrin and metalloproteases (ADAM 9, 10, and 17) (Buxbaum et al., 1998; Koike et al., 1999; Lammich et al., 1999) that cleaves APP within the Aβ sequence to generate a secreted ectodomain (sAPPα), a shorter α-cleaved C-terminal fragment of APP (α-CTF) that is also cleaved by the γ-secretase to release a short fragment (P3) - the C-terminal part of Aβ. In addition, the γ-secretase cleavage of α- and β-CTFs produces the APP intracellular domain (AICD). α-cleavage is the dominant processing step under physiological conditions, and since it cuts APP within the Aβ region it prevents Aβ formation.

Despite numerous studies, the physiological function of APP and its cleavage products remain unclear. Some evidence implies the soluble ectodomain and AICD in signaling and in a series

of physiological responses (Kimberly et al., 2001; Mattson et al., 1997). While it is possible that one does not need to understand these functions to understand the role of Aβ in AD, it is certainly not excluded that disturbance of normal APP function contributes to the disease process as well (Stokin et al., 2005). Moreover, after more than 15 years of intense research, understanding the biology of APP remains an important scientific and intellectual challenge.

1.1.3 Familial Alzheimer's disease (FAD)

From the genetical point of view, AD is a complex, heterogeneous disease that follows an age-dependent dichotomous model (Tanzi, 1999). On one hand, the early-onset familial form of AD (EOFAD) is caused by defects in any of three different genes: PS1 on chromosome 14 (Sherrington et al., 1995), PS2 on chromosome 1 (Levy-Lahad et al., 1995), and APP on chromosome 21 (Goate et al., 1991). On the other hand, late-onset AD (LOAD) is associated with genetic polymorphisms that appear to operate as risk factors and/or genetic modifiers. While the mutations in APP and the presenilins account for less than 5% of all AD cases, they are fully penetrant and therefore guarantee onset of the disease. Disease causing mutations in the APP gene are clustered around the α-, β- and particularly the γ-secretase cleavage sites, resulting in, for example, preferred amyloidogenic processing of APP (Hsiao et al., 1995) and an increased ratio of $A\beta_{42}$ to $A\beta_{40}$, thus in favor of the more hydrophobic form of Aβ (Walker et al., 2005). By far the highest number of mutations has so far been identified in the PS genes. These mutations appear to act as gain of function mutations leading to higher levels of $A\beta_{42}$ in plasma of affected patients, as well as in media of cultured fibroblasts from these patients (Scheuner et al., 1996).

1.1.4 Genetic and non-genetic risk factors for AD

The first and until now the only consistently replicated genetic risk factor for LOAD is the ε4 variant of the gene encoding the Apolipoprotein E (ApoE). The glycoprotein ApoE is the major component of very low-density lipoproteins (VLDL) and the predominant apolipoprotein in the central nervous system (Corder et al., 1993; Puglielli et al., 2003). ApoE is the principal cholesterol protein carrier in the brain and critical for the coordination of cholesterol in the repair, growth, and maintenance of myelin and neuronal membranes during development or after injury (Boyles et al., 1990; Goodrum, 1991; Ignatius et al., 1986). The *apoe* gene exists in three isoforms: ε2, ε3, and ε4. In the normal population, the ε3 allele is the most common followed by the ε4 allele (Strittmatter and Roses, 1995). Inheritance of the ε4 allele has been shown to be associated with a reduced regional cerebral blood flow in several

brain regions in non-demented carriers (Reiman et al., 2001) and several studies have shown that its inheritance is associated with elevated cholesterol levels and increased risk of developing AD compared to individuals with only the *apoe* ε2 or ε3 alleles (Corder et al., 1993; Hofman et al., 1997; Strittmatter et al., 1993). The ε4 allele has also been associated with familial hypercholesterolemia (Eto et al., 1988).

The mechanism behind the contribution of ApoE to an increased risk of AD is currently under intense investigation. *apoe* knock-out mice show a reduced deposition of Aβ (Bales et al., 1997). Furthermore, the isoform of ApoE that is derived from *apoe* ε4 expression binds with high affinicy to Aβ peptides (Beffert et al., 1998) and its expression increases the formation of Aβ fibrils, an effect that seems to be isoform specific (Holtzman et al., 2000). Under normal non-pathological conditions, ApoE is associated with a lipid source and, by adding extracellular Aβ to neuronal cell cultures, this stimulates the ApoE-mediated internalization of cholesterol (Beffert et al., 1998). An alternative mechanism by which *apoe* ε4 increases the risk of AD may however be more closely related to the intracellular homeostasis of cholesterol. Some findings suggest that the *apoe* ε4 allele is associated with a decreased cholesterol efflux compared with ε2 and ε3 alleles (Michikawa et al., 2000).

It is increasingly recognized that vascular risk factors also play a role in Alzheimer's type dementia. In the early 1990s, one found increased prevalence of senile plaques in patients with coronary artery disease, linking vascular conditions to AD neuropathology (Sparks et al., 1990; Sparks et al., 1993). Since then multiple studies have supported the idea that vascular conditions such as hypertension, atherosclerosis and hypercholesterolemia increase the risk for AD (Sjogren and Blennow, 2005). Confirmation of the role of these vascular-related conditions in dementia would suggest possible changeable risk factors that may serve as targets for strategies of prevention. With the advance of cholesterol-lowering drugs such as statins, high cholesterol levels are potentially modifiable risk factors (see paragraph 1.2).

1.1.5 Clearance of Aβ from the brain

Despite the fact that Aβ is produced as a normal consequence of APP metabolism (Haass et al., 1992), Aβ fibrils do not accumulate in large quantities in healthy individuals. This indicates the existence of clearance mechanisms and suggests that Aβ deposition is the net result of a balance between its production and catabolism. Aβ clearance occurs by at least three pathways: extracellular proteolysis, transport across the blood–brain barrier (BBB), and receptor-mediated endocytosis. Two metalloproteinases, the insulin-degrading enzyme (Qiu et al., 1998) and the membrane-anchored zinc endopeptidase neprilysin (Carson and Turner,

2002), have been implicated in the extracellular degradation of Aβ. Infusion of neutral endopeptidase inhibitors in the rat brain resulted in abnormal deposition of endogenous Aβ (Iwata et al., 2000), highlighting the importance of extracellular degradative pathways in clearing Aβ. Another important protease involved in Aβ degradation is the serin protease plasmin (Selkoe, 2001). Plasmin activity is regulated by plasminogen-activators and inhibitors as well as plasminogen activator-inhibitors and plasmin inhibitors (Collen, 1999). In addition, plasmin generation is dependent on the binding of plasminogen to the plasma membrane (Plow et al., 1995). It was shown that brain tissue from AD patients contains reduced levels of plasmin, implying that plasmin down-regulation may cause amyloid plaque deposition accompanying sporadic AD (Ledesma et al., 2000). Aβ transport across the BBB is less well understood, but gp330/megalin and its ligand ApoJ may be involved. ApoJ, the predominant Aβ-binding protein in cerebrospinal fluid, mediates binding of Aβ to gp330 (Hammad et al., 1997). Aβ can also be removed by binding to endocytic receptors, probably including the class A and class B scavenger receptors, which can bind to and internalize fibrillar forms of Aβ (Paresce et al., 1996). On the other hand, Aβ can form complexes with low-density lipoprotein-related receptor protein (LRP) ligands such as ApoE (Yang et al., 1999), which can then be internalized via LRP (Kang et al., 2000).

1.1.6 Treatments and possible treatment strategies of AD

The observation of a deficiency in cholinergic neurotransmission in AD led to the development of cholinesterase inhibitors as the first approved treatment for dementia symptoms. The cholinergic hypothesis states that decreased cholinergic transmission, due to depletion of cholinergic neurons, plays a major role in the expression of cognitive, functional, and possibly behavioral symptoms in AD (Bartus et al., 1982). The mechanism of action of cholinesterase inhibitors is to increase the availability of acetylcholine through an inhibition of the catabolic enzyme acetylcholinesterase. Another approach to the treatment of AD is to block glutamatergic neurotransmission. Glutamate is the main excitatory neurotransmitter in the brain. One of its receptors, N-methyl D-aspartate (NMDA), has been implicated in long-term potentiation, which is the neuronal mechanism responsible for learning and memory (Katsuki et al., 1997; Rondi-Reig et al., 2001). Too much stimulation, however, leads to excitotoxicity due to high intracellular concentrations of calcium, which causes neuronal dysfunction and death (Michaelis, 1998), effects involved in the pathogenic cascade of AD. Memantine, a non-competitive NMDA antagonist, blocks glutamate-mediated excitotoxicity

but leaves the physiological activation of the NMDA receptor during neurotransmission unchanged (Molinuevo et al., 2004).

Retrospective observational studies have shown that the use of two groups of widely prescribed substances may have a protective effect against the development of AD (Etminan et al., 2003; in t' Veld et al., 2001). One group combines the non-steroidal anti-inflammatory drugs (NSAIDs). In a meta-analysis of nine studies, the use of NSAIDs was associated with a lower risk of developing AD, and the benefit was greater with long-term use than with intermediate use (Etminan et al., 2003). Whether the protective effects of NSAIDs will hold up in prospective studies is an open question. The other group represents the cholesterol-lowering drugs, so called statins (see chapter 1.2).

The basis for an interesting new therapeutic approach was laid by Dale Schenk and colleagues in 1999, who actively immunized transgenic APP mice with $A\beta_{42}$. They reported that immunization of young animals essentially prevented the development of β-amyloid-plaque formation, neuritic dystrophy and astrogliosis, and treatment of the older animals also markedly reduced the extent and progression of these AD-like neuropathologies. These results raised the possibility that immunization with amyloid-β may be effective in preventing and treating AD (Schenk et al., 1999). Other studies have reproduced these results using different models (Morgan et al., 2000), and passive immunization with antibodies against human Aβ also decreased Aβ in transgenic mice and improved performance in test behaviors (DeMattos et al., 2001). Based on these preclinical findings, a multicenter randomized double-blind placebo-controlled Phase II trial was organized to test the safety and efficacy of active $A\beta_{42}$ immunization in humans, which has to be halted due to adverse effects (Gilman et al., 2005; Orgogozo et al., 2003). Despite this early halt of the trial, follow-up examinations of some of the patients revealed the presence of antibodies recognizing amyloid plaques in the immune sera of the patients (Hock et al., 2002), as well as a stabilization of the cognitive decline in immunized patients (Hock et al., 2003). Moreover, neuropathological evaluation of two immunized cases showed areas with unusually reduced amyloid burden and evidence of Aβ-associated microglia, suggesting that the immunization had increased Aβ clearance by activated microglia (Ferrer et al., 2004; Nicoll et al., 2003). Based on these observations, new vaccines are being developed at present and remain highly promising strategies for further testing and possible entry into clinical practice.

Since Aβ peptides are produced by sequential processing of APP by the two aspartyl-type proteases β- and γ-secretase, these secretases are a center of attraction for various drug discovery efforts. Although a large number of specific drug-like γ-secretase inhibitors have

been discovered, progress towards the clinic has been slowed by the broad substrate specificity of this unusual intramembrane-cleaving enzyme (Steiner and Haass, 2000). In particular, the Notch receptor depends on γ-secretase for its signaling function and, thus, γ-secretase inhibition produces distinct phenotypes related to a disturbance of this pathway in preclinical animal models. The main task now is to define the therapeutic window in human between desired central efficacy and Notch-related side effects (Beher and Shearman, 2002). In contrast, most studies with knock-out animals have indicated that β-secretase inhibition may have minimal adverse effects (Dominguez et al., 2001). However, the properties of the active site of this enzyme make it difficult to find small-molecule inhibitors that bind with high affinity (Beher and Graham, 2005).

1.2 CHOLESTEROL AND AD

Over the past decade, an increasing amount of evidence derived from genetic, epidemiological and biochemical studies has pointed to a role for cholesterol in the development of AD, and particularly in the regulation of APP processing. As mentioned above, the major risk factor, after age, is the presence of the *apoe* ε4 allele, and also other genes related to cholesterol metabolism have been linked to AD, although none as unequivocally as *apoe*. These include the gene encoding LRP (Kang et al., 2000) and *cyp46*, which encodes cholesterol 24-hydroxylase, the enzyme responsible for the catabolism of cholesterol to 24*S*-hydroxycholesterol (24*S*-OH-chol) (Lutjohann et al., 2000). Epidemiological studies reported that levels of total cholesterol and low-density lipoprotein (LDL) in serum were shown to correlate with the amount of Aβ in AD brains (Kuo et al., 1998), and there is epidemiological evidence that elevated cholesterol levels during mid-life increase the risk of developing AD (Kivipelto et al., 2001) (see also 1.1.4). Several retrospective studies have suggested that the use of statins is associated with a reduced prevalence of AD (Jick et al., 2000; Rockwood et al., 2002; Wolozin et al., 2000; Yaffe et al., 2002). Statins are a highly successful class of cholesterol lowering drugs inhibiting the Hydroxy-3-methylglutaryl coenzyme A reductase (HMGCR), a rate limiting enzyme in the isoprenoid and cholesterol biosynthesis (see 1.2.1), and thereby decrease LDL and increase high-density lipoprotein (HDL) levels (Jula et al., 2002). Clinical trials with statins in AD patients, however, revealed controversial data. Alterations in APP cleavage products such as sAPPα, sAPPβ and Aβ were detected in the cerebrospinal fluid of treated AD patients (Simons et al., 2002; Sjogren et al., 2003), while only in one study a prevented decline of cognition in AD patients was reported (Masse et al.,

2005). Several mechanisms have been suggested for the decreasing risk of AD by statin use, one of the most prevailing being that statins affect the metabolism of Aβ (see chapter 1.2.3). The causal theory of pharmacologic benefit from statins reiterates the lipid hypothesis, which states that dyslipidemia is central to the process of atherosclerosis and the clinical benefit which accrues from statin therapy is a function of the degree of lipid lowering. The non-causal theory supports the premise that clinical benefits are related primarily to pleiotropic effects of statins (Farmer, 2000). These pleiotropic effects include endothelial protection through modulation of eNOS and NO production, antioxidant and anti-inflammatory effects. Statins also reduce the levels of isoprenoids, which are derived from intermediates of the cholesterol biosynthetic pathway. These intermediates, such as farnesyl- and geranylpyrophosphate, serve as important lipid-attachment molecules for the posttranslational modification of many proteins, including heterotrimeric G proteins and small GTP-binding proteins such as RAS and Rho. These molecules play fundamental roles both in cell growth and in signal transduction and mitogenic pathways (Coleman and Olson, 2002; Olson et al., 1995). Moreover, the production of Aβ was correlated with the levels of cholesterol esters (Puglielli et al., 2001; Puglielli et al., 2003), suggesting the involvement of Acyl-coenzyme A:cholesterol acyltransferase (ACAT), the enzyme that removes excess cholesterol from membranes and converts free cholesterol to cholesterol esters for storage purpose (Rudel et al., 2001).

1.2.1 Metabolism of cholesterol

Cholesterol is provided to the cell through endogenous synthesis or uptake. Cholesterol synthesis occurs only in the liver and the brain, through a multi-component pathway that begins with the condensation of acetoacetyl-CoA with acetyl-CoA to produce mevalonate in a set of reactions that are catalyzed by Hydroxy-3-methylglutaryl coenzyme A synthase (HMGCS) and HMGCR. The first intermediate committed to the production of sterols is C30 squalene, which is converted to lanosterol. Cholesterol biosynthesis proceeds via two intersecting routes involving the same enzymes, the Kandutsch-Russell-pathway with 7-dehydrocholesterol as the direct precursor, and the Bloch synthesis pathway with desmosterol as the ultimate precursor of cholesterol (Figure 3) (Waterham et al., 2001). DHCR24, the 3β-hydroxysterol-Δ24 reductase, is crucial for cholesterol biosynthesis, as it is the mediating enzyme between the two pathways – reducing the C24 double bond of the Bloch-pathway precursors – finally leading to the production of cholesterol.

After being produced, cholesterol is secreted by a group of transport molecules, such as the ATP-binding cassette transporter A1 (ABCA1), where it binds apolipoproteins to form lipid-protein complexes. HDL complexes accept cholesterol (and other lipids) to form LDL complexes, which are transported throughout the body.

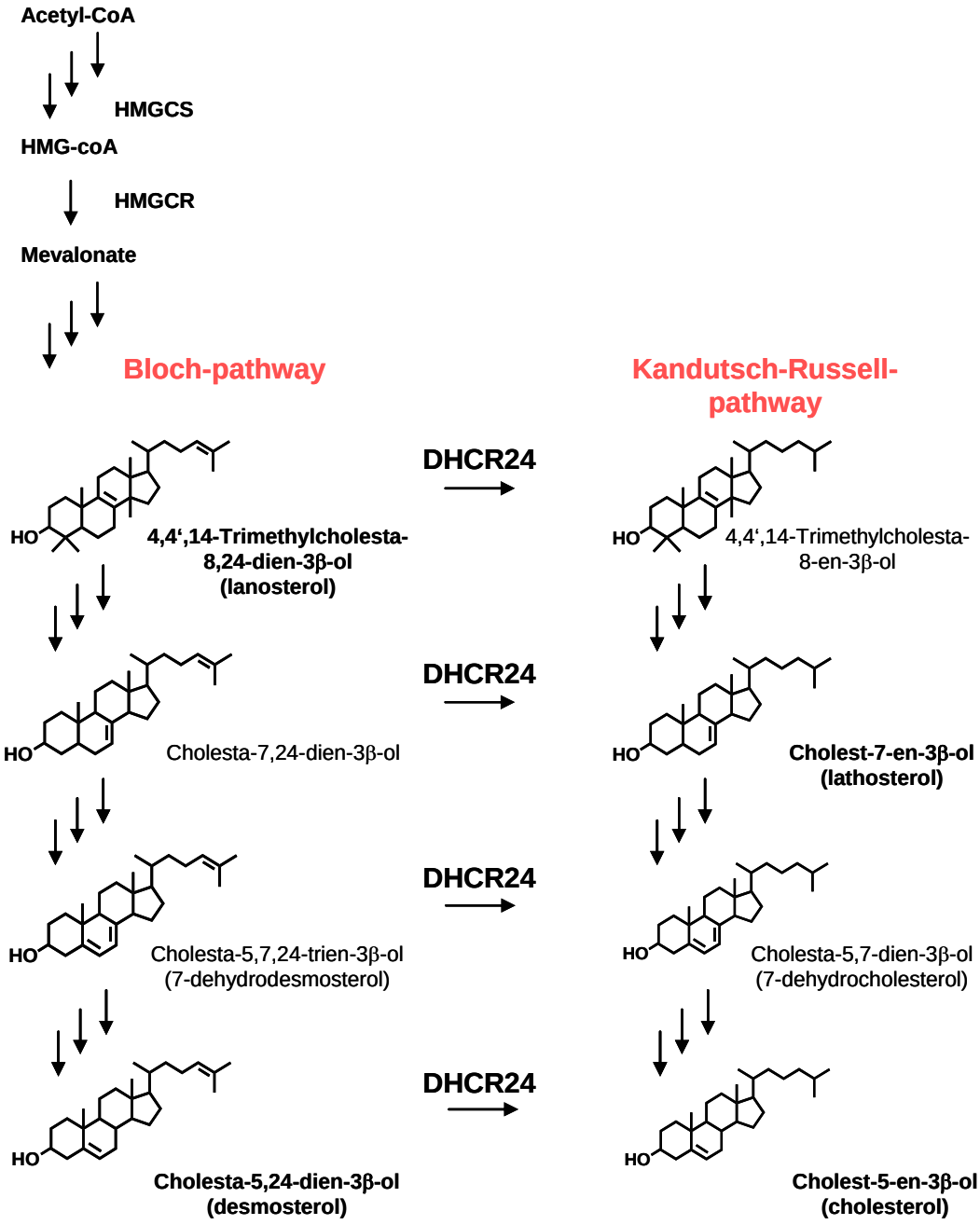

Figure 3 Cholesterol biosynthesis can proceed from lanosterol via two intersecting routes, the Bloch- or the Kandutsch-Russell-pathway. The choice of pathway is determined by the stage at which the double bond at position C24 in the sterol side chain is reduced. If this double bond is retained until the last reaction, cholesterol synthesis proceeds via desmosterol (Bloch-pathway), whereas early reduction leads to the formation of lathosterol and 7-dehydrocholesterol (Kandutsch-Russell-pathway). DHCR24 is the mediating enzyme between the two pathways.

1.2.2 Brain cholesterol

Cholesterol metabolism in the brain parallels that in the periphery, but also differs in several important aspects. In the brain, the BBB effectively prevents cholesterol uptake from the circulation, and *de novo* synthesis is responsible for practically all cholesterol present in this organ. Cholesterol is synthezised by neurons, astroglia and oligodendrocytes, but in the adult the prevalent location of cholesterol synthesis appears to be in astrocytes. Once synthesized, astrocytes secrete cholesterol predominantly via the ABCA1 transporter, where it is taken up by particles that resemble HDL (Lee and Parks, 2005). Peripheral HDL differs from brain HDL in the content of apolipoproteins. Brain HDL contains mainly ApoE and ApoJ, while peripheral HDL contains large amounts of ApoA and small amounts of ApoE. After being generated, brain HDL is taken up by lipoprotein receptors of neurons. Many types of lipoprotein receptors are present in the brain, but one of the most abundant lipoprotein receptors in neurons is LRP (Zerbinatti and Bu, 2005). The life cycle of cholesterol in the neuron begins in the endoplasmic reticulum, where cholesterol is either taken up from endosomes or synthesized *de novo*. What follows is a cyclical mechanism where membrane in the endoplasmic reticulum is progressively enriched with cholesterol.

Essentially all (about 99%) of brain cholesterol is unesterified. The majority of cholesterol present in the CNS is believed to reside in two different pools: one represented by the myelin sheaths (an estimated portion of 70%) and the other by the plasma membranes of astrocytes and neurons (Snipes and Suter, 1997). Cholesterol synthesis in the developing mammalian CNS is relatively high, but declines to a very low level in adults. This can be explained by an efficient recycling of brain cholesterol. Brain cholesterol has an extremely long half-life of about 5 years in humans (Bjorkhem et al., 1998), which makes it almost impossible to medicinally reduce brain cholesterol levels in adults. Although the cholesterol recycling system in the brain seems quite efficient, there are two known mechanisms for the excretion of cholesterol from the brain to maintain the steady state. The first is analogous to classic "reverse cholesterol transport" and is mediated by a flux of cholesterol present in ApoE containing lipoproteins through CSF into the circulation. The details of this particular mechanism for sterol transport are, however, not known (Ohyama et al., 2006). A quantitatively more important mechanism involves conversion of cholesterol to 24*S*-OH-cholesterol, a more polar sterol that is able to traverse the BBB, enter the circulation and travel to the liver (Bjorkhem et al., 1998; Lutjohann et al., 1996). 24*S*-OH-cholesterol was also shown to be a regulator for the key enzymes in cholesterol biosynthesis, as well as a precursor for steroid hormones (Edwards and Ericsson, 1998).

All genes regulated by sterols contain a sterol-responsive element (SRE) within the 5'-flanking region. Through the binding of SRE binding proteins (SREBPs), sterols are able to control the transcription of genes (Yokoyama et al., 1993).

1.2.3 Cellular membranes and lipid rafts

Plasma membranes consist of two leaflets that are asymmetric in lipid distribution, electrical charge, fluidity and function. Phosphatidylcholine and sphingomyelin (SPM) are concentrated in the brain exofacial leaflet of synaptic plasma membranes, while phosphatidylethanolamine, phosphatidylserine and phosphatidylinositol are enriched in the cytofacial leaflet. The large difference in fluidity between exo- and cytofacial leaflets is associated with the transbilayer distribution of cholesterol (Schroeder et al., 1988; Wood et al., 1989). While the exofacial leaflet is cholesterol-poor, it was shown that the cytofacial leaflet of plasma membranes from wildtype mice contains approximately 85% of the total amount of cholesterol (Igbavboa et al., 1997; Igbavboa et al., 1996), organized in exchangeable and non-exchangeable cholesterol pools (Nemecz et al., 1988). Cholesterol determines and modulates the structural characteristics of membranes (Bloch, 1979; Bloch, 1983). According to the raft hypothesis, cellular membranes are not a homogenous mixture of lipids but contain entities enriched in sphingolipids and cholesterol, so called rafts, floating in the sea of glycerophospholipids (Simons and Ikonen, 1997). It is assumed that the presence of long and saturated acyl chains in sphingolipids should allow cholesterol to become tightly intercalated with such lipids, resulting in the organization of liquid ordered phases, whereas the unsaturated phospholipids are loosely packed and form a disordered state (Recktenwald and McConnell, 1981; Sankaram and Thompson, 1990). The difference in packing ability leads to phase separation. The hypothesis postulates that distinct proteins can selectively partition into lipid rafts, because many of them need to be in a cholesterol-rich environment to be active, indicating that rafts could serve as specific sites for molecular sorting and polarized transport. For example glycosyl-phosphatidylinositol (GPI) -anchored proteins tent to be constitutively associated with raft domains, while lipid modifications on these proteins allow them to intercalate into lipid raft structure (Simons and Ehehalt, 2002). Other proteins are less closely associated, and their movement in and out of rafts can be controlled by factors such as ligand-binding or oligomerization (Harder et al., 1998). Native rafts can only be detected in living cells (Simons and Toomre, 2000). The *in vitro* counterparts are detergent resistant membrane domains (DRMs), operationally defined as domains resistant to solubilization by non-ionic detergent at 4°C (Brown and Rose, 1992), which can be isolated by cellular fractionation procedures.

However, caution needs to be exercised when equating DRMs with rafts in cell membranes (Lichtenberg et al., 2005). Lipid rafts are believed to play a central role in several cellular processes, most notably in membrane sorting and trafficking, and in signal transduction (Laude and Prior, 2004; Simons and Toomre, 2000). In these cases, rafts can act as platforms allowing particular proteins to cluster together to facilitate these processes.

1.2.4 Cholesterols' influence on APP processing

There is growing evidence that cholesterol plays an important role in AD pathology and particularly in the regulation of APP processing. Studies examining the effects of cholesterol loading in cultured cells reported inconsistent consequences on APP processing and Aβ generation, while *in vivo* data demonstrate a strong link between high cholesterol levels and increased Aβ production (Refolo et al., 2000; Sparks et al., 1994). In contrast, treatment of guinea pigs with statins resulted in lower Aβ levels (Fassbender et al., 2001). Moreover, amyloidogenic processing of APP and brain Aβ load were significantly reduced in transgenic mice treated with BM15.766, a cholesterol-lowering drug, inhibiting DHCR7 (Refolo et al., 2001). These results have been replicated in cultured cells by the use of statins and/or removal of existing cholesterol using methyl-β-cyclodextrin (Ehehalt et al., 2003; Kojro et al., 2001; Simons et al., 1998).

Recent studies suggest that amyloidogenic processing of APP may be facilitated in lipid raft domains, and may therefore be dependent on cholesterol levels. DRMs were shown to contribute in the segregation of APP from BACE (Ehehalt et al., 2003). While endogenous APP and α-secretases were predominantly found in membrane compartments not associated with lipid rafts, BACE and the γ-secretase complex were shown to reside within rafts of late Golgi and early endosomes (Cordy et al., 2003; Riddell et al., 2001; Vetrivel et al., 2004). Hence, access of α- and β-secretase to APP, and therefore Aβ generation, may be determined by dynamic interactions of APP and its secretases with lipid rafts. A moderate reduction of cholesterol up to 30% was shown to result in disorganized DRMs, and led to increased β-cleavage and higher Aβ production (Abad-Rodriguez et al., 2004). These data suggest that under physiological conditions lipids might build an invisible boundary, corralling the γ-secretase complex and BACE away from their substrate, APP (Kaether and Haass, 2004). Thus, disruption of rafts through cholesterol depletion might lessen the sequestration of γ-secretase and BACE into rafts and result in a higher proportion of these secretases in the APP containing fraction of the membrane, therefore cleaving APP more frequently, which would consequently lead to increased levels of β-CTF and Aβ (Abad-Rodriguez et al., 2004; Kaether

and Haass, 2004). However, depletion of cholesterol by a greater degree than 30% was shown to result in elevated levels of sAPPα, reduced β-cleavage and diminished Aβ production (Ehehalt et al., 2003; Kojro et al., 2001; Simons et al., 1998). This shift towards the non-amyloidogenic processing seems to be a consequence of elementary cholesterol depletion-changes in membrane organisation and secretase activity. Even though APP and its secretases are assumed to be in the same membrane compartment under these conditions, amyloidogenic processing is extensively prevented. There is some evidence that cholesterol depletion increases α-secretase activity, possibly due to the relocation of some ADAM10 from raft to non-raft fractions *in vitro* (Kojro et al., 2001). Moreover, it was shown that disrupting cholesterol transport can alter presenilin distribution within the cell and affect APP processing (Burns et al., 2003; Runz et al., 2002), and depletion of membrane cholesterol resulted in complete inhibition of γ-secretase cleavage (Wahrle et al., 2002). However, the majority of evidence indicates that alterations in β-secretase activity are largely responsible for the dependence of Aβ production on cholesterol levels. Cross linking experiments of APP and BACE in raft domains (Ehehalt et al., 2003) and targeting BACE exclusively to rafts (Cordy et al., 2003) have a remarkable effect on Aβ production that is cholesterol dependent. Furthermore, β-secretase activity in large unilamellar vesicles was shown to be directly influenced by membrane cholesterol concentrations (Kalvodova et al., 2005).

1.2.5 Cholesterol biosynthesis and transport disorders

Although the structure of cholesterol was elucidated by Wieland and Dane in 1932, the first genetic defect of the cholesterol biosynthetic pathway, mevalonic aciduria, due to deficiency of the enzyme mevalonate kinase, was identified in 1986. Since then, disorders of cholesterol biosynthesis have emerged as important errors of metabolism that collectively provided insight in many new genetic and biochemical aspects. Whereas most metabolic diseases are characterized by exclusively or largely postnatal biochemical toxicities or deficiencies, disorders of cholesterol biosynthesis are notable for their severe effects on prenatal development. The remarkable embryonic consequences of abnormal cholesterol biosynthesis are exemplified by the Smith-Lemli-Opitz syndrome (SLOS), a well-known multiple congenital anomaly syndrome only recently discovered to be caused by a deficiency in the DHCR7, the enzyme catalyzing the reduction of the ultimate precursor of cholesterol in the Kandutsch-Russel pathway (Opitz, 1999). SLOS patients reveal decreased plasma cholesterol levels and elevated concentrations of 7-dehydrocholesterol. Equally surprising has been the discovery that primary defects of cholesterol biosynthesis cause several different forms of

congenital skeletal dysplasia, most notably X-linked dominant chondrodysplasia punctata, or Conradi-Hunermann syndrome (Herman, 2003). Yet another sterol disorder, desmosterolosis, caused by defective activity of the 3β-hydroxysterol-Δ24 reductase (DHCR24), combines a severe osteosclerotic skeletal dysplasia with multiple embryonic malformations similar to those of SLOS. Only two desmosterolosis patients are known to have survived beyond birth. These patients had elevated levels of the cholesterol precursor desmosterol in plasma and tissue, while cholesterol levels were relatively normal, depending on the mutations in the *dhcr24* gene and their influence on the functional activity of DHCR24 (Andersson et al., 2002; Fitzky et al., 2001; Waterham et al., 2001). In 2002, two unrelated males with lathosterolosis were described with different mutations in the Sterol C-5-desaturase gene (Brunetti-Pierri et al., 2002). Both patients exhibited an 'SLOS-like' phenotype and had abnormal sterol profiles with accumulation of lathosterol in plasma and cultured fibroblasts.
The discovery of the biochemical basis of these diverse genetic disorders has provided accurate biochemical methods for their diagnosis and prenatal diagnosis, but the pathogenesis of these disorders is presently still unclear. One can postulate that pathogenicity results from a lack of cholesterol or related sterols, accumulation of toxic sterol intermediates above each enzyme block, abnormal feedback regulation of earlier steps in the pathway, including synthesis of key isoprenoid compounds, and/or abnormal signaling by hedgehog proteins that normally contain bound cholesterol. In 2003 it was shown that response to the hedgehog signal is compromised in mutant cells from mouse models of SLOS and lathosterolosis and in normal cells pharmacologically depleted of sterols (Cooper et al., 2003). The existence of naturally occurring or targeted mouse mutations for most of the disorders should facilitate mechanistic studies, particularly during development.

1.2.6 DHCR24 knock-out mice

C57BL/6x129SvEv mice with a targeted disruption in the *dhcr24* gene were generated and published by Wechsler and colleagues in 2003, entitled "Generation of cholesterol-free mice". Plasma and tissues of DHCR24$^{-/-}$ mice contained almost no cholesterol, and desmosterol was shown to account for 99% of total sterols (Wechsler et al., 2003). They reported that in a comprehensive patho-morphological analysis, DHCR24$^{-/-}$ mice at the age of three months revealed that all organs were normal in structure with the exception of testes, which were histological identical to degenerated testes seen in adult mice treated with a chemical inhibitor of DHCR24 (Singh and Chakravarty, 2003). The DHCR24$^{-/-}$ mice also had smaller stores of subcutaneous and mesenteric fat, and both males and females were infertile. This relatively

mild phenotype contrasts dramatically with the severe abnormalities observed in two registered patients with desmosterolosis who carry mutations in the *dhcr24* gene (Andersson et al., 2002; FitzPatrick et al., 1998). This discrepancy may be due to the fact that maternal cholesterol is not available during human embryogenesis. In mice, cholesterol can pass the placenta and this addition of maternal cholesterol seems to take over the indispensable role of endogenously synthesized cholesterol in development. Since desmosterol is accumulating in these mice, the amount of total sterols in the periphery is unchanged and the nature of the accumulating sterol may explain why DHCR24$^{-/-}$ mice are viable, whereas mice deficient in other cholesterol biosynthetic enzymes are not viable embryonically (Fitzky et al., 2001; Herz and Farese, 1999).

1.2.7 DHCR24/seladin-1

DHCR24 shares homologies with a family of flavin-adenine-dinucleotide-dependent oxidoreductases and is the human homologue of the *diminuto/dwarf1* gene, described in plants and in *C.elegans* (Klahre et al., 1998). In plants, Diminuto/Dwarf1 is required for the synthesis of brassinosteroids, which are plant sterols essential for normal growth and development. In 2000, Greeve *et al*. performed a differential display analysis and identified the mRNA of *dhcr24* being down-regulated in brain areas affected by AD compared to non affected areas (Greeve et al., 2000). This is why they named it seladin-1, the selective Alzheimer's disease indicator 1. The observed down-regulation suggested an association of seladin-1 with the selective vulnerability of neurons in these particular brain areas. Further experiments revealed a neuroprotective effect of seladin-1 over-expression in human SH-SY5Y neuroblastoma cells (unpublished results by Crameri et al.) and neuroglioma H4 cells that were protected from apoptosis induced by oxidative stress and Aβ-induced toxicity (Greeve et al., 2000). Furthermore, seladin-1 was linked to tau-related neuronal degeneration in AD, showing a close inverse correlation between the seladin-1 expression level and the presence of NFTs, neuritic plaques and paired helical filaments in temporal cortices of AD cases when compared to non-demented subjects (Iivonen et al., 2002). More recent findings give evidence of an interaction between seladin-1 and the tumor suppressor protein p53 (Wu et al., 2004). Following oncogenic and oxidative stress, Wu *et al*. could show that seladin-1 binds to p53, thus displacing the E3 ubiquitin ligase Mdm2 from p53, resulting in p53 accumulation. These data implicate an unanticipated role for seladin-1 in integrating cellular response to oncogenic and oxidative stress (Wu et al., 2004). It remains to be determined

whether the potential function of seladin-1 described above is associated with its DHCR24-function in cholesterol biosynthesis.

1.3 AIM OF THE STUDY

Given the fundamental role of cholesterol in maintaining the integrity of physiological membranes, one important objective of this thesis was the analyses of the consequences of cholesterol depletion on membrane organization and DRM formation *in vivo*. To this aim, we employed mice depleted of one *dhcr24* allele (heterozygous DHCR24$^{+/-}$ mice), as a model for a moderate cholesterol reduction of about 25%, and knock-out mice (DHCR24$^{-/-}$) depleted of both alleles, to study a chronic cholesterol deficiency. This was attempted applying various methods such as sucrose gradient fractionation, protein flotation profiling and lipid analyses. In order to assess the functional relevance of the observed alterations in DRM composition, we studied plasmin activity, APP processing, Aβ generation and signal transduction pathways as important examples of membrane-dependent cellular events. Moreover, we tried to evaluate whether cholesterol can be functionally substituted *in vivo*. Age-dependent accumulation of desmosterol in adult DHCR24$^{-/-}$ mice allowed us to examine, whether cholesterol can be physically and functionally replaced by its direct precursor.

2. METHODS

2.1 MICE

A heterozygous breeding pair with targeted depletion of one *dhcr24* allele was received from Dr. E. Feinstein (Quark Biotech, Inc.). Mice were bred to a pure FVB background and genotyped as described (Wechsler et al., 2003). In brief, DNA was extracted of tail biopsies from three week-old mice using the DNeasy tissue kit (Qiagen). PCR reaction was performed using two *dhcr24* specific primers (5'TCGCTGGCCGTGTGCGCGCT-3' and 5'-ATCCCCACTCCCACGCCCATT-3') designed to amplify a 312 bp fragment from the normal allele, and one primer specific for the Neomycin cassette, inserted in the first exon (5'-GATGGATTGCACGCAGGTTC-3'), designed to amplify a 969 bp fragment when used in combination with the upstream located *dhcr24* specific primer. The PCR reaction was carried out at the following conditions, using all three primers simultaneously: denaturation 2 min 94°C; 30 cycles of 45 sec 60°C; 2 min 72°C; 1 min 94°C. Reactions were completed by 10 min incubation at 72°C. All animal experiments and husbandry were performed compliant with national guidelines.

2.2 ANTIBODIES, WESTERN BLOTS AND QUANTIFICATION

Monoclonal anti-flotillin 1 (clone 18, Transduction Laboratories), monoclonal anti-cellular prion protein (Prp^c) (POM-1, kindly provided by Dr. A. Aguzzi, University of Zurich), monoclonal anti-transferrin receptor (TfR) (Clone CD-71, Santa Cruz Biotechnology Inc.), polyclonal anti-C-terminal APP (Sigma), monoclonal anti-N-terminal APP (22C11, Chemicon) and monoclonal m3.2 anti-APP antibody binding within residues 1-15 of mouse Aβ, recognizing mouse full length APP, sAPPα and the Aβ peptide (kindly provided by Dr. Paul M. Mathews, New York University) were used for Western blot analysis of APP processing products and sucrose gradient fractions. For signal transduction analyses anti-p-ERK Thr177/Thr160 (sc23759-R, Santa Cruz), anti-p-SAPK Thr183/Tyr185 (#9251, cell signaling), anti-GSK Ser9 (sc11757, Santa Cruz), anti-AT8 (Innogenetics), anti-p-Akt1/2/3 Ser473 and Thr 308 (sc7985-R and sc-16646-R Santa Cruz), anti-p-p38 Thr180/Tyr182 (#9211, cell signaling) and anti-RhoA 119 (sc-179, Santa Cruz) antibody were used for Western blot analysis. Monoclonal anti-β-actin (Abcam) and anti-GAPDH (Biodesign) antibodies were used as internal loading controls and for normalization of densitometric analysis of the immunoreactive bands. All antibodies were diluted in 5% fat-free milk

(Migros) in 35 mM Tris–HCl (pH 7.4) and 140 mM NaCl (TBS buffer). For Western blotting, 16% Tris-Glycine polyacrylamide–SDS gels and Novex 10-20% gradient Tricine gels (Invitrogen) were used. Proteins were transferred to a nitrocellulose membrane (0.45 mm pore; Bio-Rad). Species specific peroxidase-conjugated secondary antibodies and the ECL detection method (all from Amersham) were subsequently used. Western blot analyses were performed in 4-5 mice of each genotype and age-group. Quantification of immunoreactive bands was carried out by densitometry of the scanned films under conditions of non-saturated signals using the ImageJ software.

2.3 TISSUE PREPARATION

Mice were perfused transcardially under deep anesthesia (ketamin 100 mg, xylazine 5 mg/kg bodyweight, i.p.) using a peristaltic pump. Perfusion was performed initially with PBS pH 7.4 for 10-15 minutes on ice. For histological analyses, mice were subsequently perfused with 4% PFA. Brains were frozen or immersion-fixed in 4% PFA overnight at 4°C.

2.4 QUANTITATIVE RT-PCR

Total RNA was prepared from SH-SY5Y cells (n=4 of each condition) and half brains of mice (n=5 each) with TRIZOL (Invitrogen), DNase treated using RNase-Free DNase Set (Quiagen) and quality checked on a 2% Agarose gel. 2 μg were reversely transcribed into cDNA with the Transcriptor First Strand cDNA Synthesis Kit (Roche) and 1:4 diluted. Real-time PCR was performed in triplicates using 2 μl of cDNA in Full Velocity SYBR Green QPCR Master Mix (Stratagene) reagent (25 μl/well) according to the manufacturer's protocol. Primers were used at a final concentration of 500 nM. Sequences of the primers used for real-time PCR are listed in Table 1. To advance specificity of the reaction, primers were designed spanning genomic introns. Specificity of the reaction was also confirmed by agarose gel-electrophoresis of the PCR products. Relative mRNA levels were calculated according to the comparative threshold cycle (ΔΔCT) method (Ohyama et al., 2006). The housekeeping genes Glycerinaldehyd-3-phosphate-Dehydrogenase (*gapdh*) and *β-actin* were used as reference genes for analyses in mouse brains, and *gapdh* and phosphoglucokinase (*pgk*) were used as reference genes for SH-SY5Y cell analyses.

Table 1 Oligodeoxyribonucleotide primers used for quantitative real-time PCR analysis

Gene	Species	Forward (5'-3')	Reverse (5'-3')
dhcr24	mouse	CATCGTCCCACAAGTATG	CTCTACGTCGTCCGTCA
hmgcr	mouse	CCGGCAACAACAAGATCTGTG	ATGTACAGGATGGCGATGCA
fas	mouse	TCCTGGAACGAGAACACGATC	ATTTCCTGAAGTTTCCGCAGC
srebp1c	mouse	GGAGCCATGGATTGCACATT	GGCCCGGGAAGTCACTGT
srebp2	mouse	TGAAGCTGGCCAATCAGAAAA	ATCACTGTCCACCAGACTGCC
β-actin	mouse	TACTCTGTGTGGATCGGTGGC	TGCTGATCCACATCTGCTGG
gapdh	mouse	GGCATCTTGGGCTACACTGAG	CGAAGGTGGAAGAGTGGGAG
srebp1c	human	TGCGTCGAAGCTTTGAAGG	AGGTCGAACTGTGGAGGCC
hmgcr	human	CCACGTGAATGGCCCTAGAA	TTTCAGTCACCAACCTCCTGG
fas	human	GAACTCCTTGGCGGAAGAGAA	GGACCCCGTGGAATGTCAC
pgk	human	TGAAGGACTGTGTAGGCCCAG	TTCTTCCTCCACATGAAAGCG

2.5 HISTOLOGY

After extensive washing, the fixed tissue fragments were dehydrated through a graded series of ethanol solutions followed by xylol incubation and embedded in paraffin before making histological sections. Specimens (5 μm) were washed in xylene and dehydrated according to standard protocols. Sections were stained with hematoxylin and eosin (H/E) and used for a myelin stain (Luxol fast blue) according to standard protocols. Apoptotic cells were detected performing immunohistochemistry with an antibody against cleaved caspase-3 Asp175 (#9661, cell signaling) following the manufacturer's instructions. Terminal deoxynucleotidyl transferase mediated dUTP nick end labeling assay (TUNEL) was performed according to the manufacturer's protocol (Roche).

2.6 BRAIN SAMPLE PREPARATION

Mouse brains were homogenized in a Tris-Buffer (20 mM Tris, 137mM NaCl, pH 7.6) containing 2% SDS with protease inhibitors in a dounce homogenizer for 5 minutes on ice. The samples were centrifuged at 100,000 g for 1 hour at 4°C to pellet the insoluble debris. The supernatant was considered as total homogenate. For membrane preparations mouse brains were homogenized in 25 mM MES pH 7.0, 5 mM DTT, 2 mM EDTA and protease inhibitor without detergent in a dounce homogenizer on ice and centrifuged for 2 minutes at 2000 g to pellet the debris. Supernatants were centrifuged at 100,000 g for 1 hour at 4°C.

Pellets were considered as total membrane. Protein concentration was quantified using the DC protein assay (BIORAD).

2.7 SUCROSE GRADIENT FRACTIONATION

Detergent extraction and DRM isolation were performed as described (Crameri et al., 2006). In brief, mouse brain extracts were incubated for 1 hour at 4°C in 1% Triton X-100, 25 mM MES pH 7.0, 5 mM DTT, 2 mM EDTA and protease inhibitor. The extracts were mixed with 90% sucrose prepared in MBS buffer (25 mM MES pH 7.0, 150 mM NaCl and CLAP) over layered with a step gradient of 35% and 5% sucrose in MBS. After centrifugation at 100,000 g for 18 hours at 4°C, fractions 4-6 were identified as the DRM fraction by the presence of the DRM markers flotillin-1 and Prp^c in the control samples. Analyses were performed in three mice of each genotype and age-group.

2.8 LIPID ANALYSIS

Lipids were extracted from membrane pellets according to the Bligh-Dyer method using chloroform/methanol (Bligh and Dyer, 1959). Sphingomyelin, the ganglioside GM1 and phospholipids were determined as described (Crameri et al., 2006). Briefly, sphingomyelin was analyzed by thin-layer chromatography (TLC), GM1 by slot-blot using cholera toxin subunit B linked to a peroxidase (Sigma) and phospholipids were determined using the Phospholipid B kit (WAKO) according to the manufacturer's protocol. Analyses were performed in four mice of each genotype and age-group.

2.9 STEROL ANALYSIS

The dissected cortex specimens were dried to constant weight in a Speedvac® (Servant Instruments, Inc., Farmingdale, NY, USA). Sterols were extracted by chloroform/methanol (2:1 v/v). 50 µg 5α-cholestane (Serva Electrophoresis GmbH, Heidelberg, Germany) (50 µL from a stock solution of 5α-cholestane in cyclohexane; mg/mL), 1 µg epicoprostanol (Sigma-Aldrich, Munich, Germany) (10 µL from a stock solution epicoprostanol in cyclohexane; 100 µg/mL) were added to 500 µl of extract as internal standards. The organic solvents were evaporated under nitrogen gas at 60°C. After alkaline hydrolysis with 1 N sodium hydroxide in 90 % ethanol for one hour at 50°C the sterols were extracted twice with 3 mL cyclohexane. The combined organic phases were dried under nitrogen at 60°C. The residue was dissolved in 500 µL n-decan and the sterols were derivatised to trimethylsilyl- (TMSi) ethers by adding

20 µL of TMSi-reagent (pyridine: hexamethyldisalazane-trimethylcholorosilane; 9:3:1, by volume; all reagents were supplied by Merck) into each micro-vial and incubated for 1h at 60°C. The corresponding trimethylsilylethers of each sterol was determined by gas chromatography- flame ionisation detection as described previously (Lutjohann et al., 2004). Analyses were performed in three mice of each genotype at three weeks of age and four mice of each group at 16 weeks of age. In addition, total sterols were measured using the Amplex Red Cholesterol Kit (Molecular Probes/Invitrogen). We established that this kit detects cholesterol and desmosterol with the same sensitivity by using dilution series of commercially available sterols (Sigma). For total sterol determination, lipids were isolated from each sucrose gradient fraction and from primary neurons as described (Bligh and Dyer, 1959), solubilized in DMSO and applied to the assay.

2.10 ELISA

Murine Aβ ELISA was performed as previously described (Crameri et al., 2006; Fukumoto et al., 2002). In brief, hemi brains were homogenized in a buffer containing 100 mM Tris and 150 mM NaCl pH 7.4 and proteinase inhibitors (Roche). Total brain extracts containing soluble and membrane bound Aβ and supernatants of primary neurons were analyzed by a modified sandwich ELISA that specifically detects either $A\beta_{40}$ or $A\beta_{42}$ (Takeda, Japan) according to the provider's protocol. Aβ was captured with a specific anti-Aβ antibody (BNT77). Aβ species ending in residue 40 or 42 were measured using horseradish peroxidase-coupled monoclonal antibodies specific for $A\beta_{40}$ (HPR-conjugated BA27) and $A\beta_{42}$ (HPR-conjugated BC05) sequence. Analyses were performed for four mice of each genotype and age-group and in two independent experiments for primary neurons with four biological replicates of each genotype.

2.11 PLASMINOGEN BINDING AND PLASMIN ACTIVITY

200µg of freshly prepared membrane extracts from mouse brains (n=3 each) and SH-SY5Y cells were resuspended in Hank's balanced saline solution (HBSS) and 0.1% Ovalbumin (Sigma) and were placed in a 96 multiwell plate in the presence of 2 mM chromogenic peptide to measure endogenous plasmin activity. In parallel experiments plasminogen binding to cellular membranes was determined by addition of 2 µM human plasminogen to the same extracts. Plasmin enzymatic activity was assayed using the chromogenic substrate S-2251

(Chromogenix) specific for this protease. Absorbance was measured at 37°C and 405 nm in an ultra microplate reader Elx808iu (BioteK instruments, INC) every 5 minutes.

2.12 SECRETASE ACTIVITY ASSAYS

Secretase activities were measured using α-, β- and γ-secretase activity Kits (R&D systems). These assays rely on the cleavage of secretase-specific peptides that are conjugated to the reporter molecules EDANS and DABCYL. In the uncleaved form the fluorescent emissions from EDANS are quenched by the physical proximity of the DABCYL moiety which exhibits maximal absorbance at the same wavelength (495 nm). Cleavage of the peptide by the secretase physically separates the EDANS and DABCYL allowing for the release of a fluorescent signal. Reactions were carried out according to the manufacture's instructions using provided buffers. In brief, half brains (n=5 each) were homogenized in cell extraction buffer to a final concentration of 2 mg/ml. Homogenates were incubated on ice for 10 minutes and centrifuged at 10,000 g for 1 minute. Supernatant, 2x reaction buffer and substrates were added to each well, gently mixed and incubated in the dark at 37°C for 1-2 hours. The plate was read in a fluorescent micro plate reader using 355 nm wavelengths for excitation and 510 nm for emission with a 495 nm cutoff.

2.13 PRIMARY NEURONAL CULTURES

Primary neuronal cultures were prepared from wildtype, DHCR24$^{+/-}$ and DHCR24$^{-/-}$ embryos at E13-16. The cortex was dissected, and kept in ice-cold Hank's balanced salt solution (HBSS; 10 mM HEPES, pH 7.3) (Invitrogen). Meninges were removed and the cortical tissues were incubated for 10 minutes in 2.4 U/ml Dispase (Roche) and 0.2 mg/ml deoxyribonuclease (Sigma) and then dissociated to single cells by gentle trituration. The cell suspension was mixed with Neurobasal-Medium supplemented with B27 (Invitrogen), 0.5 mM glutamine, 50 U/ml penicillin, and 50 µg/ml streptomycin. The cell suspension was centrifuged at 310 g for 3 minutes and the resulting pellets were resuspended in the medium described above and plated onto polyornithin/laminin (Sigma) coated 12-well plates with one coated glass cover slip for immunocytochemical staining in each well. The cells were cultured in a CO_2 incubator (5% v/v, 37°C) for 3-5 days. For Western blot analysis of sAPPα, the supernatant was collected, acetone precipitated and dissolved in loading buffer. For detection of Aβ in supernatants of primary neurons, cells were grown in 12-well plates in cholesterol- and serum-free medium complemented with B27 (Invitrogen) for 3 days *in vitro*. Medium was removed, cells were washed with PBS and overlaid with 350 µl of fresh serum-free medium.

After 24 hours, 150 µl of the supernatant was used for ELISA without further processing. For Western blot analysis of full length APP primary neurons were homogenized in a Tris-Buffer containing 2% SDS with protease inhibitors. Analyses were performed in two independent experiments with four biological replicates of each genotype.

2.14 IMMUNOCYTOCHEMISTRY

Neurons were fixed with 4% PFA for 10 minutes at room temperature, blocked and permeabilized with 5% horse serum containing 0.1% Triton X-100 for 2 hours. Anti-Map2 antibody and anti-GFAP antibody (both from Sigma) were used to determine the percentage of neurons and astrocytes according to the manufacturer's instructions. Species specific fluorescence-labeled secondary antibodies (Amersham) were diluted in blocking buffer and cells were stained for 2-4 hours in the dark. The cells were washed and embedded in Moviol (Merck).

2.15 CELL CULTURE

SH-SY5Y cells were cultured in DMEM NUT-F12 medium (Invitrogen) containing 10% foetal calf serum (FCS), 5% horse serum (HS) and 5000U/ml penicillin and 5000µg/ml streptomycin. Sterols were dissolved in 95% EtOH. Cells were grown in serum-free media containing 10 µg/ml lanosterol, 10 µg/ml desmosterol, 10 µg/ml lanosterol plus 10 µg/ml desmosterol, or control reagent only (95% EtOH) for four days. After sterol treatment of SH-SY5Y cells and before Aβ measurement in the medium of primary neurons, the viability of the individual cultures was determined using the MTT (Sigma) and the LDH assay (Sigma) according to the manufacturer's instructions. For desmosterol addition and cholesterol reduction in SH-SY5Y cells, desmosterol and methyl-β-cyclodextrin (Sigma) were complexed as described previously for cholesterol (Klein et al., 1995). These complexes containing 0.3 mM desmosterol were added to the medium of SH-SY5Y cells at a final 1:10 dilution together with 2 µg/ml free desmosterol and incubated for 1h at 37°C. To moderately reduce cholesterol from SH-SY5Y cells, the cells were incubated for 48 hours with 0.4 µM mevilonin (Sigma) and 1 mM methyl-β-cyclodextrin to extract 30% cholesterol as described previously (Abad-Rodriguez et al., 2004). The incorporation of desmosterol was monitored by TLC using pure desmosterol (Sigma) as standard. Cholesterol reduction in mevilonin and methyl-β-cyclodextrin treated cells was monitored by the Amplex red kit (Molecular Probes/Invitrogen) as described above. Cell viability after these treatments was not affected, as determined as described above.

2.16 STATISTICAL ANALYSIS

Data were collected by investigators blinded to the experimental setup and were statistically analyzed by non-parametric Mann-Whitney U-test. In all graphs, mean±SEM (standard error of the mean) are shown unless otherwise noted. In tables, mean±SD (standard deviation of the mean) are shown. p-values <0.05 were considered to be statistically significant. *$p<0.05$, **$p<0.01$.

3. RESULTS

3.1 VIABILITY AND NEUROPATHOLOGICAL STATUS OF DHCR24$^{-/-}$ MICE

DHCR24 knock-out mice (DHCR24$^{-/-}$) were born at a lower frequency than expected (10-17%) and were about 25% smaller in size than their heterozygous (DHCR24$^{+/-}$) and wildtype (wt) littermates, as previously described (Wechsler et al., 2003). DHCR24$^{+/-}$ littermates showed no obvious phenotype. After backcrossing DHCR24$^{+/-}$ mice (C57BL/6x129SvEv) to a pure FVB background the frequency of born knock-out mice from heterozygous matings was increased to an almost normal rate (15-20%). To ensure surviving of the visibly smaller knock-out mice, the number of littermates was decreased to 2-3 mice per mating.

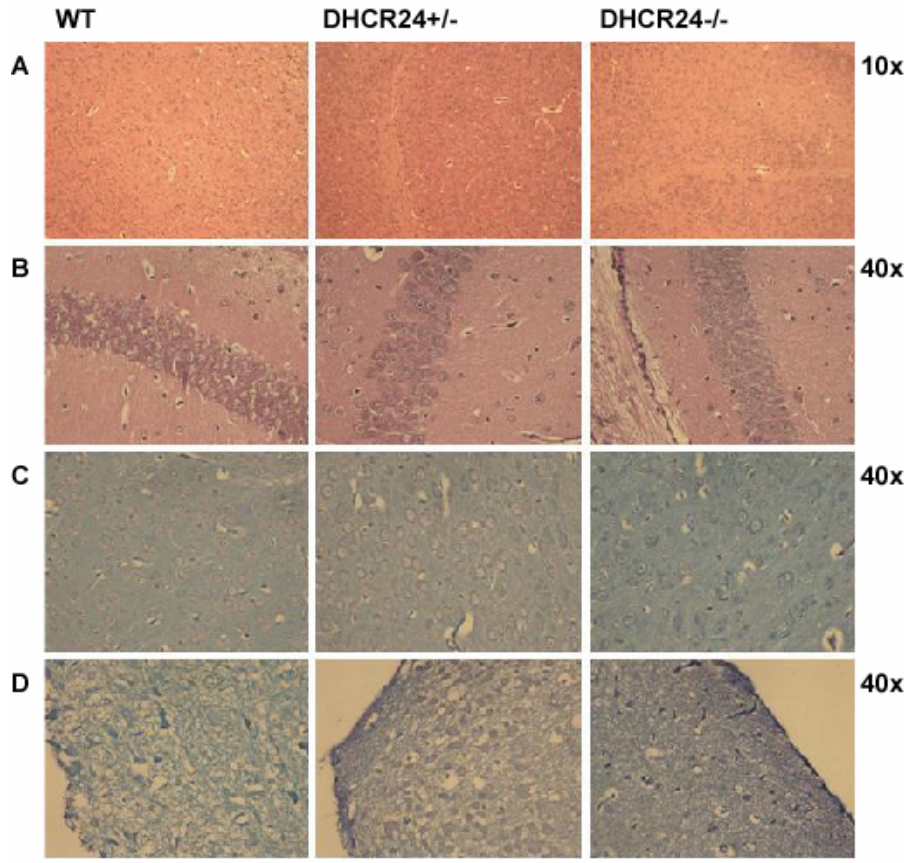

Figure 4 Neuropathological analyses of three week-old wt and DHCR24 depleted mice. Histolgical H/E stainings of cortical (A) and hippocampal (B) sections and Luxol fast blue stainings of different cortical areas (C and D) revealed no structural or morphological differences between the three genotypes.

Under these conditions maternal care was ensured. The knock-out mice were able to suck, determined by an evident full stomach, and developed normally, although with poorer growth characteristics. While some DHCR24$^{-/-}$ mice reached about normal weight 10-12 weeks after

birth, the average weight of knock-out mice was below the level of wildtype and heterozygous littermates, as previously described (Wechsler et al., 2003). Neuropathological examinations of mice at the age of three weeks and four months applying different histological methods such as hematoxylin/eosin (H/E) and myelin staining (Luxol fast blue) revealed that there were no detectable morphological or structural differences between wildtype, heterozygous and knock-out mice (Figure 4). These analyses were confirmed by Dr. vet. Monika Hilbe at the Tierspital in Zurich, who analyzed brains from mice of all three genotypes at different ages (two days, three weeks and four months). Furthermore, no differences in apoptotic events were detected in brains of DHCR24$^{-/-}$ mice as revealed by TUNEL and cleaved caspase-3 staining of histological brain sections (data not shown).

3.2 YOUNG DHCR24 DEPLETED MICE

It was shown that cholesterol biosynthesis is high in the brain of newborn mammals but is reduced during postnatal development, while it levels off about 2-3 weeks after birth (Ohyama et al., 2006). We therefore examined the brains of three week-old (young) wt, DHCR24$^{+/-}$ and DHCR24$^{-/-}$ mice.

3.2.1 Brain sterol synthesis and elimination

To eventually produce cholesterol from lanosterol a series of enzyme reactions is required. DHCR24 reduces the C24 double bond of all sterols of the Bloch-pathway, starting from lanosterol as the first substrate. Desmosterol is the ultimate precursor of cholesterol and the last possible substrate for DHCR24 of the Bloch-pathway. The synthesis of sterols of the Kandutsch-Russel pathway including lathosterol and cholesterol is essentially dependent on DHCR24 (see Figure 3 in chapter 1.2.1). We analyzed the sterol distribution in brains of young wt, DHCR24$^{+/-}$ and DHCR24$^{-/-}$ mice using gas-chromatography/mass-spectrometry. With DHCR24 depletion sterols of the Bloch-pathway were accumulating, whereas components of the Kandutsch-Russel pathway were reduced (Figure 5A and Table 2). Cholesterol was significantly reduced in brains of DHCR24$^{+/-}$ mice (77±11%, p=0.016) and dramatically diminished in DHCR24$^{-/-}$ brains (4.2±1%, p=0.025) compared to wt mice. The ultimate substrate of DHCR24, desmosterol, was markedly increased in DHCR24$^{+/-}$ brains (383±138%, p=0.004) and tremendously increased in brains of DHCR24$^{-/-}$ mice (4783±56%, p=0.025). Whereas lanosterol, the first substrate of DHCR24, was moderately elevated with

DHCR24 depletion (126±44%, p=0.167 in DHCR24$^{+/-}$ brains and 189±44%, p=0.025 in DHCR24$^{-/-}$ brains, respectively), lathosterol and the brain specific catabolic product of cholesterol, 24*S*-OH-cholesterol, were significantly decreased in brains of DHCR24$^{+/-}$ mice (72±13%, p=0.042 and 75±10%, p=0.028, respectively) and were virtually absent in knock-out mouse brains (6.3±2%, p=0.025 and 4.3±2%, p=0.025, respectively).

The major sterol in wt brains was cholesterol, accounting for over 99% of all sterols, while desmosterol represented less than 1% of all sterols in wt brains (Figure 5B and Table 2). Since desmosterol is the last sterol of the Bloch-pathway and its reduction is solely catalyzed by DHCR24, this sterol was increased in DHCR24$^{+/-}$ brains and greatly accumulated in brains of knock-out mice. However, compared to the total amount of cholesterol in brains of young wt mice, desmosterol concentration reached about 8% in DHCR24$^{+/-}$ brains, in DHCR24$^{-/-}$ mice about 50% of wt cholesterol levels; therefore the amount of total sterols was reduced by approximately 15% in brains of DHCR24$^{+/-}$ mice, presenting a model of moderate cholesterol reduction with slightly increased levels of desmosterol. Total sterols in brains of DHCR24$^{-/-}$ mice were reduced by 47%, while desmosterol accounted for over 95% of these sterols. The small proportion of cholesterol in DHCR24$^{-/-}$ mice was most probably maternal cholesterol that traversed the placenta and did not derive from *de novo* cholesterol biosynthesis. All together, these data clarify the role of DHCR24 in brain sterol biosynthesis and suggest that other enzymes of the two pathways, for example DHCR14, are not capable of taking over the reductase function of DHCR24, as proposed earlier (Peri et al., 2005).

Table 2 Brain concentrations (ng/mg wet weight; mean ±SD) of cholesterol, desmosterol, lanosterol, lathosterol and 24*S*-OH-cholesterol of young (three week-old) wt, DHCR24$^{+/-}$ and DHCR24$^{-/-}$ mice

Genotype	Lanosterol	Desmosterol	Lathosterol	Cholesterol	24*S*-OH-Chol
wt	37±7	567±84	391±87	59,623±7,305	340±53
DHCR24$^{+/-}$	46±16	2,172±777**	281±49*	45,730±5,962*	256±33*
DHCR24$^{-/-}$	70±16*	27,141±47*	25±1*	2,496±66*	15±7*

*p<0.05, **p<0.01 vs. aged-matched controls. Exact p-values are given in the text

In conclusion, these data reveal that young DHCR24$^{+/-}$ mice demonstrate a model for a moderate cholesterol reduction of about 25%, whereas DHCR24$^{-/-}$ mice present a model that is entirely devoid of cholesterol but accumulates desmosterol over time. Wechsler *et al*. could

show that desmosterol levels already increased during embryonic development of DHCR24$^{-/-}$ mice (Wechsler et al., 2003). Our findings support this theory of desmosterol accumulation and suggest that there is no efficient catabolism of desmosterol in the murine brain.

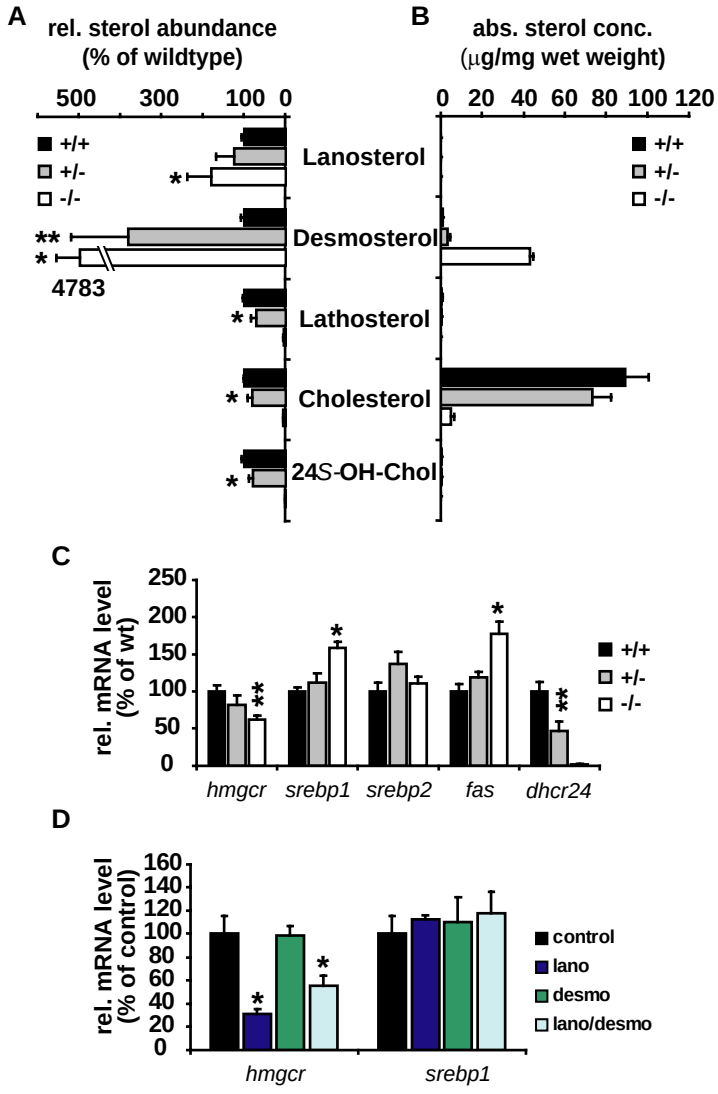

Figure 5 Sterol distribution and differential gene expression in brains of wt and DHCR24 depleted mice. (A) Lanosterol was moderately increased with DHCR24 depletion, while desmosterol accumulated gradually in DHCR24$^{+/-}$ and DHCR24$^{-/-}$ brains. Cholesterol, lathosterol and 24*S*-OH-chol were significantly reduced in DHCR24$^{+/-}$ brains and virtually absent in DHCR24$^{-/-}$ brains. Sterol levels in wt brains were considered as 100%. (B) In wt and DHCR24$^{+/-}$ brains cholesterol was the major sterol, accounting for almost 99% of all sterols, while desmosterol was the predominant sterol in DHCR24$^{-/-}$ brains. Absolute desmosterol concentrations in young DHCR24$^{-/-}$ brains were only half of the cholesterol concentrations in wt mice. (C) Expression analyses of genes involved in brain cholesterol and lipid homeostasis were determined by real-time PCR. Elevations in *fas* and *srebp1* expression and reduced *hmgcr* expression in DHCR24$^{-/-}$ brains were apparent, whereas no significant effect was observed for *srebp2* in DHCR24 depleted brains. DHCR24 expression was significantly reduced in DHCR24$^{+/-}$ brains and DHCR24 mRNA was absent in DHCR24$^{-/-}$ brains. Data were normalized to the mean value of the two housekeeping genes *gapdh* and *β-actin*. (D) SH-SY5Y cells were treated with lanosterol, desmosterol and a combination of both sterols. Lanosterol significantly reduced *hmgcr* expression, also in combination with desmosterol, while desmosterol alone did not alter *hmgcr* expression. Sterol treatment did not affect *srebp1* expression. Relative mRNA levels of the respective genes in wt brains were considered as 100% (*p<0.03, **p<0.009).

3.2.2 Differential expression of cholesterol related genes

To identify changes in gene expression that are associated with cholesterol depletion, we isolated total RNA from hemi brains of young DHCR24$^{+/-}$, DHCR24$^{-/-}$ and wt littermates and performed real-time PCR experiments (Figure 5C). Expression analysis of genes involved in cholesterol and fatty acid biosynthesis revealed a trend towards an increased expression of fatty acid synthase (*fas*) in DHCR24$^{+/-}$ brains (119±6.8%, p=0.076), while *fas* expression was significantly increased in DHCR24$^{-/-}$ brains (177±17.1%, p=0.027). Expression of the sterol-regulatory element binding protein 1 (*srebp1*) was unchanged in DHCR24$^{+/-}$ brains, but highly elevated in DHCR24$^{-/-}$ brains (158±8.6%, p=0.014), whereas expression of *srebp2* was unchanged with DHCR24 depletion compared to controls. Expression of the *hmgcr* gene, encoding for the rate-limiting enzyme in cholesterol biosynthesis, showed a trend towards a reduction in DHCR24$^{+/-}$ brains (81.9±12.5%, p=0.072) and was significantly reduced in brains of young DHCR24$^{-/-}$ mice (62.1±5.4%, p=0.002).

Analyses of *dhcr24* expression revealed a gene dose-dependent effect in DHCR24$^{+/-}$ mice (46.3±13.6%, p=0.009), explaining the reduced cholesterol levels in heterozygous brains and the increase of desmosterol in these mice. DHCR24 mRNA was not detectable in DHCR24$^{-/-}$ mice. The expression of the housekeeping genes *gapdh* and *β-actin* was not altered between the three genotypes (not shown). Relative mRNA levels of the respective genes were normalized to the mean value of both housekeeping genes.

Analyses of sterol distribution and expression of the rate-limiting enzyme HMGCR suggest a possible feedback mechanism from early Bloch-sterols such as lanosterol on *hmgcr* expression. Previous studies showed that lanosterol and its naturally occurring oxygenated derivative oxylanosterol can influence cholesterol biosynthesis and HMGCR activity, by mediating post-transcriptional modification and stimulating the degradation of HMGCR (Panini et al., 1992; Panini et al., 1986; Song et al., 2005). Therefore, we treated SH-SY5Y neuroblastoma cells with lanosterol, desmosterol and a combination of both sterols (5 µg/ml each in 95% ethanol) and determined *hmgcr* expression in these cultures (Figure 5D). Lanosterol treated cultures and cultures treated with both sterols showed a significant decrease in *hmgcr* expression compared to control cultures that were treated with 95% ethanol, while desmosterol treatment alone did not alter *hmgcr* expression. These results suggest that lanosterol or its naturally occurring oxygenated derivative might be part of a feedback mechanism on cholesterol biosynthesis, thus regulating the expression of the rate-limiting enzyme HMGCR. Treatment of SH-SY5Y cells with sterols as described above did not reveal

any differences in expression of *srebp1* (Figure 5D) and fas (data not shown), suggesting that cholesterol paucity might be responsible for the observed elevation of *srebp1* and *fas* expression in DHCR24$^{-/-}$ brains, rather than the increase of lanosterol or desmosterol.

3.2.3 Membrane organization: DRM protein and lipid composition

Given the fundamental role of cholesterol in maintaining the integrity of physiological membranes and lateral membrane domains we next tested whether changes in *dhcr24* expression affect the protein and lipid composition of DRMs. To this aim, total brain extracts from young wt, DHCR24$^{+/-}$ and DHCR24$^{-/-}$ mice were incubated with 1% Triton X-100 at 4°C and centrifuged in a sucrose gradient. This procedure allows the separation of detergent-insoluble membrane portions (DRMs) from soluble parts of the membrane. Ten fractions were collected from the top of each tube, while the first fraction was discarded. Fractions 4-6 were identified as DRM fractions by the presence of the raft markers cellular Prion protein (Prp^c), flotillin-1 and the raft-specific ganglioside GM1 in the control samples. Determination of the total amount of protein in each fraction revealed significantly lower protein levels in the DRM fractions with DHCR24 depletion (Figure 6A). While in wt mice 20.2±2.5% of total protein was found in DRM fractions, this percentage was significantly decreased in DHCR24$^{+/-}$ (13.9±2.7%, p=0.02) and DHCR24$^{-/-}$ mice (3.1±0.8%, p=0.025). Analysis of the flotation profile of Prp^c revealed significantly less Prp^c in DRM fractions of the DHCR24 depleted mice (Figure 6B and Table 3). A similar pattern was observed analyzing the flotation profile of another raft marker, flotillin-1, that was significantly reduced in DRM fractions of DHCR24$^{+/-}$ mice and even absent in these fractions in DHCR24$^{-/-}$ brains (Figure 6C and Table 3).

Table 3 Percentages of the total amounts of the respective proteins and lipids (set as 100%) in brain DRM sucrose gradients fractions of young (three week-old) wildtype, DHCR24$^{+/-}$ and DHCR24$^{-/-}$ mice.

Genotype	Prp^c	flotillin-1	Cholesterol	SPM	GM1
wt	40.5±5%	12.3±1%	53.5±9%	37.6±6%	71.8±6%
DHCR24$^{+/-}$	12.5±5% p=0.02	5.1±2% p=0.021	36±7% p=0.043	17±7% p=0.043	62±3% p=0.048
DHCR24$^{-/-}$	3.5±1% p=0.025	-	-	6.0±3% p=0.025	2.4±1% p=0.025

p-values vs. aged-matched wildtype mice

The total protein level of both raft markers in brain homogenates were similar in all three genotypes (Figure 6E), suggesting that cholesterol depletion influenced merely the subcellular distribution of these proteins, while total protein levels were not affected.

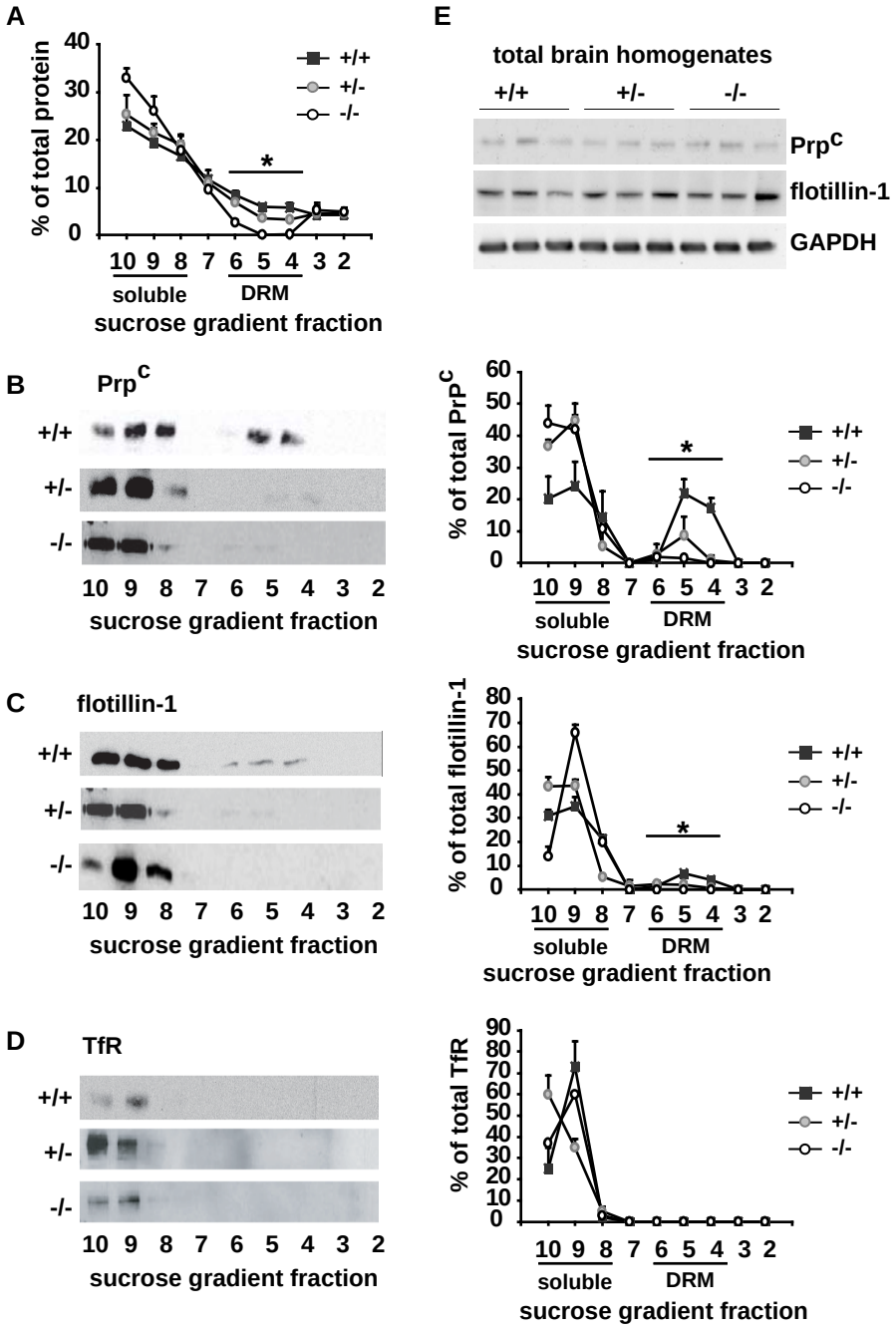

Figure 6 Protein analyses of sucrose gradient fractions. (A) Percentage of total protein in DRM fractions 4-6 were significantly reduced with DHCR24 depletion. Western blot analyses of flotation profiles of Prp^c (B) and flotillin-1 (C) revealed an altered subcellular distribution of the two raft marker with DHCR24 depletion, while no differences were detected in the distribution of the non-raft marker TfR (D). Western blots on the left show representative examples. Graphs on the right show the distribution of Prp^c, flotillin-1 and TfR in each fraction as percentage of the total amount of the respective protein along the entire gradient. (E) Total levels of Prp^c and flottillin-1 were unchanged in brain homogenates of all three genotypes. GAPDH was used as loading control (*$p<0.03$).

The non-raft protein Transferrin receptor (TfR) remained in the heavy fractions to a comparable extent in brains of all three genotypes (Figure 6D).

Analysis of the distribution of membrane constituents in soluble (8-10) and DRM fractions (4-6) revealed a significant decrease of total sterols in DRM fractions of DHCR24$^{+/-}$ mice (82±1.7%, p=0.043, Figure 7A). In DHCR24$^{-/-}$ mice, total sterols were significantly reduced in soluble fractions 8-10 of the sucrose gradients (47.8±14.3%, p=0.021), and even below detection level in their DRM fractions (Figure 7A). Because endogenous desmosterol levels represent only about 1% of total sterols in wt brains (Table 2), we conclude that cholesterol accounts for the majority of total sterols in wt and DHCR24$^{+/-}$ soluble and DRM fractions. In contrast, the detected amount of sterols in DHCR24$^{-/-}$ brains is most probably merely desmosterol, the predominant sterol in these mice. Analyses of sucrose gradient fractions by TLC for cholesterol (Figure 7B and Table 3) confirmed these findings, revealing a significant reduction of cholesterol in DRM fraction of DHCR24$^{+/-}$ brains. Cholesterol was not detectable by TLC of sucrose gradient fractions of DHCR24$^{-/-}$ brains. These data suggest that moderate cholesterol depletion in DHCR24$^{+/-}$ mice mainly affected cholesterol pools in lateral membrane domains such as DRMs, whereas cholesterol levels in soluble membrane fractions were apparently not disturbed.

Lipid analyses of sucrose gradient fractions revealed major changes in the distribution of sphingomyelin (SPM) and the ganglioside GM1 in DHCR24$^{+/-}$ and DHCR24$^{-/-}$ brains compared to wt controls (Figure 7C,D and Table 3). Both lipids were significantly reduced in DRM fractions with DHCR24 depletion, whereas the total brain levels were similar in all three genotypes (data not shown). Analysis of total brain homogenates also revealed no differences in the levels of phospholipids between the three genotypes (Figure 7E). These results show that the distribution of raft proteins, sterols and lipids is significantly altered with moderate cholesterol depletion in young DHCR24$^{+/-}$ brains. Moreover, these data point out that total cholesterol deficiency in DHCR24$^{-/-}$ mice has deleterious effects on membrane organization, challenging the very existence of lipid rafts in these mice.

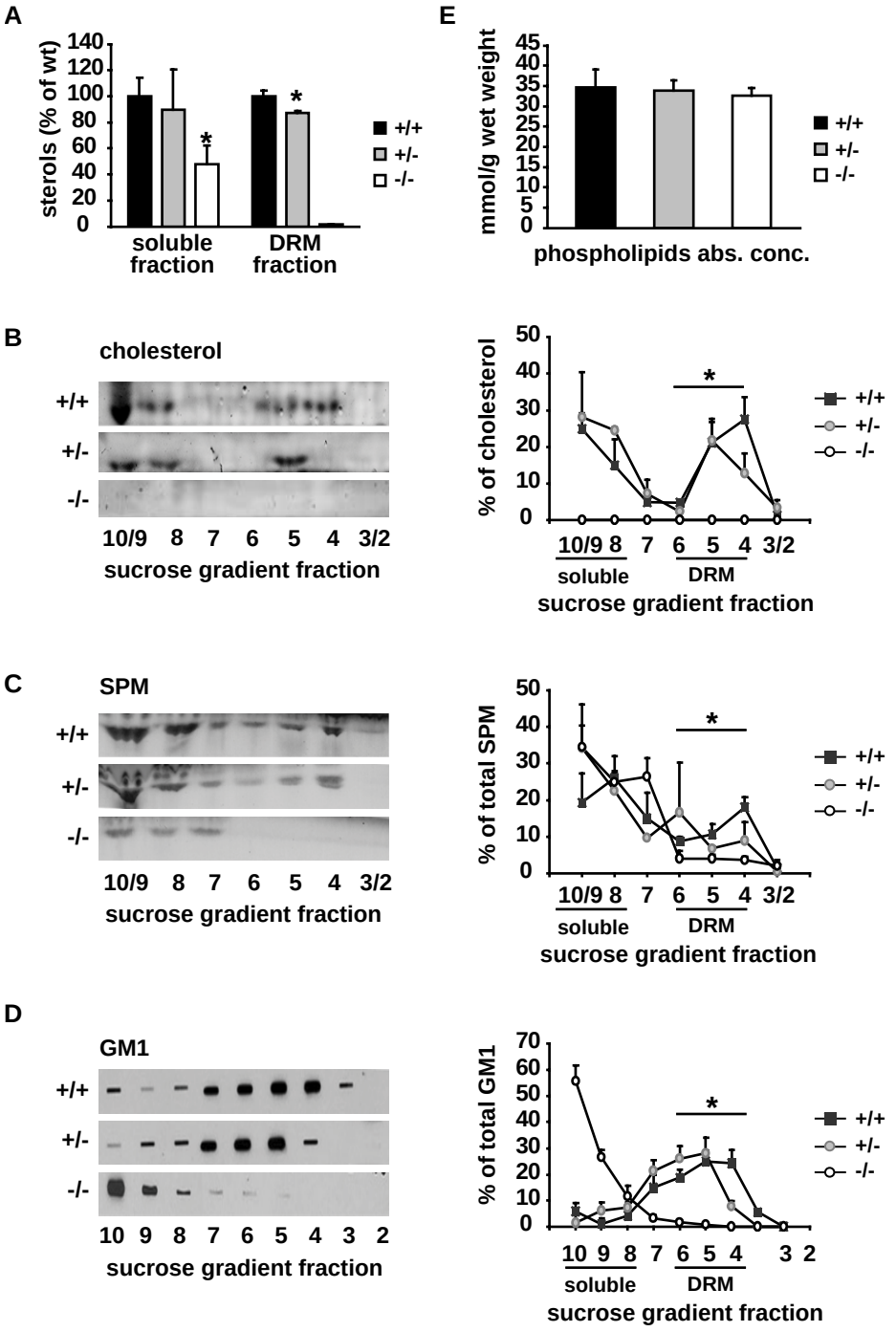

Figure 7 Lipid analyses of sucrose gradient fractions. (A) Measurement of total sterols in soluble (8-10) and DRM (4-6) fractions revealed a significant decrease of sterols in DRM fractions of DHCR24$^{+/-}$ brains. The level of total sterols was significantly reduced in soluble fractions of DHCR24$^{-/-}$ brains, while sterols were below detection level in DRM fractions of these mice. Data from wt mice were considered as 100%. TLC of cholesterol (B) and SPM (C) distribution in sucrose gradient fractions showed a significant reduction of cholesterol in DRM fractions with DHCR24 depletion. (D) Slot blot analyses of GM1 distribution in sucrose gradient fractions revealed a significant reduction of this ganglioside in DRM fractions of DHCR24 depleted brains. Pictures on the left show representative examples. Graphs on the right show the distribution of cholesterol, SPM and GM1 in each fraction as percentage of the total amount of the respective lipid along the entire gradient. (E) Phospholipid concentration in total brain homogenates was not altered between the three genotypes. Data from wt mice were considered as 100% (*$p<0.05$).

3.2.4 Analyses of DRM-dependent functions: plasminogen binding and plasmin activation

To evaluate the functional consequences of the observed disturbances in DRM composition in DHCR24 depleted mice, we analyzed plasmin activity in plasma membranes of DHCR24$^{+/-}$ and DHCR24$^{-/-}$ mouse brains. Plasmin activity is regulated by plasminogen activators, plasminogen activator inhibitors and plasmin inhibitors (Collen, 1999). In addition, plasmin generation is dependent on the binding of plasminogen to the plasma membrane (Plow et al., 1995). This occurs via the association with molecules such as α-enolase (Miles et al., 1991), annexin II (Hajjar and Acharya, 2000), amphoterin (Parkkinen and Rauvala, 1991) or the ganglioside GM1 (Miles et al., 1989). Experimental data point to DRMs as the sites where the plasminogen binding and activation take place. Moreover, plasminogen-binding molecules are enriched in rafts of neurons (Ledesma et al., 2003), and plasmin is almost exclusively present in these neuronal microdomains (Ledesma et al., 2000).

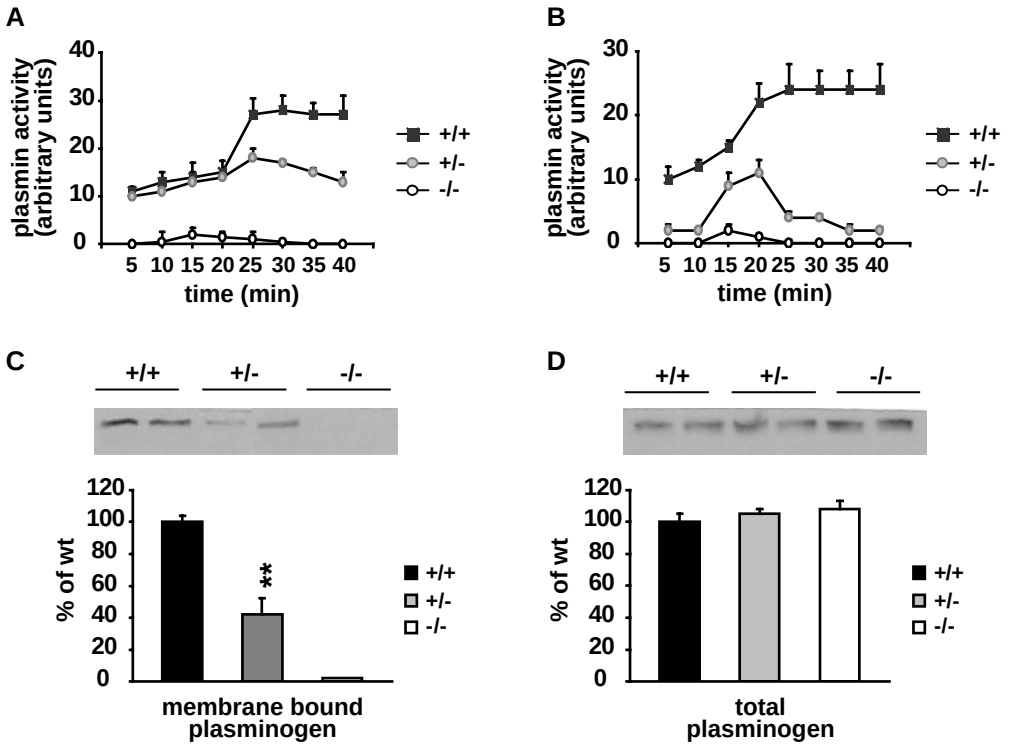

Figure 8 Analyses of DRM-dependent plasminogen binding and plasmin activation. Plasmin activity (expressed in arbitrary units) was measured at the indicated times in membranes isolated from young wt, DHCR24$^{+/-}$ and DHCR24$^{-/-}$ mouse brains. (A) DHCR24 depletion led to decreased plasmin activity in mouse brains in a dose dependant manner. (B) Plasmin activity was significantly reduced with DHCR24 depletion after addition of exogenous plasminogen, pointing to a reduced ability of membranes to bind plasminogen in DHCR24 depleted mice. (C) Membrane bound plasminogen was significantly reduced in DHCR24$^{+/-}$ and was absent in knock-out brains. (D) Endogenous levels of cellular plasminogen were not altered in any of the groups. The graphs below show the mean values and standard errors from the densitometric quantification of the Western blots from two independent experiments. Data were normalized to the amount of membrane bound GAPDH (not shown) and are expressed as percentage of the values obtained in the wt mice (**$p<0.006$).

We measured plasmin enzymatic activity using the chromogenic substrate S-2251 specific for this protease. Plasmin activity in isolated membranes of DHCR24$^{+/-}$ brains was significantly reduced and an even more drastic decrease was observed in DHCR24$^{-/-}$ brains (Figure 8A). Additionally, to analyze plasminogen binding exogenous plasminogen was added to isolated membranes and plasmin activity was measured. Concurrently, DHCR24 depletion resulted in reduced plasmin activity indicating a diminished ability of these membranes to bind plasminogen (Figure 8B). Accordingly, the amount of endogenous plasminogen bound to the membrane was clearly reduced in DHCR24$^{+/-}$ brains (42.9±10.9% p=0.005) and undetectable in DHCR24$^{-/-}$ brains (Figure 8C), while the endogenous levels of total plasminogen were similar in all mouse brains (Figure 8D).

3.2.5 BACE1-APP membrane compartmentalization, APP processing and Aβ generation

APP metabolism is a membrane-related process, since the substrate APP and its cleaving enzymes are transmembrane proteins, influenced by membrane composition and organization. Several studies examining the effects of cholesterol depletion on APP processing demonstrate a strong link between membrane cholesterol concentrations and the production of Aβ. Recent studies indicate that amyloidogenic processing seems to highly depend on how much cholesterol is extracted from cellular membranes: while a moderate reduction of cholesterol resulted in increased Aβ production in primary neurons (Abad-Rodriguez et al., 2004), extensive cholesterol depletion resulted in significantly reduced Aβ levels in cellular models (Ehehalt et al., 2003; Kojro et al., 2001; Parvathy et al., 2004; Simons et al., 1998). In these studies, cholesterol lowering drugs and/or cholesterol extracting agents were used to reduce cellular and membrane cholesterol concentrations. To study the effects of cholesterol reduction on BACE and APP membrane segregation and their functional interaction *in vivo*, we analyzed DHCR24$^{+/-}$ mice exhibiting a moderate cholesterol depletion of approximately 25% and DHCR24$^{-/-}$ mice as a model for a chronic cholesterol deficiency. While in wt brains 36.4±3.6% of BACE was present in DRM fractions 4-6, this portion was significantly reduced (9.7±1.9%, p=0.025) in DHCR24$^{+/-}$ brains. In DHCR24$^{-/-}$ brains BACE was completely shifted to APP containing soluble fractions (Figure 9A). Endogenous APP is known to reside mainly outside rafts and remained in the soluble fractions 8-10 to a similar extent in all three genotypes (Figure 9B). Levels of cellular full-length APP were similar in all three groups, and there was no significant alteration in membrane bound fractions of full-length APP (Figure 9C and E). To test if the changes in membrane compartmentalization had a functional

consequence on APP processing we measured the levels of CTFs in brains of these mice (Figure 9C-F). While the amount of α-CTF was not significantly changed between the genotype groups, the β-CTF was markedly increased in DHCR24$^{+/-}$ brains (201±16%, p=0.021, Figure 9C and D) but significantly reduced in DHCR24$^{-/-}$ brains (54±5.6%, p=0.009) when compared to wt mice (Figure 9E and F). To determine to which extent these changes in APP processing and membrane compartmentalization affect Aβ generation, we determined the concentration of murine Aβ by specific ELISA (Fukumoto et al., 2002) (Figure 9G). $A\beta_{40}$ levels were significantly increased in DHCR24$^{+/-}$ brains (152±16%, p=0.027) but markedly decreased in brains of DHCR24$^{-/-}$ mice (42.9±4.3%, p=0.021). Since endogenous $A\beta_{42}$ levels in young mice are extremely low (Refolo et al., 2001), $A\beta_{42}$ was below detection level in brains of all three genotypes (Figure 9G).

In conclusion, these data provide evidence that APP processing and Aβ generation are strongly influenced by DHCR24 disruption in a cholesterol-dependent manner *in vivo*. It was previously shown that the proteolytic activity of the β-secretase is lipid dependent and directly influenced by membrane cholesterol concentrations (Kalvodova et al., 2005) and γ-secretase activity was shown to be modulated by cellular cholesterol levels (Burns and Duff, 2002; Runz et al., 2002; Wahrle et al., 2002).

Figure 9 BACE-APP membrane compartmentalization and APP processing in DHCR24 depleted mice. (A) BACE1 distribution along the sucrose gradient fractions was significantly altered with DHCR24 depletion, while flotation profiles of APP (B) did not reveal any differences between the genotypes. Left pictures show representative examples. Graphs on the right indicate the amount of BACE1 and APP in each fraction as a percentage of total BACE1 and APP, respectively. APP β-cleavage was analyzed by Western blot of cellular extracts containing equal amount of protein prepared from wt and DHCR24$^{+/-}$ (C), and wt and DHCR24$^{-/-}$ (E) brains. APP CTFs were normalized to the amount of full length APP and the percentages in wt mice were considered as 100%. Levels of α-CTF were similar in all three genotypes (C-F). DHCR24$^{+/-}$ mice revealed a significant increase in β-cleavage (D), while β-CTF in brains of DHCR24$^{-/-}$ mice was significantly reduced (F). Murine Aβ ELISA measurements showed an increase of $A\beta_{40}$ in DHCR24$^{+/-}$ brains, while this peptide was significantly decreased in knock-out brains. $A\beta_{42}$ peptides were below detection level in brains of all three genotypes (G). Proteolytic activity of APP cleaving secretases was unchanged in DHCR24$^{+/-}$ brains, whereas β- and γ-secretase were significantly decreased in knock-out brains (H) (*p<0.04, **p<0.01).

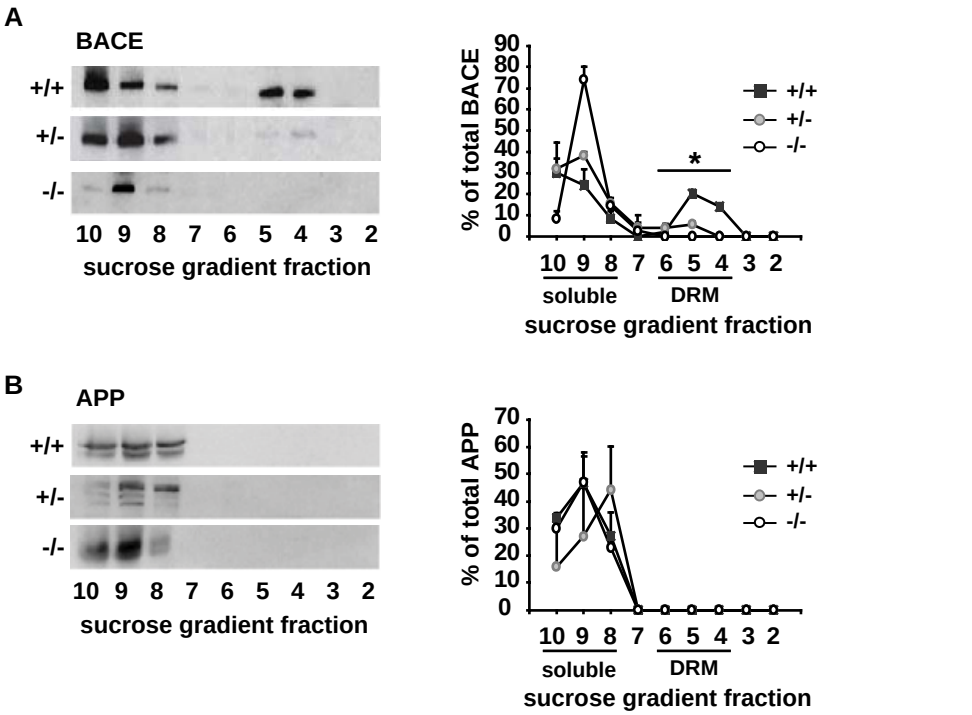
A
BACE
+/+
+/-
-/-
10 9 8 7 6 5 4 3 2
sucrose gradient fraction
% of total BACE
soluble
DRM
B
APP
% of total APP

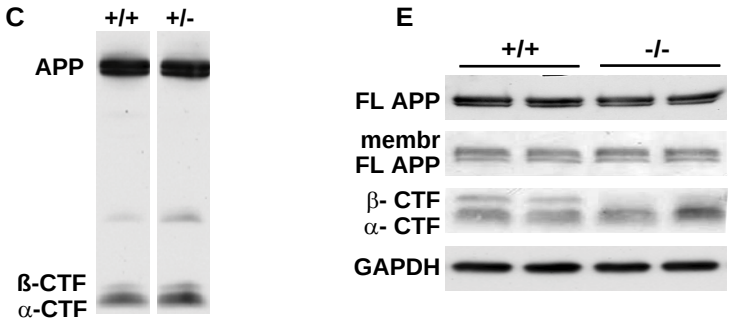
C
+/+
+/-
APP
ß-CTF
α-CTF
E
FL APP
membr FL APP
β- CTF
α- CTF
GAPDH

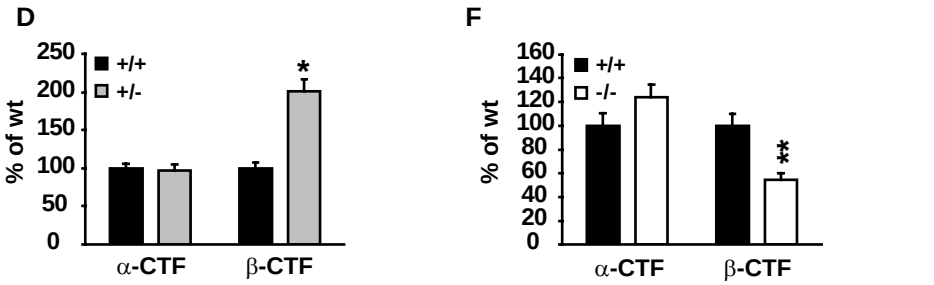
D
% of wt
α-CTF
β-CTF
F
-/-

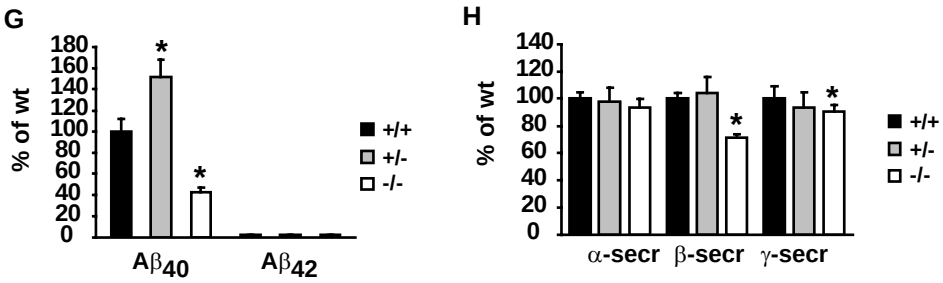
G
Aβ40
Aβ42
H
α-secr
β-secr
γ-secr

Therefore, to evaluate whether the changes in APP processing and Aβ generation were due to altered activities of involved secretases, we determined α-, β- and γ-secretase activity in brain homogenates of DHCR24 depleted and wt mice (Figure 9H). Brain activity levels of all three secretases were unchanged in DHCR24$^{+/-}$ mice, whereas a significant reduction of β-secretase activity (71.4±2.4%, p=0.025) and a moderate but still significant decrease in γ-secretase activity (90.2±5%, p=0.039) was found in DHCR24$^{-/-}$ mouse brains, which is likely to contribute to the observed changes in Aβ production in DHCR24$^{-/-}$ brains. These data suggest that the observed increase in amyloidogenic processing of APP in DHCR24$^{+/-}$ brains is most probably due to the changes in BACE and APP distribution throughout membrane compartments, rather than a consequence of altered secretase activity. However, impaired β- and γ-secretase activity in DHCR24$^{-/-}$ mice suggests that the membrane composition present in brains of these mice is not optimal to ensure full secretase activity.

Our data of the young DHCR24$^{-/-}$ mice analyses are in agreement with the observation of reduced amyloidogenic APP cleavage in situations of drastic cholesterol depletion (Ehehalt et al., 2003; Simons et al., 1998). Moreover, we could confirm the *in vitro* data published by Abad-Rodriguez *et al*. suggesting that a moderate cholesterol reduction leads to disturbances in DRM formation and increased amyloidogenic processing of APP in our DHCR24$^{+/-}$ mouse model *in vivo*. We therefore conclude that proper raft organization is necessary to maintain a certain steady state level of Aβ.

3.2.6 Protein abundance and phosphorylation

Lipid rafts sequester signaling proteins of many kinds, including heterotrimeric G protein subunits, receptor tyrosine kinases, and Src-like kinases. Although their biological function is still poorly understood, rafts have been shown to act as membrane platforms for regulating signal transduction in many cell types (Simons and Toomre, 2000). In a preliminary experiment, we analyzed phosphorylation of the main mitogen-activated protein kinases (MAPKs) in wt and DHCR24 depleted mice to determine pathways that are possibly altered with moderate cholesterol shortage, as modeled in DHCR24$^{+/-}$ mice, and chronic cholesterol deficiency as determined in DHCR24$^{-/-}$ mice. The stress activated protein kinases (SAPKs) and p38 kinases constitute together with extracellular signal-regulated kinases (ERKs) the family of MAPKs. It was shown that the phosphorylation status of many MAPKs is influenced by the subcellular distribution and concentration of cholesterol (Ballard-Croft et al., 2006; Dobreva et al., 2005) and altered signaling events were described in mouse models

with enzyme defects in cholesterol biosynthesis and impaired cholesterol transport such as Niemann Pick disease (NPD) (Cooper et al., 2003; Sawamura et al., 2003; Sawamura et al., 2001).

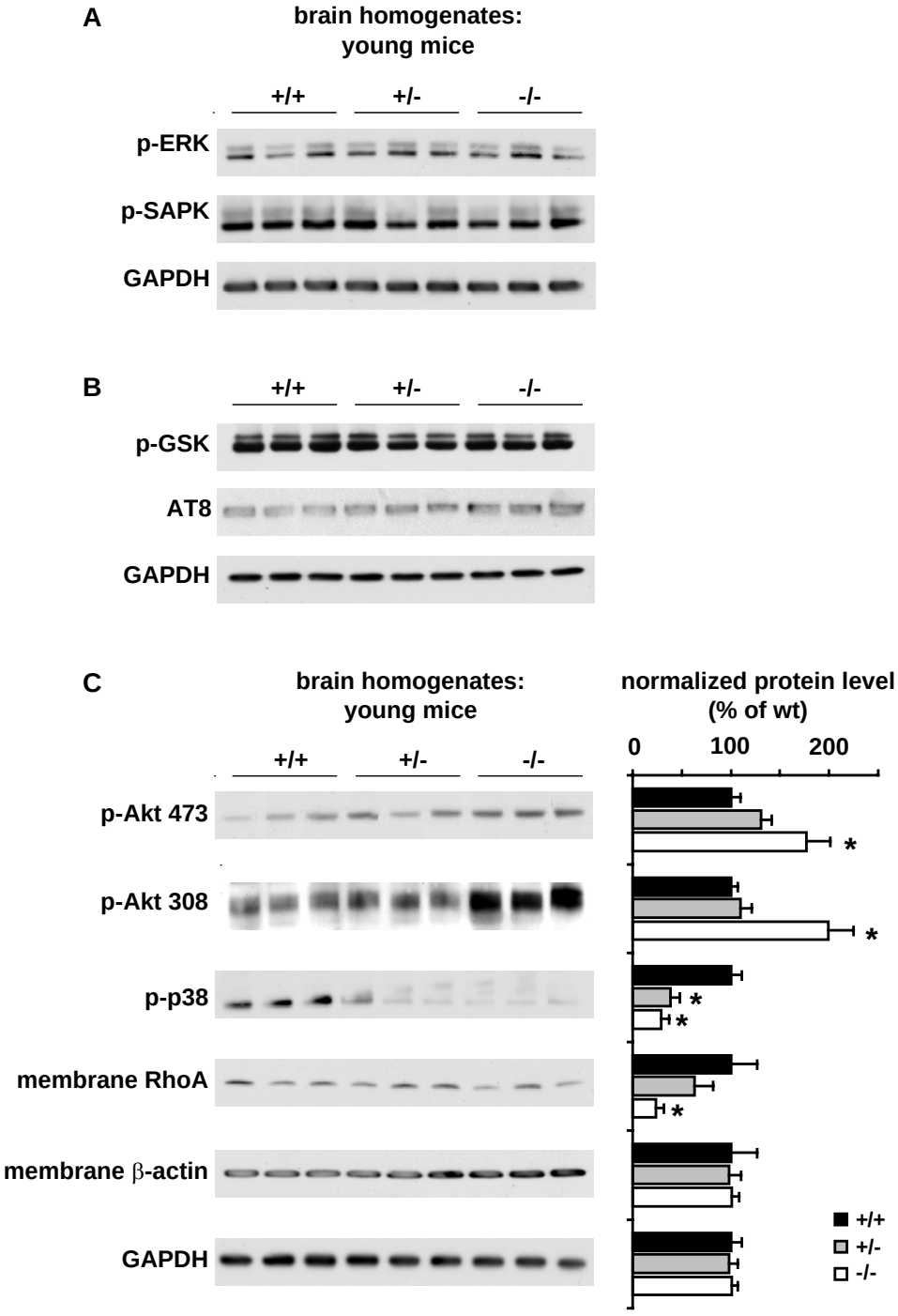

Figure 10 Protein phosphorylation and abundance in brains of DHCR24 depleted mice. Western blot analyses of signaling cascades involving ERK and SAPK (A) and GSK and TAU (B) did not reveal any difference in phosphorylation of these proteins between the three genotypes. (C) The phosphorylation of both phospho-sites of PKB/Akt (Ser473 and Thr308) was significantly increased in DHCR24$^{-/-}$ brains, whereas no difference was detected between DHCR24$^{+/-}$ and wt brains. p38 phosphorylation was significantly reduced in DHCR24$^{+/-}$ and knock-out mice and the levels of membrane associated RhoA were markedly diminished in knock-out brains (*$p<0.021$).

Moreover, we determined phosphorylation and protein concentration of a variety of proteins known to be involved in signaling cascades affected by cholesterol depletion such as Glycogen Synthase Kinase 3β (GSK) and Tau (Yu et al., 2005), Protein Kinase B (Akt/PKB) (Porstmann et al., 2005), and membrane associated Rho GTPase A (Pedrini et al., 2005). Phosphorylation of Erk and SAPK was similar in all three genotypes (Figure 10A) and additionally, phosphorylated GSK and S202 phosphorylated Tau did not reveal any differences between the genotypes (Figure 10B). However, PKB/Akt phosphorylation at both activation sites (Ser473 and Thr308) was significantly increased in DHCR24$^{-/-}$ brains (176±21%, p=0.041 and 199±25%, p=0.019, respectively, Figure 10C). In contrast, p38 phosphorylation was markedly reduced in brains of DHCR24$^{+/-}$ and DHCR24$^{-/-}$ mice (39±9.1%, p=0.012 and 29.5±8.2%, p=0.012, respectively, Figure 10C) and membrane associated RhoA was also significantly decreased in DHCR24$^{-/-}$ brains (28.1±8.1%, p=0.021, Figure 10C). These findings suggest that cholesterol paucity may influence certain cell signaling events while others remain unaffected.

3.3 MODELED DESMOSTEROL INCREASE IN SH-SY5Y CELLS

To determine whether the decrease in cholesterol and not the increase in desmosterol levels is responsible for the observed changes in DHCR24+/- mouse brains, we artificially increased the levels of desmosterol in SH-SY5Y neuroblastoma cells, while cellular cholesterol levels were not altered, and determined DRM formation, plasmin activity and APP β-cleavage in these cells. Methyl-β-cyclodextrin is a cyclic oligosaccharide, consisting of seven glucopyranose units, which was demonstrated to efficiently remove cholesterol from a variety of cells in culture. Hydrophobic guest molecules, such as cholesterol or other sterols can be incorporated into the cavity of cyclodextrin by displacing water. The resulting complex is water-soluble, although the guest molecule can be easily released. Methyl-β-cyclodextrin can also be used for the reverse purpose: coupling of the oligosaccharide with a guest molecule allows its addition to encountering cellular membranes. The capacity of membranes to incorporate additional sterols is limited and depends on the nature of the integrating molecule. We incubated desmosterol/methyl-β-cyclodextrin inclusion complexes for 1 hour (desmo) with SH-SY5Y cells. TLC analysis revealed that this treatment induced an average six-fold increase in the amount of desmosterol compared to untreated control (contr) cells (Figure 11A).

Ceramide levels, shown as a loading control, were not significantly changed between the two groups. To also model cholesterol deficiency in SH-SY5Y cells, we treated cells with the statin mevilonin and methyl-β-cyclodextrin to reduce about 30% of cellular cholesterol (mev/CD).

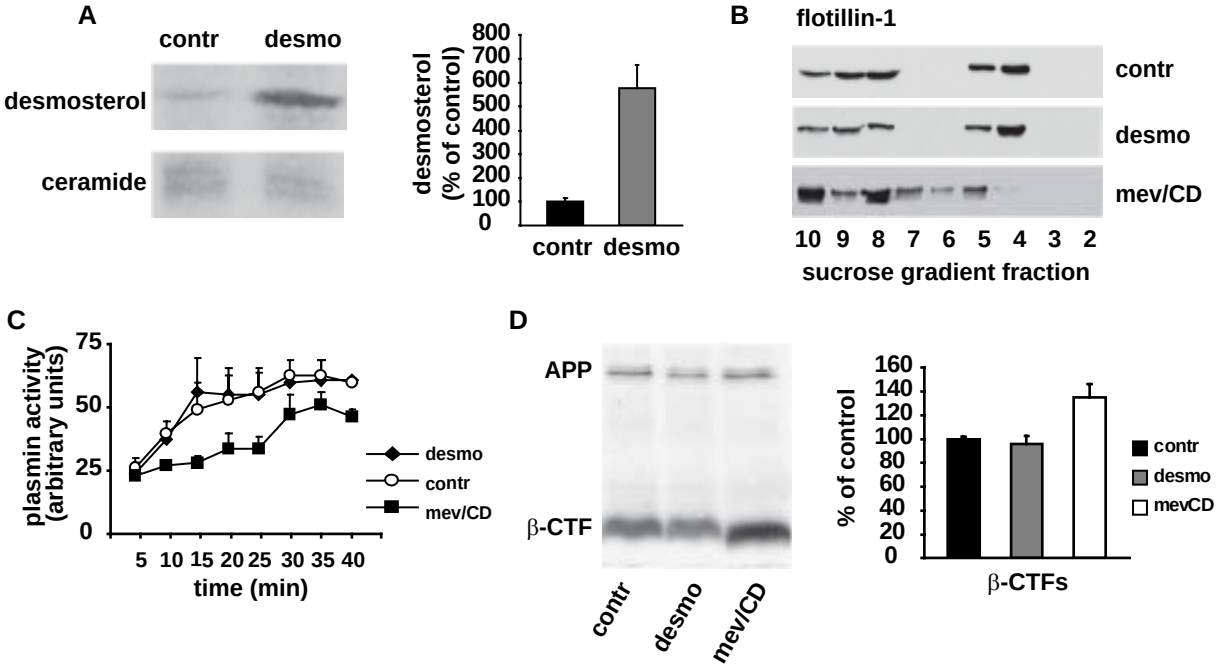

Figure 11 Methyl-β-cyclodextrin mediated desmosterol increase and cholesterol extraction from SH-SY5Y cells. SH-SY5Y cells were treated with desmosterol/Methyl-β-cyclodextrin compexes (desmo) or Methyl-β-cyclodextrin alone (mev/CD) and compared to untreated cells (control). (A) Increased desmosterol levels were verified by TLC. Ceramide levels, shown as a loading control, were not significantly changed. The graph on the right shows the mean values and standard error from the densitometric analysis of the TLCs from two independent experiments. Desmosterol content is given as the fold-increase in treated with respect to the corresponding level of the untreated cells. (B) Flotation profiles revealed that reduced cholesterol concentrations, but not increased desmosterol levels resulted in displacement of the DRM marker protein from the DRM fractions. (C) Activity assays showed that plasmin activity of cellular membranes is reduced with cholesterol reduction but not in cells with higher desmosterol levels. (D) Western blot analyses revealed an increase in β-CTF in cholesterol depleted cells, while desmosterol increase did not affect APP processing. The graph on the right shows the mean values and standard errors from the densitometric quantification of the Western blots from two independent experiments. Data were normalized to the amount of APP and are expressed as percentage of the values obtained in the untreated cells.

The flotation profile of the raft marker flotillin-1 revealed that reduced cholesterol level, but not increased desmosterol levels resulted in displacement of the raft marker protein from DRM fractions (Figure 11B). Plasmin activity expressed in arbitrary units measured in freshly prepared membranes of SH-SY5Y cells treated as described above revealed that cholesterol reduction, but not higher desmosterol levels in the DRMs, reduced the plasmin activity of cellular membranes (Figure 11C). Western blot analyses using the 6E10 antibody that specifically recognizes full length APP and its β-CTF revealed not significant changes

between desmosterol/methyl-β-cyclodextrin complex and control cells, whereas β-CTF levels were significantly increased in mevilonin/cyclodextrin treated cells (135±7%, p=0.021) that exhibited a moderate cholesterol reduction, a situation comparable to that in young DHCR24$^{+/-}$ mice (Figure 11D). These data clearly show that moderately reduced cholesterol resulted in increased β-cleavage of APP in SH-SY5Y cells, whereas an average six-fold increase in the amount of desmosterol does not affect DRM formation, plasmin activity and APP processing. Efforts to model the membrane sterol constitution of DHCR24$^{-/-}$ mice in SH-SY5Y cells were unsuccessful. The inhibition of cholesterol biosynthesis by statin treatment and the complete removal of cholesterol using methyl-β-cyclodextrin before replenishing membranes with desmosterol is a harsh method, apparently delimitating cell viability.

3.4 APP PROCESSING IN PRIMARY NEURONS OF DHCR24 DEPLETED MICE

To examine the effects of DHCR24 depletion on APP ectodomain shedding and Aβ generation *in vitro*, without perturbing cell viability with numerous treatments, we prepared primary cortical neurons of wt and DHCR24 depleted mice in serum- and cholesterol-free medium complemented with B27. Immunocytochemistry using the neuron specific antibody anti-Map2 revealed no obvious differences in morphological appearance between wt, DHCR24$^{+/-}$ and DHCR24$^{-/-}$ neurons (Figure 12A). Additionally, there were no differences in cell viability between the neuronal cultures as determined by the *in vitro* toxicology assays based on Lactate-Dehydrogenase (LDH) and on Tox-1 (MTT) (Figure 12B). Sterol analysis revealed that the total level of sterols was significantly reduced in primary neurons of DHCR24$^{-/-}$ mice (56±5.6%, p=0.021), whereas in neurons of DHCR24$^{+/-}$ mice the levels were unchanged compared to wt neurons after 5 days *in vitro* (Figure 12C). Because DHCR24$^{-/-}$ neurons are devoid of cholesterol, these data suggest that, like in young mouse brains, desmosterol accumulated as a consequence of DHCR24 deficiency in primary neurons. The finding that sterol levels were not altered in DHCR24$^{+/-}$ neurons might be due to a generally reduced cholesterol biosynthesis in primary neurons *in vitro* when compared to young animals. A reduced rate of synthesis would result in full cholesterol production, because the amount of DHCR24 in heterozygous mice is sufficient to completely convert accruing substrates. Analysis of the medium from neuronal cultures revealed that the level of sAPPα in supernatants of DHCR24$^{+/-}$ neurons was unchanged, but markedly increased in DHCR24$^{-/-}$ neurons compared to control cultures (143±12.5%, p=0.023, Figure 12D).

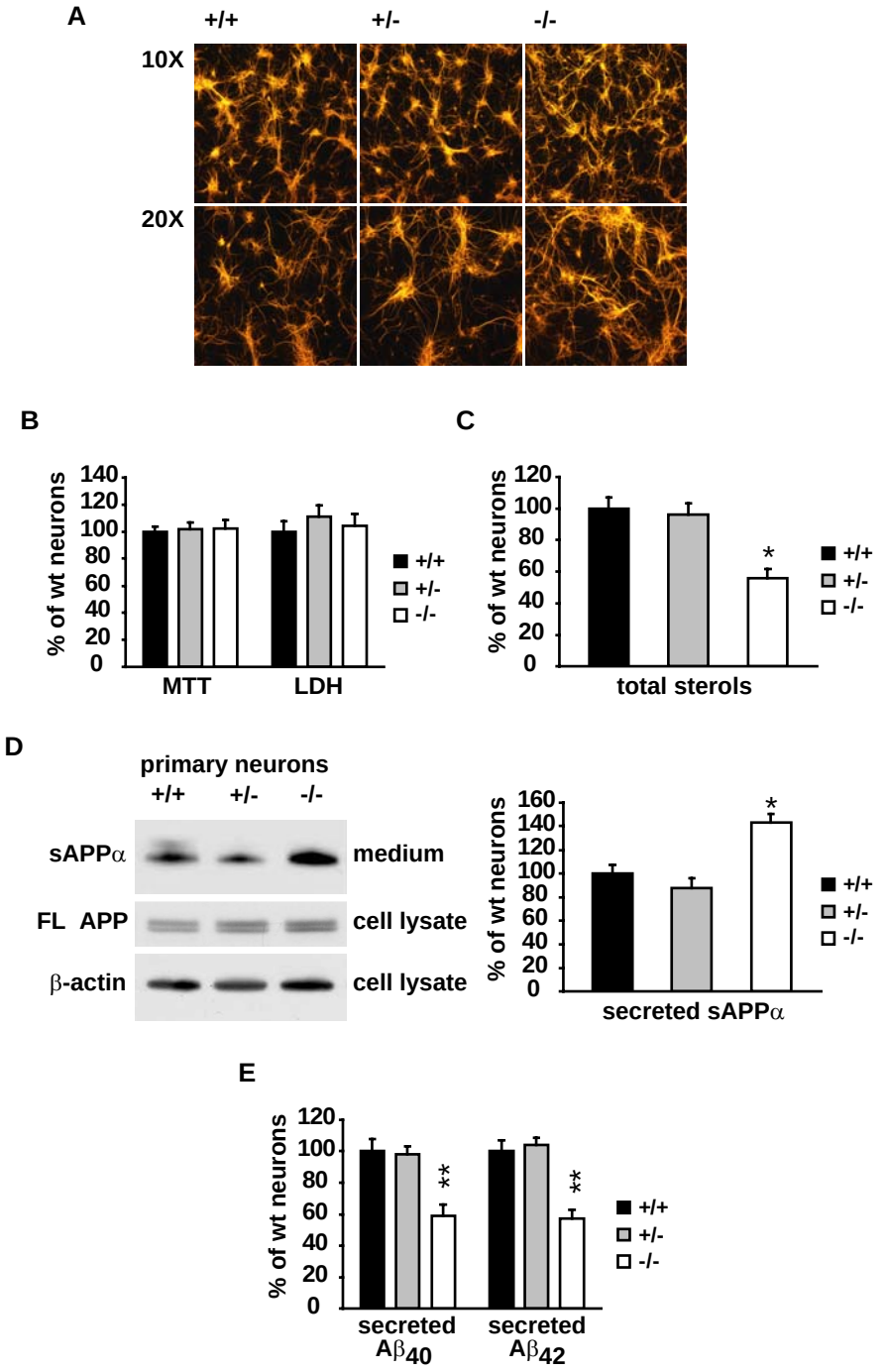

Figure 12 APP processing in primary neurons of DHCR24 depleted mice. Anti-Map2 staining (A) and cell viability assays (B) of primary neurons of each genotype did not reveal any significant differences between the cultures. (C) Sterol measurements show that DHCR24$^{-/-}$ neurons contained significantly less amounts of total sterols, whereas sterol levels in DHCR24$^{+/-}$ neurons were similar to that in wt neurons. (D) Secreted sAPPα levels were increased in the medium of DHCR24$^{-/-}$ neurons, while no significant changes were detected between DHCR24$^{+/-}$ and wt cultures. The graph on the right shows the mean values and standard error from the densitometric analysis of the Western blots from two independent experiments. (E) ELISA measurements of the medium revealed no difference in Aβ levels between DHCR24$^{+/-}$ and wt cultures, but a significant decrease of $A\beta_{40}$ and $A\beta_{42}$ in the medium of DHCR24$^{-/-}$ neurons. Data were normalized to the amount of proteins in the respective cultures and are expressed as percentage of the values obtained from wt cultures (*$p<0.03$, **$p<0.002$).

The level of full length APP in cell homogenates was similar in all three genotypes (Figure 12D). Measurements of $A\beta_{40}$ and $A\beta_{42}$ peptides in the medium of the neuronal cultures by murine Aβ ELISA revealed no differences between wt and DHCR24$^{+/-}$ neurons, while these peptides were significantly reduced in supernatants of DHCR24$^{-/-}$ neurons (58.7±21.1%, p=0.001 and 57.4±15.9%, p=0.001, respectively, Figure 12E). These results show that extensive cholesterol deficiency in DHCR24$^{-/-}$ neurons resulted in increased α-secretase type ectodomain shedding and decreased Aβ generation.

3.5 ADULT DHCR24 DEPLETED MICE

Taking the central role of cholesterol in development, in cell viability and various cell functions and in membrane organization, the question arises why cholesterol-free DHCR24$^{-/-}$ mice show such a mild phenotype. One possible explanation is the fact that maternal cholesterol is able to traverse the murine placenta and is therefore available during mouse embryogenesis. Although cholesterol accounts for over 99% of all sterols in wt brains, DHCR24$^{-/-}$ mice showed only a partial reduction of total sterol levels in the brain due to desmosterol accumulation. The nature of the accumulating sterol might be a second important factor determining the biophysical properties and functionality of membranes containing the substitutional sterol. On the one hand, our data clearly show that in brains of young DHCR24$^{-/-}$ mice, membrane organization and function is significantly disturbed, resulting in deficient DRM formation and altered membrane-related functions such as APP processing. On the other hand, cell viability and several signaling cascades are not affected in these mice, suggesting at least a partial replacement of cholesterol by desmosterol. The finding that desmosterol is greatly accumulating in young DHCR24$^{-/-}$ mice without getting efficiently catabolized rises the question, if desmosterol concentrations increase to even higher levels in adult knock-out brains and, if so, whether desmosterol is capable of efficiently substituting cholesterol in the adult brain. We therefore analyzed adult wt, DHCR24$^{+/-}$ and DHCR24$^{-/-}$ mice at the age of 16 weeks. This time point was chosen to ensure a good state of health of DHCR24$^{-/-}$ mice.

3.5.1 Sterol concentrations and gene expression analysis

Brain sterol concentrations were determined in adult wt, DHCR24$^{+/-}$ and DHCR24$^{-/-}$ mice by gas-chromatography/mass-spectrometry (Figure 13A and Table 4). Lanosterol levels were unchanged in DHCR24$^{+/-}$, but significantly reduced in DHCR24$^{-/-}$ mice (72.6±2.9%, p=0.021).

Table 4 Brain concentrations (ng/mg wet weight; mean ±SD) of cholesterol, desmosterol, lanosterol, lathosterol and 24*S*-OH-cholesterol of adult (16 week-old) wildtype, DHCR24$^{+/-}$ and DHCR24$^{-/-}$ mice

Genotype	Lanosterol	Desmosterol	Lathosterol	Cholesterol	24*S*-OH-Chol
wt	27±3	463±24	140±14	75,240±2,118	157±7
DHCR24$^{+/-}$	23±2	1,263±122*	96±9*	77,115±3,255	148±5
DHCR24$^{-/-}$	19±2*	96,751±10,956*	1±0.4*	3,065±319*	10±2*

*p<0.03 vs. aged-matched controls. Exact p-values are given in the text

Desmosterol accumulation in adult DHCR24$^{+/-}$ mice (463±23%, p=0.021) was comparable to that in young DHCR24$^{+/-}$ mice (see Figure 5A), while adult DHCR24$^{-/-}$ mice revealed an even greater build-up of desmosterol (21743±1182% of wt, p=0.021, Figure 13A). Quantitatively, the brain concentration of desmosterol in 16 week-old DHCR24$^{-/-}$ mice was comparable to the concentration of cholesterol in aged-matched wt mice (Figure 13B and Table 4). Lathosterol was significantly reduced in adult DHCR24$^{+/-}$ mice (68.6±3.6%, p=0.021), whereas the levels of cholesterol and its catabolite 24*S*-OH-cholesterol were unchanged between adult wt and heterozygous mice. These results suggest that the reduced levels of DHCR24 in heterozygous mice are necessarily capable of maintaining cholesterol homeostasis in adult DHCR24$^{+/-}$ mice, particularly since cholesterol biosynthesis is drastically reduced during postnatal development. This finding is in concert with data obtained from heterozygous desmosterolosis patients who show mildly increased levels of desmosterol in tissue and plasma but normal levels of cholesterol (Andersson et al., 2002). In adult DHCR24$^{-/-}$ brains lathosterol, cholesterol and 24*S*-OH-cholesterol were virtually absent (0.87±0.15%, 4.07±0.21% and 6.39±0.64%, p<0.03, respectively, Figure 13A), corroborating the hypothesis that no other enzyme of the two pathways is able to take over the function of DHCR24.

Expression analysis of cholesterol and fatty acid synthesis related genes revealed no significant differences between adult DHCR24$^{+/-}$ and wt brains (Figure 13C). Expression of *dhcr24* was significantly reduced in DHCR24$^{+/-}$ brains (48.3±6.4%, p=0.021, Figure 13C), suggesting that *dhcr24* expression is not influenced by chronic cholesterol paucity or desmosterol accumulation. Sterol analyses in adult DHCR24$^{-/-}$ brains revealed that the observed changes in *fas* expression in three week-old DHCR24$^{-/-}$ mouse brains were abolished in adult knock-out mice (Figure 13C), indicating that high concentrations of desmosterol might substitute the role of cholesterol in this feedback mechanism. Moreover, the detected

down-regulation of *hmgcr* in young DHCR24$^{-/-}$ brains was abolished in adult knock-out mice, which showed expression levels similar to those in wt mice (Figure 13C). Since lanosterol levels were also reduced in the adult knock-out mice, these data support the theory of a possible feedback mechanism from early Bloch-sterols or their derivatives on the transcriptional level of the rate-limiting enzyme HMGCR.

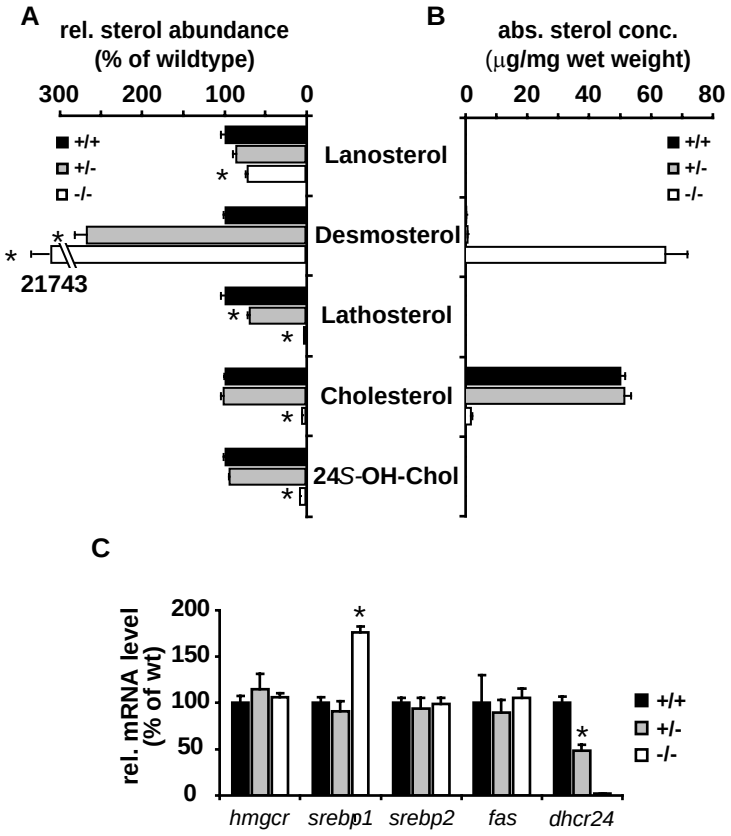

Figure 13 Brain sterol synthesis and elimination and gene expression analyses in adult DHCR24 depleted mice. (A) Lanosterol levels were unchanged in DHCR24$^{+/-}$ brains and a small but significant reduction was detected in DHCR24$^{-/-}$ brains. Desmosterol concentrations in adult DHCR24$^{+/-}$ mice were increased, while desmosterol tremendously accumulated in adult knock-out brains. Lathosterol levels were significantly reduced in DHCR24$^{+/-}$ brains and virtually absent in DHCR24$^{-/-}$ brains. Cholesterol concentrations and levels of 24*S*-OH-chol were not altered in DHCR24$^{+/-}$ brains but vastly diminished in knock-out brains. (B) In adult DHCR24$^{+/-}$ brains cholesterol levels were recovered when compared to aged-matched controls. Absolute desmosterol concentrations in 16 week-old DHCR24$^{-/-}$ brains were similar to those of cholesterol concentrations in wt mice. (C) Changes in gene expression detected in young DHCR24 depleted mice were annulled in adult mice, except a significant up-regulation of *srebp1* in DHCR24$^{-/-}$ brains, which was similar to that seen in young knock-out mice. DHCR24 expression was reduced in DHCR24$^{+/-}$ brains to the same extent as in young heterozygous mice and absent in adult DHCR24$^{-/-}$ brains. Data were normalized to the mean value of the two housekeeping genes *gapdh* and *β-actin*. Relative mRNA levels of the respective genes in wt brains were considered as 100% (*p<0.03).

In parallel to three week-old mice and in agreement with published results (Ohyama et al., 2006) the *srebp1* expression in adult DHCR24$^{-/-}$ brains was significantly higher than that in wt controls (176±6.5%, p=0.012, Figure 13C), suggesting that desmosterol accumulation did not

influence *srebp1* expression in the brain, as already indicated by the results of the *in vitro* treatment of SH-SY5Y with sterols (Figure 5D). Having demonstrated that membrane organization and DRM formation is disturbed in brains of young DHCR24$^{-/-}$ mice (Figure 6 and Figure 7), which show desmosterol levels accounting for approximately 50% of wt cholesterol levels, we next addressed the question if higher levels of desmosterol can functionally substitute cholesterol in brains of adult DHCR24$^{-/-}$ mice. Since heterozygous mice at the age of 16 weeks did not reveal any differences in brain cholesterol concentration compared to their wt littermates, we focused on adult knock-out and wt mice for further analyses.

3.5.2 Membrane organization: DRM protein distribution and sterol repartition

To evaluate if the observed increase in desmosterol concentration in adult DHCR24$^{-/-}$ mice has an effect on membrane organization we analyzed DRM formation and protein composition in adult DHCR24$^{-/-}$ brains. The total amount of protein in each fraction did not significantly differ between the two genotypes (Figure 14A). Analysis of the flotation profile of Prp^{c} revealed the presence of comparable percentages (13.8±4.2% and 15.8±3.7%, respectively, Figure 14B) of this raft marker in DRM fractions of adult DHCR24$^{-/-}$ and wt brains. Compared to young knock-out mice, adult DHCR24$^{-/-}$ mice exhibited a drastic increment of Prp^{c} in the DRM fractions, suggesting major differences in membrane organization of DHCR24$^{-/-}$ mice between the two age groups.

The non-raft protein APP remained in the soluble fractions of the gradients to the same extent in brains of both genotypes (Figure 14C). Analysis of the total sterol levels in soluble and DRM fractions of the gradients revealed no significant changes of sterol levels in heavy fractions 8-10 of adult DHCR24$^{-/-}$ brains (Figure 14D). In marked contrast to three week-old mice (Figure 7A), a substantial amount of sterols was detected in DRM fractions of adult DHCR24$^{-/-}$ brains (83.2±6.2% of wt, Figure 14D), suggesting that desmosterol associated with DRM fractions of adult DHCR24$^{-/-}$ brains. The amount of phospholipids was unchanged between the two genotypes (Figure 14E). Taken together, these results show that in membranes entirely lacking cholesterol, high concentrations of desmosterol allow DRM formation and protein recruitment of raft marker in these domains. Furthermore, these observations suggest that desmosterol in adult DHCR24$^{-/-}$ mice principally resides in the same flotation fractions of brain extracts as cholesterol in wt controls. However, it remains to be determined if high desmosterol concentrations can functionally replace cholesterol *in vivo*.

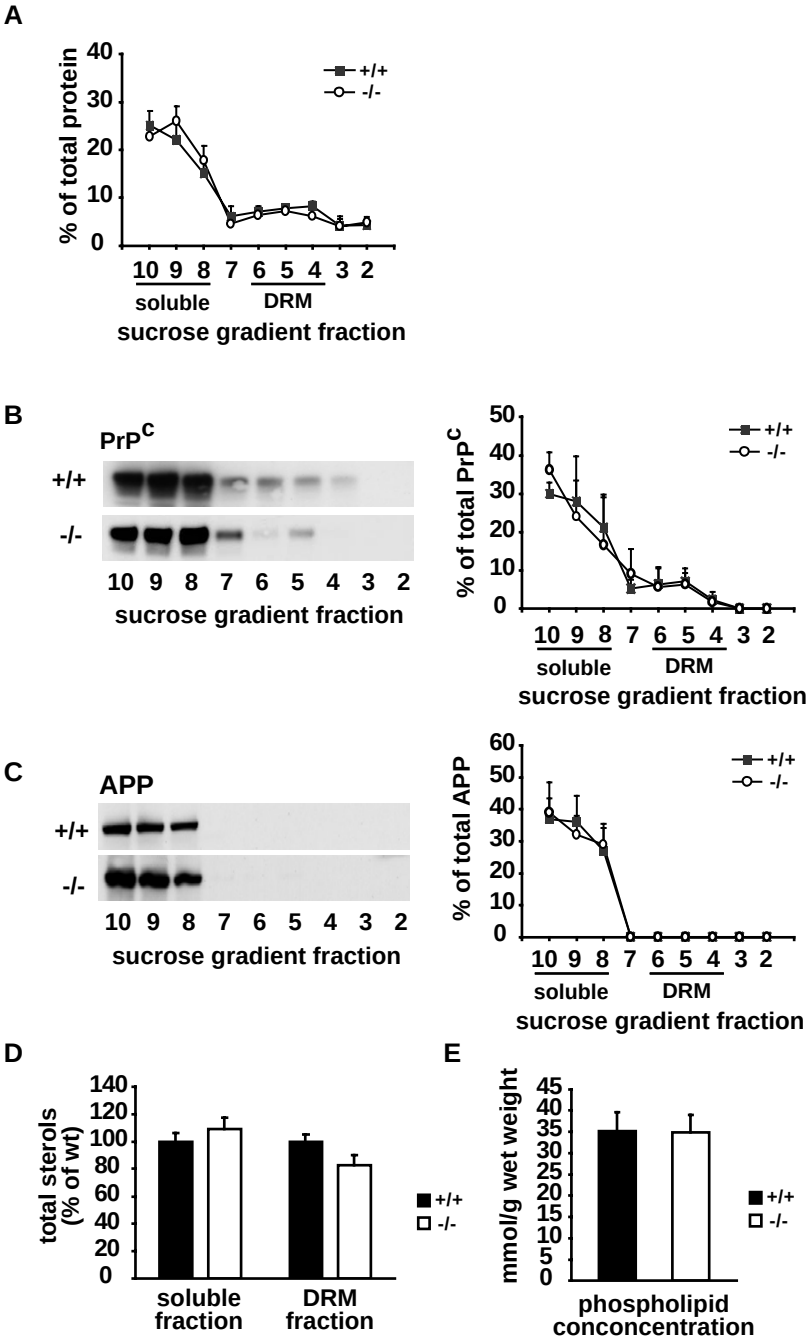

Figure 14 Effects of desmosterol substitution of cholesterol on membrane protein distribution and lipid composition in adult DHCR24$^{-/-}$ brains. (A) Percentages of total protein in DRM fractions 4-6 were unchanged between adult knock-out and wt mice. Western blot analyses of flotation profiles of the raft marker Prp^{c} (B) and the non-raft protein APP (C) revealed no significant differences in the distribution of the two proteins. Graphs on the right show the distribution of both proteins in each fraction as a percentage of the total amount of the respective proteins along the entire gradient. (D) Sterol analysis in soluble and DRM fractions of the gradient revealed a considerable amount of sterols present in DRM fractions of DHCR24$^{-/-}$ mice. Therefore, no significant difference were detected between adult DHCR24$^{-/-}$ and wt mouse brains. While cholesterol is assumed to represent most sterols in wt fractions, desmosterol accounts for the majority of sterols in knock-out fractions (see Table 4). (E) Phospholipid concentrations in total brain extracts are similar in adult mice of both genotypes.

3.5.3 Functional replacement of cholesterol by desmosterol

Therefore, we determined if membrane-related functions such as APP processing and Aβ generation occur at normal levels in brains of these mice. Levels of cellular full-length APP were similar in both genotypes (Figure 15A). Additionally, analysis of APP processing products revealed no detectable changes in levels of α-CTF and β-CTF in adult DHCR24$^{-/-}$ mouse brains (Figure 15A and B) when compared to wt mice. To determine if Aβ generation is influenced by the presence of membrane desmosterol we performed murine Aβ ELISA. Measurements of total extracts containing soluble and membrane bound portions of Aβ peptides revealed no detectable changes in the concentration of $A\beta_{40}$ between adult DHCR24$^{-/-}$ and wt mice (Figure 15C), in contrast to reduced $A\beta_{40}$ levels detected in young DHCR24$^{-/-}$ mice (Figure 9G). In 16 week-old mice $A\beta_{42}$ peptides were also detectable in total extracts of both genotypes, which did not differ between adult knock-out and wt mice (Figure 15C). To evaluate whether the observed changes in proteolytic activity of involved secretases in young DHCR24$^{-/-}$ mice were abolished by desmosterol membrane repartition, we determined α-, β- and γ-secretase activity in brain homogenates of adult DHCR24$^{-/-}$ and wt mice (Figure 15D).

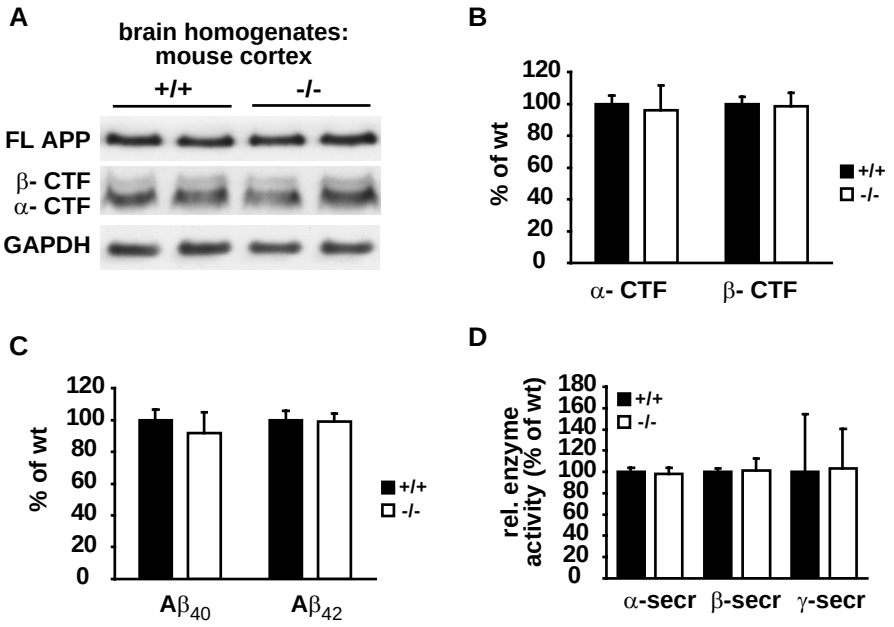

Figure 15 Functional replacement of cholesterol by desmosterol. (A) Representative Western blots show that cellular levels of full length (FL) APP and its cleavage products α- and β-CTF are unchanged between adult DHCR24$^{-/-}$ and wt mice. (B) The graph shows the mean values and standard error from the densitometric analysis of the Western blots. (C) $A\beta_{40}$ and $A\beta_{42}$ levels are similar in adult knock-out brains when compared to wt controls. (D) Full proteolytic activity of all three secretases involved in APP processing is ensured in brains of adult DHCR24$^{-/-}$ mice.

Brain activity levels of all three secretases were unchanged in adult DHCR24$^{-/-}$ compared to wt mice, suggesting that desmosterol influences membrane organization in a way that full β- and γ-secretase activity is maintained. Moreover, quantitative analyses of phosphorylated proteins involved in signal transduction revealed that the observed changes in Akt and p38 phosphorylation were abolished in adult DHCR24 depleted mice (Figure 16).

In addition, membrane association of RhoA in adult DHCR24$^{-/-}$ mice was not altered compared to aged-matched control mice. These data provide the evidence that desmosterol - insofar it is abundant enough - can substitution cholesterol in biological membranes leading to its functional replacement in APP metabolism *in vivo*. Furthermore, the steady state phosphorylation status of signaling peptides known to be modulated by altered cholesterol concentrations is maintained in adult DHCR24 depleted mice, confirming the functional replacement of cholesterol by desmosterol.

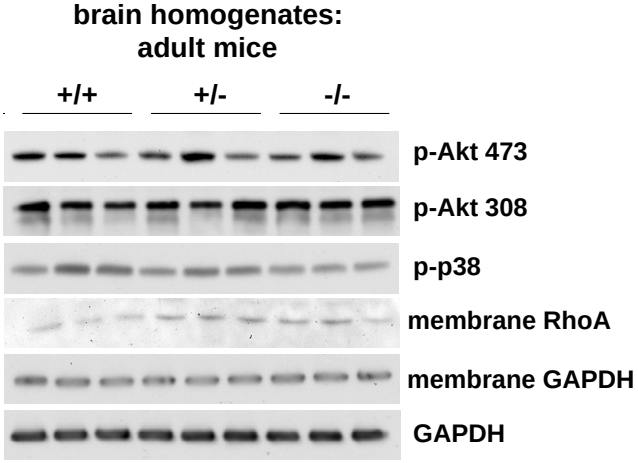

Figure 16 Protein phorsphorylation and abundance in brains of adult DHCR24 depleted mice. Western blot analyses revealed no differences in the phosphorylation of both phospho-sites of Akt (Ser473 and Thr308) and p38 phosphorylation between the three genotypes. In addition, no difference was detected in membrane associated RhoA between wt, DHCR24$^{+/-}$ and DHCR24$^{-/-}$ brains. GAPDH on total brains homogenates and membrane preparations was stained as loading control.

4. DISCUSSION

4.1 DHCR24 DEPLETED MICE

The results presented in this thesis show that brain cholesterol levels can be modulated by modifying the expression of the cholesterol-synthesizing enzyme, DHCR24. Our approach is different from previous work that relied on pharmacological inhibition of early steps of cholesterol synthesis or on using lipid extracting drugs that has led to controversial results (Ehehalt et al., 2003; Fassbender et al., 2001; Simons et al., 1998; Sparks et al., 1994). We show that the depletion of one *dhcr24* allele resulted in a moderate cholesterol reduction of about 25% in brains of DHCR24$^{+/-}$ mice, whereas complete *dhcr24* disruption led to total cholesterol deficiency in DHCR24$^{-/-}$ brains. As a consequence, membrane organization and DRM composition and function were significantly altered in a cholesterol-dependent manner, revealing major changes in membrane-related functions such as plasmin activation, APP processing and Aβ generation.

Considering that cholesterol is an essential component of vertebrate cell membranes and exhibits essential biological roles, it is striking that DHCR24 knock-out mice survive beyond birth. The question arises which mechanism/s enable the DHCR24$^{-/-}$ mice to reach embryonic maturation and postnatal development. With mice, in contrast to humans, cholesterol passes the placenta. Therefore, one reasonable answer is that circulating cholesterol, contributed from the heterozygous mother, suffices for early development. In this scenario, soon after birth DHCR24$^{-/-}$ mice are compromised due to the deficiency in synthesizing cholesterol and seriously depend on maternal care. Though cholesterol ingested with breast milk is kept from the brain through the BBB, it does supply the pup's periphery, and most likely contributes to a normal postnatal development. Since the DHCR24 knock-outs are smaller in size and probably also exhibit other abnormal symptoms recognized by the mother, such as differences in hormones or dermatological attributes (Mirza et al., 2006), some pups were killed by the mother within hours of birth. In addition, many knock-out pups died within days after birth as a consequence of weakness to assert themselves against their healthy littermates in terms of feeding. Moreover, the reduced frequency of born knock-out mice indicates some prenatal death, although knock-out mice in our colony were born to an even higher frequency (15-20%) as previously described (Wechsler et al., 2003). Neuronal preparation from embryos at E13-16 revealed a comparable frequency of knock-out embryos, indicating that prenatal death occurs earlier in embryonic development.

Embryonic development and the postnatal survival of the DHCR24 knock-out mice may also depend on the nature of the substituting sterol. This issue is discussed in detail in section 4.4. Once DHCR24$^{-/-}$ mice established themselves during the first weeks after birth, their surviving was warranted. Strikingly, neuropathological and biochemical analysis did not reveal any differences concerning morphology, viability or apoptotic and inflammatory events in brains of DHCR24$^{-/-}$ mice of different age-groups. We did not examine any peripheral parameters like serum components, hormone levels or bile acids and therefore we can not rule out potential differences, which possibly affect the general health status of knock-out mice.

In brains of young DHCR24 depleted mice, cholesterol was reduced due to a gene dose-dependent effect in DHCR24$^{+/-}$ brains, whereas in DHCR24-/- brains cholesterol was virtually absent. It was shown that cholesterol biosynthesis is high in the brain of newborn mammals but is reduced during postnatal development (Ohyama et al., 2006). This change in biosynthetic activity possibly explains why adult DHCR24$^{+/-}$ mice did not show any differences in cholesterol concentrations, as observed in young heterozygous mice. Since no up-regulation of *dhcr24* expression was detected in adult DHCR24$^{+/-}$ mice, we conclude that *dhcr24* expression is not directly regulated by cholesterol levels. Another mechanism that could contribute to the gain-back of cholesterol in adult heterozygous mice is a reduced catabolism of cholesterol by diminished conversion to 24*S*-OH-cholesterol. Early sterols of the Bloch-pathway such as lanosterol accumulated in young DHCR24$^{-/-}$ brains, while this accumulation was not observed in adult knock-out mice. In contrast, lanosterol levels in adult DHCR24$^{-/-}$ brains were significantly reduced, implying a generally decreased activity of cholesterol biosynthesis in these mice, possibly mediated by tremendously increasing desmosterol levels. Since desmosterol is the last sterol of the Bloch-pathway and is solely converted by DHCR24, it gradually accumulated in spite of reduced biosynthetic activity. Given that desmosterol concentrations in adult DHCR24$^{-/-}$ mice are even overtopping cholesterol concentration in aged-matched wt controls, we have to assume that other possible feedback mechanism are set off, maybe similar to those caused by high cholesterol levels. One indication for this hypothesis is the normalized regulation of *fas* expression in adult knock-out mice compared to controls, while in young knock-out mice a clear up-regulation was detected, when compared to wt controls. Analyses of sterol distribution and expression of cholesterol and fatty acid biosynthesis related genes also suggest possible other feedback mechanisms: The accumulation of lanosterol in young DHCR24$^{-/-}$ mouse brains seems to influence transcription of *hmgcr*, the rate-limiting enzyme in cholesterol biosynthesis.

Previous studies showed that oxylanosterol, an oxygenated derivative of lanosterol, is involved in regulation of HMGCR-activity and cholesterol biosynthesis (Panini et al., 1992; Panini et al., 1986). Moreover, lanosterol was shown to play a major role in post-transcriptional regulation of HMGCR, by stimulating its degradation (Song et al., 2005). The finding that *hmgcr* expression is not altered in adult DHCR24$^{-/-}$ mice, which do not accumulate lanosterol and treatment of SH-SY5Y cells with lanosterol further revealed evidence for the hypothesis of a possible feedback mechanism of lanosterol on *hmgcr* expression. However, treatment of SH-SY5Y cells with high levels of desmosterol did not influence gene-expression, suggesting that the observed changes in gene expression in knock-out mouse brains were most probably due to the paucity of cholesterol, rather than to the accumulation of desmosterol.

4.2 MODERATE CHOLESTEROL REDUCTION IN DHCR24$^{+/-}$ MICE

In a recent study, a moderate reduction of cholesterol through methyl-β-cyclodextrin mediated extraction from primary neurons resulted in disorganized DRMs, leading to increased amyloidogenic processing and elevated Aβ generation in these cells (Abad-Rodriguez et al., 2004). It was hypothesized that the disruption of rafts through cholesterol depletion might lessen the sequestration of γ-secretase and BACE into rafts and result in a higher proportion of these secretases in the APP containing fractions of the membrane, therefore cleaving APP more frequently (Kaether and Haass, 2004). In our DHCR24$^{+/-}$ mice that bring out a good model for *in vivo* cholesterol reduction of about 30%, we could reproduce the findings from Abad-Rodriguez and colleagues, corroborating the belief that DRMs play a major role in the segregation process of APP from BACE, suggesting that proper DRM organization are essential to maintain the steady-state levels of Aβ.

The finding that low expression of DHCR24 paralleled a reduction in brain membrane cholesterol offers a new perspective on the role that DHCR24 in might play in AD pathology. Because DHCR24 was shown to be down-regulated in vulnerable areas of brains in AD patients (Greeve et al., 2000) it is reasonable to think that lower levels of DHCR24, promoted by yet to be identified causes, are responsible for the membrane cholesterol reduction and disorganization of DRMs found in such brains (Ledesma et al., 2003a). This would consequently lead to Aβ accumulation via a combination of inefficient Aβ degradation, possibly due to low plasmin activity, and increased APP amyloidogenic cleavage. Iivonen et al., in contrast, could not find an association between reduced DHCR24 transcription levels in

AD brains and Aβ content (Iivonen et al., 2002). The fact that cholesterol levels were not measured in this study together with the low number of samples analyzed precludes drawing a definitive conclusion. Indeed, cholesterol loss has been observed in a significant number but not in all AD brains (Ledesma et al., 2003a). Altogether these data suggest that compensatory mechanisms to the effects of DHCR24 deficiency on cholesterol levels might exist that would differ among AD patients. Moreover, alternative mechanisms (i.e. mutations in APP or presenilins) might be responsible for Aβ accumulation in certain AD cases. Further research, including large scale studies, is required to clarify these matters.

4.3 CHRONIC CHOLESTEROL DEFICIENCY IN YOUNG DHCR24$^{-/-}$ MICE

Our *in vivo* approach analyzing the brains of DHCR24$^{-/-}$ mice substantiates previous findings, that depletion of cholesterol by a degree greater than 30% resulted in elevated levels of sAPPα, reduced β-cleavage and diminished Aβ generation (Ehehalt et al., 2003; Kojro et al., 2001; Parvathy et al., 2004; Refolo et al., 2001; Simons et al., 1998). However, in these studies, cholesterol lowering drugs or cholesterol extracting agents were used to reduce cellular and membrane cholesterol levels. We could show that chronic cholesterol deficiency in young DHCR24$^{-/-}$ brains leads to decreased amyloidogenic processing, resulting in reduced Aβ production. In addition to the deficient formation of DRMs in brains of young DHCR24$^{-/-}$ mice the proteolytic activity of BACE and the γ-secretase complex were significantly reduced, suggesting that the membrane composition in brains of these mice was suboptimal to maintain full enzymatic activity of the two secretases. This is in concert with several previous findings that disrupting cholesterol transport can alter presenilin distribution within the cell and affect APP processing (Burns et al., 2003; Runz et al., 2002), and depletion of membrane cholesterol resulted in complete inhibition of γ-secretase cleavage of APP (Wahrle et al., 2002). Moreover, it was shown that alterations in β-secretase activity might be responsible for the dependence of Aβ production on cholesterol levels. Cross linking experiments of APP and BACE in raft domains (Ehehalt et al., 2003) and targeting BACE exclusively to rafts (Cordy et al., 2003) remarkably affect Aβ production in a cholesterol-dependent manner. Furthermore, BACE activity in large unilamellar vesicles was shown to be directly influenced by membrane cholesterol concentrations (Kalvodova et al., 2005).

Primary neurons of DHCR24$^{-/-}$ mice revealed decreased levels of total sterols after 5 days in culture, and the effects of this reduction on APP processing were similar to those detected in

young DHCR24$^{-/-}$ mice. Unfortunately, we were not able to reproducibly culture these neurons for the time period needed to increase desmosterol concentrations to considerably higher levels. However, in single experiments analyzed neurons cultured for 2 and for 8 days, revealed gradually increasing sterol levels (data not shown), indicating that desmosterol concentrations rise over time, just as it was observed in knock-out mice. Viability and endurance of primary neurons sensitively depend on general conditions like medium-supplements, temperature, age of embryos for preparation, coating conditions of plates, etc. Therefore, we consider it possible to generally culture primary neurons of DHCR24$^{-/-}$ mice and wt controls for a longer period *in vitro* and suggest this for future experiments. Granted that desmosterol levels in aged primary neurons of DHCR24$^{-/-}$ mice reach such high levels as cholesterol in wt neurons or even higher, one could nicely show the correlation between cholesterol paucity, desmosterol increase and Aβ production. Furthermore, this cellular model would serve as an excellent system to analyze other effects of desmosterol on membrane organization and function, such as signaling, endocytic activity and also biophysical properties such as curvature and lipid packing.

In a first screen of protein phosphorylation in brains of DHCR24 depleted mice, we determined an altered phosphorylation status of PKB/Akt and the stress kinase p38, and differences in the proportion of membrane bound RhoA in brains of young knock-out mice. Surprisingly, phosphorylation and protein abundance of other MAPK and of many other proteins were not altered in young DHCR24 depleted mice, suggesting cholesterol independent mechanisms.

Porstmann *et al*. could recently show that PKB/Akt activation is necessary to induce transcription of enzymes involved in cholesterol and fatty acid biosynthesis via activation of SREBP (Porstmann et al., 2005). Since we found respective genes differentially expressed in young DHCR24$^{-/-}$ mice, we analyzed PKB/Akt phosphorylation to determine possible regulatory mechanisms, and determined a hyperphosphorylation of Akt at both phospho-epitopes in young DHCR24$^{-/-}$ brains. Moreover, these findings are in concert with data observed from aged primary neurons. Aging of wt neurons in culture led to a reduction of cholesterol concentration in these cells and this decrease was accompanied by a hyperphosphorylation of PKB/Akt due changes in DRM protein composition (Prof. Carlos Dotti, personal communication). PKB/Akt activation triggers a surviving cascade, possibly responsible for the long endurance of aging neurons *in vitro* and there are several explanations how cholesterol-dependent alterations in DRM composition could influence PKB/Akt

phosphorylation. In its inactive state, Akt is located in the cytosol; however, when the phosphoinositide phosphate, phosphoinoside 3,4,5-trisphosphate, is activated by phosphoinositide 3-kinase (PI3K) it recruits Akt and 3-phosphoinositide-dependent protein kinase 1 (PDK1) to the lipid bilayer. There, Akt is activated via phosphorylation on two residues, Thr308 and Ser473 (Alessi et al., 1996). Recruitment of proteins into lipid rafts and their phosphorylation/activation within rafts has previously been described for many different proteins, including PKB/Akt (Remacle-Bonnet et al., 2005) and the insulin receptor (Ikonen and Vainio, 2005; Vainio et al., 2005). One other possible mechanism is the subcellular dislocation of components in or out of lipid rafts that are responsible for Akt-activation such as the Trk receptor (Rajagopal et al., 2004).

The finding that the stress kinase p38 is hypophosphorylated in brains of DHCR24 depleted mice is in line with previous findings that cholesterol is the major component of native lipoproteins activating the p38 mitogen-activated protein kinases (Dobreva et al., 2005).

However, some changes determined in DHCR24$^{-/-}$ brains might not directly be associated with DRM composition. The finding that the membrane bound portions of RhoA were reduced in young DHCR24$^{-/-}$ mouse brains may be possible effects of the determined down-regulation of *hmgcr* in brains of these mice. One popular hypothesis for statin action is related to the drugs' inhibition of the isoprenoid pathway by inhibiting HMGCR, thereby modulating the activities of the Rho family of small GTPases - RhoA, B, and C - that need isoprenoid compounds for membrane coupling and activity. Rho proteins exert many of their effects via Rho-associated protein kinase (ROCKs) and a dominant negative form of ROCK was shown to increase sAPPα shedding, suggesting that altered APP processing induced by statin treatment is a consequence of changes in the Rho-ROCK protein phosphorylation pathway. The detected decrease in membrane associated RhoA therefore possibly contributes to the observed changes in APP processing and Aβ generation in DHCR24$^{-/-}$ mice.

4.4 REPLACEMENT OF CHOLESTEROL BY DESMOSTEROL IN ADULT DHCR24$^{-/-}$ MICE

In contrast to many relatives of cholesterol, desmosterol is an abundant structural membrane component in mammalian cells, such as spermatozoa and astrocytes (Lin et al., 1993; Mutka et al., 2004). Reduced ability to convert desmosterol to cholesterol leads to the human disorder desmosterolosis (as described in paragraph 1.2.5). This rare malformation syndrome is characterized by severe developmental defects and cognitive impairment (Andersson et al.,

2002; FitzPatrick et al., 1998; Herman, 2003; Waterham et al., 2001). Instead, DHCR24 knock-out mice that accumulate high amounts of desmosterol over time, exhibit an unexpectedly mild phenotype, being small and infertile but viable (see paragraph 1.2.6). This raises the question in how far desmosterol can be a substitute for cholesterol concerning membrane organization, DRM formation and membrane-related functions.

Taking the central role of cholesterol in membrane composition and function, a variety of other sterols were analyzed towards their biophysical behavior in model membranes. Some of them were found to be "membrane-active sterols", defined as sterols that decrease the membrane permeability, increase the order in the lipid acyl chains near the terminal methyl group, and enable the growth of sterol auxotroph microorganisms (Barenholz, 2002; Stottrup and Keller, 2006). For example, lathosterol, a distant precursor of cholesterol also lacking the C24 double bond, was shown to associate with rafts of cellular membranes at least as efficiently as cholesterol (Lusa et al., 2003; Wang et al., 2004). The effect of desmosterol on membrane lipid order, phase separation and lipid packing was found to be similar to that of cholesterol in model membranes, while significantly lower ordering effects of lanosterol were observed, a more distant precursor of cholesterol in the Bloch-pathway (Huster et al., 2005).

Our analyses of adult DHCR24$^{-/-}$ mice suggest that desmosterol is capable in substituting cholesterol in biological membranes leading to its functional replacement in APP metabolism *in vivo*. We could show that the observed changes in membrane composition and DRM structure in brains of young DHCR24$^{-/-}$ mice, affecting secretase activity, β-cleavage of APP and Aβ generation, were annulled in adult knock-out mice. Therefore, we conclude that age-related desmosterol accumulation and integration in membranes of adult DHCR24$^{-/-}$ mice is responsible for a normal distribution of membrane constituents, DRM formation and sustained APP metabolism.

However, in model membranes desmosterol was shown to promote the formation and stability of ordered domains somewhat less efficiently than cholesterol (Vainio et al., 2006). Moreover, Vainio *et al*. found that in mammalian cell membranes desmosterol associated less avidly with DRMs than cholesterol. Their model is different from ours in that they use CHO cells containing high amounts of endogenous desmosterol concentrations, but normal levels of cholesterol, therefore they can not rule out that the presence of cholesterol affects desmosterol-DRM association. Despite this difference, our results are consistent with their findings that desmosterol is capable to associate with DRMs, although maybe not as fervently as cholesterol. Moreover, Vainio *et al*. also showed that exchanging of ~70% of cholesterol by desmosterol in mammalian cell membranes impaired raft-dependent signaling via the insulin

receptor, whereas protein secretion, a process highly dependent on membrane composition and properties (Gondre-Lewis et al., 2006), was not affected by cholesterol substitution with desmosterol. These findings suggest that cholesterol replacement in DRMs may influence certain raft-dependent functions while others remain unaffected. Thus, we found no significant differences in APP processing, Aβ generation and proteolytic activity of secretases between adult DHCR24$^{-/-}$ and aged-matched wt mice, confirming the functional activity of desmosterol containing membranes in adult DHCR24$^{-/-}$ brains. Convincingly, the observed changes in protein phosphorylation of PKB/Akt and p38 and the membrane association of RhoA in young DHCR24$^{-/-}$ mice were annulled in adult knock-out mice, suggesting that either cholesterol deficit in early postnatal development has other effects than it has in an adult organism, or that desmosterol is indeed capable of efficiently taking over cholesterols' function concerning these pathways.

Cell membranes need to contain sterols that condense lipids, form lipid domains as rafts (Simons and Ikonen, 1997), and provide the basis for a proper organization and function of membranes. From the point of view of biophysics, it was stated that cholesterol and desmosterol are identical sterols (Huster et al., 2005), and our study provides detailed evidence of the effective functional substitution of cholesterol by desmosterol. However, in living organisms desmosterol does probably not serve for all functions of cholesterol. For example, cholesterol is an essential component of crucial metabolic pathways, e.g above all, essentially involved in the synthesis of steroid hormones. The most prominent effect of the absenteeism of cholesterol regarding these functions is infertility of the DHCR24$^{-/-}$ mice.

4.5 CONCLUSION AND OUTLOOK

The aim of this study was the analyses of DRM associated membrane organization in DHCR24 depleted mice and to evaluate the possible effects on a membrane-related, functional level. DHCR24 depletion resulted in reduced brain cholesterol concentrations, affecting DRM formation, composition and function in a cholesterol-dependent manner. Surprisingly, the entire replacement of cholesterol by desmosterol revealed an efficient functional substitution of cholesterol by its direct precursor.

The two mouse models used in this study, the DHCR24$^{+/-}$ and DHCR24$^{-/-}$ mice were shown to be suitable models for cholesterol depletion *in vivo*, avoiding the disturbing method of pharmacological cholesterol extraction. However, interference in cholesterol biosynthesis on the level of cholesterol synthesizing enzymes always involves changes in the level of sterol

intermediates. Like DHCR7 deficiency in SLOS leads to reduced cholesterol levels paralleled by increased levels of 7-dehydrocholesterol, altered DHCR24 activity results in desmosterol accumulation. Therefore, one has to take into account that cholesterol reduction in DHCR24 depleted mice is not necessarily the sole underlying basis for possible resulting effects. The observed alterations could also be the consequence of a combination of basal circumstances. We tried to evaluate the effects of as many other implicated factors as possible, to rule out that alterations other than cholesterol reduction might be jointly responsible for the observed findings in DHCR24 depleted mouse brains.

One other possibly affected mechanism that could contribute to altered APP processing and Aβ generation in DHCR24$^{-/-}$ brains is the mechanism of endo- and exocytosis. It is generally agreed that non-amyloidogenic processing mainly occurs at the cell surface where α-secretases are present, whereas amyloidogenic processing involves transit through the endocytic organelles where APP encounters β- and γ-secretase (Vetrivel and Thinakaran, 2006). Previous work has reported that inhibition of endocytosis leads to increased α-secretase type ectodomain shedding and thus to decreased β-cleavage and reduced release of Aβ (Carey et al., 2005; Ehehalt et al., 2003). Since depletion of cholesterol is also known to decrease the rate of endocytosis (Rodal et al., 1999), this is likely to contribute to the observed changes in APP processing after cholesterol extraction.

Endocytosis of various plasma membrane molecules occurs in the absence of functional clathrin-coated pits. Most of these molecules are found in lipid rafts, which suggests that at least some clathrin-independent endocytosis may be raft specific or raft mediated (Lamaze et al., 2001). This process seems to be cholesterol sensitive and dependent on dynamin, a high-molecular weight GTPase, which forms oligomeric rings around the neck of the forming vesicle, and aids in the internalisation by severing it from the plasma membrane (Mousavi et al., 2004). In ongoing experiments we already started to analyze whether DHCR24 and consequent cholesterol depletion affect endocytic activity in brains and primary neurons of DHCR24$^{-/-}$ mice. In addition, we want to evaluate the influence of total cholesterol deficiency on intracellular trafficking of APP and thus on APP ectodomain shedding.

First experiments determining endocytic activity of primary neurons and the membrane distribution of dynamin suggest that endocytic activity and APP internalization is decreased in DHCR24 knock-out neurons. However, further experiments are necessary to confirm these date and work out the involved mechanism. In a next set of experiments we want to determine, which specific endocytic pathway is affected by DHCH24 deficiency. Therefore,

one could infect primary neurons of DHCR24 knock-out and wildtype mice with a variant of the SV40, infecting murine cells. SV40 enters the cell specifically via raft-mediated endocytosis. Control experiments like Transferrin uptake, which is known to be clathrin mediated will reveal possible differences between the two genotypes regarding endocytic activity of these primary neurons. Furthermore, one could follow APP internalization *in vitro* using living cell microscopy.

One very surprising result was the finding that melin staining applying histological techniques did not reveal any obvious difference between wt and DHCR24 knock-out mice. Since up to 70% of the brain cholesterol was estimated to be associated with myelin and myelin consists to more that 70% of lipids when related to its dry weight, the question arises how the structure of myelin is maintained in cholesterol-free knock-out brains. GC/MS analysis and determination of myelin protein composition would be an interesting first investigation and examining the structure of myelin from DHCR24$^{-/-}$ brains by electronmicroscopic means would be a challenging topic to focus on in future experiments.

Data presented in this document have partially been published in The EMBO Journal, January 2006 (see attachment at the end of the document). Two other manuscripts were submitted in July and October 2006.

5. MATERIAL

5.1 PRODUCTS

Product	Provider
10-20% Tricine Gels	Invitrogen
Acetone	Merck
Agarose	Invitrogen
B27	Invitrogen
BSA	Sigma
Chemicals	Merck or Sigma
Chloroform	Sigma
Complete Protease Inhibitor	Roche
DEPC	Sigma
DMEM / F12	Invitrogen
DMSO	Sigma
DNA ladder 100 bp, 2 log	Invitrogen
dNTP mix 10mM	Sigma
DTT	Sigma
ECL	Amersham
Ethanol	Merck
Ethidiumbromide	Sigma
FCS	Invitrogen
Glycerol	Sigma
HPLC grade H_2O	Aldrich
Isopropanol	Sigma
L-Glutamine	Invitrogen
MES	Sigma
Methanol	Merck
methyl-β-cyclodextrin	Sigma
Mevilonin	Sigma
Neurobasal medium	Invitrogen
Nitrocellulose membrane 0.45µm	BioRad
Oligonucleotides	Microsynth / Sigma
Paraformaldehyd	Sigma
PCR Buffer II 10x	Applied Biosystems
RNase away	Catalys
SDS	Sigma
Sterols	Sigma
Triton X-100	Sigma
Trizol	Invitrogen
Tween-20	Sigma
Xomat LS Films	Kodak
β-mercaptoethanol	Sigma

5.2 BUFFERS

Buffer	Components
DEPC water	500 µl Diethylpyrocarbonate, ddH_2O ad 1000 ml
DNA loading dye	0.25 g Bromophenol blue, 0.25 g Xylene cyanol FF, 30 g Glycerol, ddH_2O ad 10 ml
EDTA 0.5 M, pH 8.4	186.1 g $Na_2EDTA \times 2H_2O$, ddH_2O ad 1000 ml
Laemmli Buffer 4x	2.5 ml Tris-HCl 1 M pH 6.8, 4 ml Glycerol, 5 ml SDS 10%, 50 µl Bromophenol blue 1%, 1 ml β-mercaptoethanol, ddH_2O ad 10 ml
PBS 10x	90 g NaCl, 2 g KCl, 18 g $Na_2HPO_4 \times 2H_2O$, 2.4 g K_2HPO_4, ddH_2O ad 1000 ml
TBS 10x	24.2 g Tris base, 86.7 g NaCl, ddH_2O ad 1000 ml
TBST 1x	500 µl Tween-20, TBS 1x ad 1000 ml
Tricine running buffer 10x	121 g Tris base, 179 g Tricine, 10 g SDS, ddH_2O ad 1000 ml
Tris Glycine transfer buffer	2.9 g Glycine, 5.8 g Tris, 0.37 g SDS, 200 ml Methanol, ddH_2O ad 1000 ml

5.3 INSTRUMENTS

Instrument	Provider
7900 **ABI** PRISM® Sequence Detection System	Applied Biosystems
Bio Photometer	Eppendorf
Centrifuge: 5417C, 5417R, 5804R	Eppendorf
GeneAmp PCR System 9700	PE Applied Biosystems
Kodak X-OMAT 2000 Processor	Kodak
Memmert waterbath	Fisher
MP 220 pH meter	Mettler Toledo
Nicon Eclipse TE300	Nikon
Nikon Eclipse E800	Nikon
NUAIRE Autoflow CO_2 Incubator	Inotech
SKAN VSE-2000-120 sterile hood	Skan
Sorvall RC 26 Plus	Kendro
Spectra Max Fluorescence Reader	Bucher
Thermomixer	Eppendorf

5.4 KITS

Kit	Provider
Amplex Red	Molecular Probes/Invitrogen
DC Protein Assay	BioRad
DNeasy Kit	QIAGEN
ECL Advance Kit	Amersham Biosciences
Full Velocity SYBR Green QPCR Master Mix	Stratagene
RNase-Free DNase Kit	QIAGEN
RNeasy Kit	QIAGEN
Secretase assays	R&D Systems
SuperSignal West femto	Pierce
Transcriptor First Strand cDNA Synthesis Kit	Roche Diagnostics

ABBREVATIONS

-/-	knock-out
+/-	heterozygous
+/+	Wildtype
aaa	Gene encoding protein Aaa
AAA/Aaa	Protein A
ABCA1	ATP-Binding Cassette Transporter A1
ACAT	Acyl-coenzyme A: cholesterol acyltransferase
AD	Alzheimer's disease
AICD	APP intracellular domain
ApoE	Apolipoprotein E
APP	Amyloid precursor protein
ATP	Adenosine triphosphate
Aβ	Amyloid β-peptide
BACE	β-site APP cleaving enzyme
BSA	Bovine Serum Albumin
cDNA	Complementary deoxyribonucleic acid
CE	Cholesteryl ester
CNS	Central nervous system
CSF	Cerebrospinal fluid
CTF	C-terminal fragment
ddH_2O	Double distilled water
DEPC	Diethyl pyrocarbonate
DHCR24	3β-hydroxysterol-Δ24 reductase
DNA	Deoxyribonucleic acid
dNTP	Deoxynucleotide
DRM	Detergent resistant membrane domain
DTT	Dithiothreitol
ECL	Enhanced chemiluminescence
EDTA	Ethylendiamintetraacetic acid
ELISA	Enzyme-linked immunosorbent assay
EOFAD	Early onset familial Alzheimer's disease
ER	Endoplasmatic reticulum
FAD	Familial form of Alzheimer's disease
FAS	Fatty acid synthase
FCS	Fetal calf serum
GAPDH	Glyceraldehydes-3-phosphate dehydrogenase
GPI	Glycosyl-phosphatidylinositol
HDL	High density lipoprotein
HMGCR	Hydroxy-3-methylglutaryl coenzyme A reductase
HMGCS	Hydroxy-3-methylglutaryl coenzyme A synthase
HRP	Horse radish peroxidase
kDa	Kilo dalton
LDL	Low density lipoprotein
LOAD	Late onset Alzheimer's disease

mRNA	Messenger ribonucleic acid
NFT	Neurofibrillary tangles
P/S	Penicillin / Streptomycin
PBGD	porphobilinogen deaminase
PBS	Phosphate buffered saline
PCR	Polymerase chain reaction
PGK	Phosphoglycerate kinase
PS	Presenilin
QPCR	Quantitative PCR
RNA	Ribonucleic acid
RT	Room temperature or reverse transcription
sAPP	Secreted APP ectodomain
SD	Standard deviation
SDS	Sodium dodecyl sulfate
SDS-PAGE	Sodium dodecyl sulfate polyacrylamide gel electrophoreses
SEM	Standard error of the mean
SH-SY5Y	Human neuroblastoma cells
SLOS	Smith-Lemli-Opitz syndrome
SPM	Sphingomyelin
SREBP	Sterol-responsive element binding protein
TBS	Tris buffered saline
TBST	Tris buffered saline + Tween 20
wt	Wildtype

REFERENCES

Abad-Rodriguez, J., Ledesma, M.D., Craessaerts, K., Perga, S., Medina, M., Delacourte, A., Dingwall, C., De Strooper, B. and Dotti, C.G. (2004) Neuronal membrane cholesterol loss enhances amyloid peptide generation. *J Cell Biol*, **167**, 953-960.

Alessi, D.R., Andjelkovic, M., Caudwell, B., Cron, P., Morrice, N., Cohen, P. and Hemmings, B.A. (1996) Mechanism of activation of protein kinase B by insulin and IGF-1. *Embo J*, **15**, 6541-6551.

Andersson, H.C., Kratz, L. and Kelley, R. (2002) Desmosterolosis presenting with multiple congenital anomalies and profound developmental delay. *Am J Med Genet*, **113**, 315-319.

Arriagada, P.V., Growdon, J.H., Hedley-Whyte, E.T. and Hyman, B.T. (1992a) Neurofibrillary tangles but not senile plaques parallel duration and severity of Alzheimer's disease. *Neurology*, **42**, 631-639.

Arriagada, P.V., Marzloff, K. and Hyman, B.T. (1992b) Distribution of Alzheimer-type pathologic changes in nondemented elderly individuals matches the pattern in Alzheimer's disease. *Neurology*, **42**, 1681-1688.

Bales, K.R., Verina, T., Dodel, R.C., Du, Y., Altstiel, L., Bender, M., Hyslop, P., Johnstone, E.M., Little, S.P., Cummins, D.J., Piccardo, P., Ghetti, B. and Paul, S.M. (1997) Lack of apolipoprotein E dramatically reduces amyloid beta-peptide deposition. *Nat Genet*, **17**, 263-264.

Ballard-Croft, C., Locklar, A.C., Kristo, G. and Lasley, R.D. (2006) Regional Myocardial Ischemia Induced Activation of MAPKs is Associated With Subcellular Redistribution of Caveolin and Cholesterol. *Am J Physiol Heart Circ Physiol*.

Barenholz, Y. (2002) Cholesterol and other membrane active sterols: from membrane evolution to "rafts". *Prog Lipid Res*, **41**, 1-5.

Bartus, R.T., Dean, R.L., 3rd, Beer, B. and Lippa, A.S. (1982) The cholinergic hypothesis of geriatric memory dysfunction. *Science*, **217**, 408-414.

Beffert, U., Aumont, N., Dea, D., Lussier-Cacan, S., Davignon, J. and Poirier, J. (1998) Beta-amyloid peptides increase the binding and internalization of apolipoprotein E to hippocampal neurons. *J Neurochem*, **70**, 1458-1466.

Begley, J.G., Duan, W., Chan, S., Duff, K. and Mattson, M.P. (1999) Altered calcium homeostasis and mitochondrial dysfunction in cortical synaptic compartments of presenilin-1 mutant mice. *J Neurochem*, **72**, 1030-1039.

Beher, D. and Graham, S.L. (2005) Protease inhibitors as potential disease-modifying therapeutics for Alzheimer's disease. *Expert Opin Investig Drugs*, **14**, 1385-1409.

Beher, D. and Shearman, M.S. (2002) Gamma-secretase inhibition. *Biochem Soc Trans*, **30**, 534-537.

Bjorkhem, I., Lutjohann, D., Diczfalusy, U., Stahle, L., Ahlborg, G. and Wahren, J. (1998) Cholesterol homeostasis in human brain: turnover of 24S-hydroxycholesterol and evidence for a cerebral origin of most of this oxysterol in the circulation. *J Lipid Res*, **39**, 1594-1600.

Bligh, E.G. and Dyer, W.J. (1959) A rapid method of total lipid extraction and purification. *Can J Biochem Physiol*, **37**, 911-917.

Bloch, K.E. (1979) Speculations on the evolution of sterol structure and function. *CRC Crit Rev Biochem*, **7**, 1-5.

Bloch, K.E. (1983) Sterol structure and membrane function. *CRC Crit Rev Biochem*, **14**, 47-92.

Boyles, J.K., Notterpek, L.M. and Anderson, L.J. (1990) Accumulation of apolipoproteins in the regenerating and remyelinating mammalian peripheral nerve. Identification of

apolipoprotein D, apolipoprotein A-IV, apolipoprotein E, and apolipoprotein A-I. *J Biol Chem*, **265**, 17805-17815.

Braak, H. and Braak, E. (1995) Staging of Alzheimer's disease-related neurofibrillary changes. *Neurobiol Aging*, **16**, 271-278; discussion 278-284.

Brown, D.A. and Rose, J.K. (1992) Sorting of GPI-anchored proteins to glycolipid-enriched membrane subdomains during transport to the apical cell surface. *Cell*, **68**, 533-544.

Brunetti-Pierri, N., Corso, G., Rossi, M., Ferrari, P., Balli, F., Rivasi, F., Annunziata, I., Ballabio, A., Russo, A.D., Andria, G. and Parenti, G. (2002) Lathosterolosis, a novel multiple-malformation/mental retardation syndrome due to deficiency of 3beta-hydroxysteroid-delta5-desaturase. *Am J Hum Genet*, **71**, 952-958.

Burns, M. and Duff, K. (2002) Cholesterol in Alzheimer's disease and tauopathy. *Ann N Y Acad Sci*, **977**, 367-375.

Burns, M., Gaynor, K., Olm, V., Mercken, M., LaFrancois, J., Wang, L., Mathews, P.M., Noble, W., Matsuoka, Y. and Duff, K. (2003) Presenilin redistribution associated with aberrant cholesterol transport enhances beta-amyloid production in vivo. *J Neurosci*, **23**, 5645-5649.

Buxbaum, J.D., Liu, K.N., Luo, Y., Slack, J.L., Stocking, K.L., Peschon, J.J., Johnson, R.S., Castner, B.J., Cerretti, D.P. and Black, R.A. (1998) Evidence that tumor necrosis factor alpha converting enzyme is involved in regulated alpha-secretase cleavage of the Alzheimer amyloid protein precursor. *J Biol Chem*, **273**, 27765-27767.

Carey, R.M., Balcz, B.A., Lopez-Coviella, I. and Slack, B.E. (2005) Inhibition of dynamin-dependent endocytosis increases shedding of the amyloid precursor protein ectodomain and reduces generation of amyloid beta protein. *BMC Cell Biol*, **6**, 30.

Carson, J.A. and Turner, A.J. (2002) Beta-amyloid catabolism: roles for neprilysin (NEP) and other metallopeptidases? *J Neurochem*, **81**, 1-8.

Coleman, M.L. and Olson, M.F. (2002) Rho GTPase signalling pathways in the morphological changes associated with apoptosis. *Cell Death Differ*, **9**, 493-504.

Collen, D. (1999) The plasminogen (fibrinolytic) system. *Thromb Haemost*, **82**, 259-270.

Cooper, M.K., Wassif, C.A., Krakowiak, P.A., Taipale, J., Gong, R., Kelley, R.I., Porter, F.D. and Beachy, P.A. (2003) A defective response to Hedgehog signaling in disorders of cholesterol biosynthesis. *Nat Genet*, **33**, 508-513.

Corder, E.H., Saunders, A.M., Strittmatter, W.J., Schmechel, D.E., Gaskell, P.C., Small, G.W., Roses, A.D., Haines, J.L. and Pericak-Vance, M.A. (1993) Gene dose of apolipoprotein E type 4 allele and the risk of Alzheimer's disease in late onset families. *Science*, **261**, 921-923.

Cordy, J.M., Hussain, I., Dingwall, C., Hooper, N.M. and Turner, A.J. (2003) Exclusively targeting beta-secretase to lipid rafts by GPI-anchor addition up-regulates beta-site processing of the amyloid precursor protein. *Proc Natl Acad Sci U S A*, **100**, 11735-11740.

Crameri, A., Biondi, E., Kuehnle, K., Lutjohann, D., Thelen, K.M., Perga, S., Dotti, C.G., Nitsch, R.M., Ledesma, M.D. and Mohajeri, M.H. (2006) The role of seladin-1/DHCR24 in cholesterol biosynthesis, APP processing and Abeta generation in vivo. *Embo J*, **25**, 432-443.

Daigle, I. and Li, C. (1993) apl-1, a Caenorhabditis elegans gene encoding a protein related to the human beta-amyloid protein precursor. *Proc Natl Acad Sci U S A*, **90**, 12045-12049.

Davis-Salinas, J. and Van Nostrand, W.E. (1995) Amyloid beta-protein aggregation nullifies its pathologic properties in cultured cerebrovascular smooth muscle cells. *J Biol Chem*, **270**, 20887-20890.

De Strooper, B. (2003) Aph-1, Pen-2, and Nicastrin with Presenilin generate an active gamma-Secretase complex. *Neuron*, **38**, 9-12.

De Strooper, B. and Annaert, W. (2000) Proteolytic processing and cell biological functions of the amyloid precursor protein. *J Cell Sci*, **113 (Pt 11)**, 1857-1870.

DeMattos, R.B., Bales, K.R., Cummins, D.J., Dodart, J.C., Paul, S.M. and Holtzman, D.M. (2001) Peripheral anti-A beta antibody alters CNS and plasma A beta clearance and decreases brain A beta burden in a mouse model of Alzheimer's disease. *Proc Natl Acad Sci U S A*, **98**, 8850-8855.

Dobreva, I., Zschornig, O., Waeber, G., James, R.W. and Widmann, C. (2005) Cholesterol is the major component of native lipoproteins activating the p38 mitogen-activated protein kinases. *Biol Chem*, **386**, 909-918.

Dominguez, D.I., De Strooper, B. and Annaert, W. (2001) Secretases as therapeutic targets for the treatment of Alzheimer's disease. *Amyloid*, **8**, 124-142.

Edwards, P.A. and Ericsson, J. (1998) Signaling molecules derived from the cholesterol biosynthetic pathway: mechanisms of action and possible roles in human disease. *Curr Opin Lipidol*, **9**, 433-440.

Ehehalt, R., Keller, P., Haass, C., Thiele, C. and Simons, K. (2003) Amyloidogenic processing of the Alzheimer beta-amyloid precursor protein depends on lipid rafts. *J Cell Biol*, **160**, 113-123.

Esler, W.P. and Wolfe, M.S. (2001) A portrait of Alzheimer secretases--new features and familiar faces. *Science*, **293**, 1449-1454.

Etminan, M., Gill, S. and Samii, A. (2003) Effect of non-steroidal anti-inflammatory drugs on risk of Alzheimer's disease: systematic review and meta-analysis of observational studies. *Bmj*, **327**, 128.

Eto, M., Watanabe, K., Chonan, N. and Ishii, K. (1988) Familial hypercholesterolemia and apolipoprotein E4. *Atherosclerosis*, **72**, 123-128.

Farmer, J.A. (2000) Pleiotropic effects of statins. *Curr Atheroscler Rep*, **2**, 208-217.

Fassbender, K., Simons, M., Bergmann, C., Stroick, M., Lutjohann, D., Keller, P., Runz, H., Kuhl, S., Bertsch, T., von Bergmann, K., Hennerici, M., Beyreuther, K. and Hartmann, T. (2001) Simvastatin strongly reduces levels of Alzheimer's disease beta -amyloid peptides Abeta 42 and Abeta 40 in vitro and in vivo. *Proc Natl Acad Sci U S A*, **98**, 5856-5861.

Ferrer, I., Boada Rovira, M., Sanchez Guerra, M.L., Rey, M.J. and Costa-Jussa, F. (2004) Neuropathology and pathogenesis of encephalitis following amyloid-beta immunization in Alzheimer's disease. *Brain Pathol*, **14**, 11-20.

Fitzky, B.U., Moebius, F.F., Asaoka, H., Waage-Baudet, H., Xu, L., Xu, G., Maeda, N., Kluckman, K., Hiller, S., Yu, H., Batta, A.K., Shefer, S., Chen, T., Salen, G., Sulik, K., Simoni, R.D., Ness, G.C., Glossmann, H., Patel, S.B. and Tint, G.S. (2001) 7-Dehydrocholesterol-dependent proteolysis of HMG-CoA reductase suppresses sterol biosynthesis in a mouse model of Smith-Lemli-Opitz/RSH syndrome. *J Clin Invest*, **108**, 905-915.

FitzPatrick, D.R., Keeling, J.W., Evans, M.J., Kan, A.E., Bell, J.E., Porteous, M.E., Mills, K., Winter, R.M. and Clayton, P.T. (1998) Clinical phenotype of desmosterolosis. *Am J Med Genet*, **75**, 145-152.

Fox, N.C., Warrington, E.K., Freeborough, P.A., Hartikainen, P., Kennedy, A.M., Stevens, J.M. and Rossor, M.N. (1996) Presymptomatic hippocampal atrophy in Alzheimer's disease. A longitudinal MRI study. *Brain*, **119 (Pt 6)**, 2001-2007.

Fukumoto, H., Cheung, B.S., Hyman, B.T. and Irizarry, M.C. (2002) Beta-secretase protein and activity are increased in the neocortex in Alzheimer disease. *Arch Neurol*, **59**, 1381-1389.

Geula, C., Wu, C.K., Saroff, D., Lorenzo, A., Yuan, M. and Yankner, B.A. (1998) Aging renders the brain vulnerable to amyloid beta-protein neurotoxicity. *Nat Med*, **4**, 827-831.

Gilman, S., Koller, M., Black, R.S., Jenkins, L., Griffith, S.G., Fox, N.C., Eisner, L., Kirby, L., Rovira, M.B., Forette, F. and Orgogozo, J.M. (2005) Clinical effects of Abeta immunization (AN1792) in patients with AD in an interrupted trial. *Neurology*, **64**, 1553-1562.

Goate, A., Chartier-Harlin, M.C., Mullan, M., Brown, J., Crawford, F., Fidani, L., Giuffra, L., Haynes, A., Irving, N., James, L. and et al. (1991) Segregation of a missense mutation in the amyloid precursor protein gene with familial Alzheimer's disease. *Nature*, **349**, 704-706.

Gondre-Lewis, M.C., Petrache, H.I., Wassif, C.A., Harries, D., Parsegian, A., Porter, F.D. and Loh, Y.P. (2006) Abnormal sterols in cholesterol-deficiency diseases cause secretory granule malformation and decreased membrane curvature. *J Cell Sci*, **119**, 1876-1885.

Goodrum, J.F. (1991) Cholesterol from degenerating nerve myelin becomes associated with lipoproteins containing apolipoprotein E. *J Neurochem*, **56**, 2082-2086.

Greeve, I., Hermans-Borgmeyer, I., Brellinger, C., Kasper, D., Gomez-Isla, T., Behl, C., Levkau, B. and Nitsch, R.M. (2000) The human DIMINUTO/DWARF1 homolog seladin-1 confers resistance to Alzheimer's disease-associated neurodegeneration and oxidative stress. *J Neurosci*, **20**, 7345-7352.

Haass, C., Schlossmacher, M.G., Hung, A.Y., Vigo-Pelfrey, C., Mellon, A., Ostaszewski, B.L., Lieberburg, I., Koo, E.H., Schenk, D., Teplow, D.B. and et al. (1992) Amyloid beta-peptide is produced by cultured cells during normal metabolism. *Nature*, **359**, 322-325.

Hajjar, K.A. and Acharya, S.S. (2000) Annexin II and regulation of cell surface fibrinolysis. *Ann N Y Acad Sci*, **902**, 265-271.

Hammad, S.M., Ranganathan, S., Loukinova, E., Twal, W.O. and Argraves, W.S. (1997) Interaction of apolipoprotein J-amyloid beta-peptide complex with low density lipoprotein receptor-related protein-2/megalin. A mechanism to prevent pathological accumulation of amyloid beta-peptide. *J Biol Chem*, **272**, 18644-18649.

Harder, T., Scheiffele, P., Verkade, P. and Simons, K. (1998) Lipid domain structure of the plasma membrane revealed by patching of membrane components. *J Cell Biol*, **141**, 929-942.

Hardy, J.A. and Higgins, G.A. (1992) Alzheimer's disease: the amyloid cascade hypothesis. *Science*, **256**, 184-185.

Herman, G.E. (2003) Disorders of cholesterol biosynthesis: prototypic metabolic malformation syndromes. *Hum Mol Genet*, **12 Spec No 1**, R75-88.

Herz, J. and Farese, R.V., Jr. (1999) The LDL receptor gene family, apolipoprotein B and cholesterol in embryonic development. *J Nutr*, **129**, 473S-475S.

Hock, C., Konietzko, U., Papassotiropoulos, A., Wollmer, A., Streffer, J., von Rotz, R.C., Davey, G., Moritz, E. and Nitsch, R.M. (2002) Generation of antibodies specific for beta-amyloid by vaccination of patients with Alzheimer disease. *Nat Med*, **8**, 1270-1275.

Hock, C., Konietzko, U., Streffer, J.R., Tracy, J., Signorell, A., Muller-Tillmanns, B., Lemke, U., Henke, K., Moritz, E., Garcia, E., Wollmer, M.A., Umbricht, D., de Quervain, D.J., Hofmann, M., Maddalena, A., Papassotiropoulos, A. and Nitsch, R.M. (2003) Antibodies against beta-amyloid slow cognitive decline in Alzheimer's disease. *Neuron*, **38**, 547-554.

Hofman, A., Ott, A., Breteler, M.M., Bots, M.L., Slooter, A.J., van Harskamp, F., van Duijn, C.N., Van Broeckhoven, C. and Grobbee, D.E. (1997) Atherosclerosis, apolipoprotein

E, and prevalence of dementia and Alzheimer's disease in the Rotterdam Study. *Lancet*, **349**, 151-154.

Holtzman, D.M., Bales, K.R., Tenkova, T., Fagan, A.M., Parsadanian, M., Sartorius, L.J., Mackey, B., Olney, J., McKeel, D., Wozniak, D. and Paul, S.M. (2000) Apolipoprotein E isoform-dependent amyloid deposition and neuritic degeneration in a mouse model of Alzheimer's disease. *Proc Natl Acad Sci U S A*, **97**, 2892-2897.

Hsiao, K.K., Borchelt, D.R., Olson, K., Johannsdottir, R., Kitt, C., Yunis, W., Xu, S., Eckman, C., Younkin, S., Price, D. and et al. (1995) Age-related CNS disorder and early death in transgenic FVB/N mice overexpressing Alzheimer amyloid precursor proteins. *Neuron*, **15**, 1203-1218.

Huster, D., Scheidt, H.A., Arnold, K., Herrmann, A. and Muller, P. (2005) Desmosterol may replace cholesterol in lipid membranes. *Biophys J*, **88**, 1838-1844.

Igbavboa, U., Avdulov, N.A., Chochina, S.V. and Wood, W.G. (1997) Transbilayer distribution of cholesterol is modified in brain synaptic plasma membranes of knockout mice deficient in the low-density lipoprotein receptor, apolipoprotein E, or both proteins. *J Neurochem*, **69**, 1661-1667.

Igbavboa, U., Avdulov, N.A., Schroeder, F. and Wood, W.G. (1996) Increasing age alters transbilayer fluidity and cholesterol asymmetry in synaptic plasma membranes of mice. *J Neurochem*, **66**, 1717-1725.

Ignatius, M.J., Gebicke-Harter, P.J., Skene, J.H., Schilling, J.W., Weisgraber, K.H., Mahley, R.W. and Shooter, E.M. (1986) Expression of apolipoprotein E during nerve degeneration and regeneration. *Proc Natl Acad Sci U S A*, **83**, 1125-1129.

Iivonen, S., Hiltunen, M., Alafuzoff, I., Mannermaa, A., Kerokoski, P., Puolivali, J., Salminen, A., Helisalmi, S. and Soininen, H. (2002) Seladin-1 transcription is linked to neuronal degeneration in Alzheimer's disease. *Neuroscience*, **113**, 301-310.

Ikonen, E. and Vainio, S. (2005) Lipid microdomains and insulin resistance: is there a connection? *Sci STKE*, **2005**, pe3.

in t' Veld, B.A., Ruitenberg, A., Hofman, A., Launer, L.J., van Duijn, C.M., Stijnen, T., Breteler, M.M. and Stricker, B.H. (2001) Nonsteroidal antiinflammatory drugs and the risk of Alzheimer's disease. *N Engl J Med*, **345**, 1515-1521.

Iwata, N., Tsubuki, S., Takaki, Y., Watanabe, K., Sekiguchi, M., Hosoki, E., Kawashima-Morishima, M., Lee, H.J., Hama, E., Sekine-Aizawa, Y. and Saido, T.C. (2000) Identification of the major Abeta1-42-degrading catabolic pathway in brain parenchyma: suppression leads to biochemical and pathological deposition. *Nat Med*, **6**, 143-150.

Jick, H., Zornberg, G.L., Jick, S.S., Seshadri, S. and Drachman, D.A. (2000) Statins and the risk of dementia. *Lancet*, **356**, 1627-1631.

Jula, A., Marniemi, J., Huupponen, R., Virtanen, A., Rastas, M. and Ronnemaa, T. (2002) Effects of diet and simvastatin on serum lipids, insulin, and antioxidants in hypercholesterolemic men: a randomized controlled trial. *Jama*, **287**, 598-605.

Juottonen, K., Laakso, M.P., Insausti, R., Lehtovirta, M., Pitkanen, A., Partanen, K. and Soininen, H. (1998) Volumes of the entorhinal and perirhinal cortices in Alzheimer's disease. *Neurobiol Aging*, **19**, 15-22.

Kaether, C. and Haass, C. (2004) A lipid boundary separates APP and secretases and limits amyloid beta-peptide generation. *J Cell Biol*, **167**, 809-812.

Kalvodova, L., Kahya, N., Schwille, P., Ehehalt, R., Verkade, P., Drechsel, D. and Simons, K. (2005) Lipids as modulators of proteolytic activity of BACE: involvement of cholesterol, glycosphingolipids, and anionic phospholipids in vitro. *J Biol Chem*, **280**, 36815-36823.

Kang, D.E., Pietrzik, C.U., Baum, L., Chevallier, N., Merriam, D.E., Kounnas, M.Z., Wagner, S.L., Troncoso, J.C., Kawas, C.H., Katzman, R. and Koo, E.H. (2000) Modulation of amyloid beta-protein clearance and Alzheimer's disease susceptibility by the LDL receptor-related protein pathway. *J Clin Invest*, **106**, 1159-1166.

Katsuki, H., Izumi, Y. and Zorumski, C.F. (1997) Removal of extracellular calcium after conditioning stimulation disrupts long-term potentiation in the CA1 region of rat hippocampal slices. *Neuroscience*, **76**, 1113-1119.

Kimberly, W.T., Zheng, J.B., Guenette, S.Y. and Selkoe, D.J. (2001) The intracellular domain of the beta-amyloid precursor protein is stabilized by Fe65 and translocates to the nucleus in a notch-like manner. *J Biol Chem*, **276**, 40288-40292.

Kivipelto, M., Helkala, E.L., Laakso, M.P., Hanninen, T., Hallikainen, M., Alhainen, K., Soininen, H., Tuomilehto, J. and Nissinen, A. (2001) Midlife vascular risk factors and Alzheimer's disease in later life: longitudinal, population based study. *Bmj*, **322**, 1447-1451.

Klahre, U., Noguchi, T., Fujioka, S., Takatsuto, S., Yokota, T., Nomura, T., Yoshida, S. and Chua, N.H. (1998) The Arabidopsis DIMINUTO/DWARF1 gene encodes a protein involved in steroid synthesis. *Plant Cell*, **10**, 1677-1690.

Klein, U., Gimpl, G. and Fahrenholz, F. (1995) Alteration of the myometrial plasma membrane cholesterol content with beta-cyclodextrin modulates the binding affinity of the oxytocin receptor. *Biochemistry*, **34**, 13784-13793.

Koike, H., Tomioka, S., Sorimachi, H., Saido, T.C., Maruyama, K., Okuyama, A., Fujisawa-Sehara, A., Ohno, S., Suzuki, K. and Ishiura, S. (1999) Membrane-anchored metalloprotease MDC9 has an alpha-secretase activity responsible for processing the amyloid precursor protein. *Biochem J*, **343 Pt 2**, 371-375.

Kojro, E., Gimpl, G., Lammich, S., Marz, W. and Fahrenholz, F. (2001) Low cholesterol stimulates the nonamyloidogenic pathway by its effect on the alpha -secretase ADAM 10. *Proc Natl Acad Sci U S A*, **98**, 5815-5820.

Kuo, Y.M., Emmerling, M.R., Bisgaier, C.L., Essenburg, A.D., Lampert, H.C., Drumm, D. and Roher, A.E. (1998) Elevated low-density lipoprotein in Alzheimer's disease correlates with brain abeta 1-42 levels. *Biochem Biophys Res Commun*, **252**, 711-715.

Lamaze, C., Dujeancourt, A., Baba, T., Lo, C.G., Benmerah, A. and Dautry-Varsat, A. (2001) Interleukin 2 receptors and detergent-resistant membrane domains define a clathrin-independent endocytic pathway. *Mol Cell*, **7**, 661-671.

Lambert, M.P., Barlow, A.K., Chromy, B.A., Edwards, C., Freed, R., Liosatos, M., Morgan, T.E., Rozovsky, I., Trommer, B., Viola, K.L., Wals, P., Zhang, C., Finch, C.E., Krafft, G.A. and Klein, W.L. (1998) Diffusible, nonfibrillar ligands derived from Abeta1-42 are potent central nervous system neurotoxins. *Proc Natl Acad Sci U S A*, **95**, 6448-6453.

Lammich, S., Kojro, E., Postina, R., Gilbert, S., Pfeiffer, R., Jasionowski, M., Haass, C. and Fahrenholz, F. (1999) Constitutive and regulated alpha-secretase cleavage of Alzheimer's amyloid precursor protein by a disintegrin metalloprotease. *Proc Natl Acad Sci U S A*, **96**, 3922-3927.

Laude, A.J. and Prior, I.A. (2004) Plasma membrane microdomains: organization, function and trafficking. *Mol Membr Biol*, **21**, 193-205.

Ledesma, M.D., Abad-Rodriguez, J., Galvan, C., Biondi, E., Navarro, P., Delacourte, A., Dingwall, C. and Dotti, C.G. (2003a) Raft disorganization leads to reduced plasmin activity in Alzheimer's disease brains. *EMBO Rep*, **4**, 1190-1196.

Ledesma, M.D., Da Silva, J.S., Crassaerts, K., Delacourte, A., De Strooper, B. and Dotti, C.G. (2000) Brain plasmin enhances APP alpha-cleavage and Abeta degradation and is reduced in Alzheimer's disease brains. *EMBO Rep*, **1**, 530-535.

Ledesma, M.D., Da Silva, J.S., Schevchenko, A., Wilm, M. and Dotti, C.G. (2003) Proteomic characterisation of neuronal sphingolipid-cholesterol microdomains: role in plasminogen activation. *Brain Res*, **987**, 107-116.

Lee, J.Y. and Parks, J.S. (2005) ATP-binding cassette transporter AI and its role in HDL formation. *Curr Opin Lipidol*, **16**, 19-25.

Levy-Lahad, E., Wasco, W., Poorkaj, P., Romano, D.M., Oshima, J., Pettingell, W.H., Yu, C.E., Jondro, P.D., Schmidt, S.D., Wang, K. and et al. (1995) Candidate gene for the chromosome 1 familial Alzheimer's disease locus. *Science*, **269**, 973-977.

Lichtenberg, D., Goni, F.M. and Heerklotz, H. (2005) Detergent-resistant membranes should not be identified with membrane rafts. *Trends Biochem Sci*, **30**, 430-436.

Lin, D.S., Connor, W.E., Wolf, D.P., Neuringer, M. and Hachey, D.L. (1993) Unique lipids of primate spermatozoa: desmosterol and docosahexaenoic acid. *J Lipid Res*, **34**, 491-499.

Lusa, S., Heino, S. and Ikonen, E. (2003) Differential mobilization of newly synthesized cholesterol and biosynthetic sterol precursors from cells. *J Biol Chem*, **278**, 19844-19851.

Lutjohann, D., Breuer, O., Ahlborg, G., Nennesmo, I., Siden, A., Diczfalusy, U. and Bjorkhem, I. (1996) Cholesterol homeostasis in human brain: evidence for an age-dependent flux of 24S-hydroxycholesterol from the brain into the circulation. *Proc Natl Acad Sci U S A*, **93**, 9799-9804.

Lutjohann, D., Papassotiropoulos, A., Bjorkhem, I., Locatelli, S., Bagli, M., Oehring, R.D., Schlegel, U., Jessen, F., Rao, M.L., von Bergmann, K. and Heun, R. (2000) Plasma 24S-hydroxycholesterol (cerebrosterol) is increased in Alzheimer and vascular demented patients. *J Lipid Res*, **41**, 195-198.

Lutjohann, D., Stroick, M., Bertsch, T., Kuhl, S., Lindenthal, B., Thelen, K., Andersson, U., Bjorkhem, I., Bergmann Kv, K. and Fassbender, K. (2004) High doses of simvastatin, pravastatin, and cholesterol reduce brain cholesterol synthesis in guinea pigs. *Steroids*, **69**, 431-438.

Martin-Morris, L.E. and White, K. (1990) The Drosophila transcript encoded by the beta-amyloid protein precursor-like gene is restricted to the nervous system. *Development*, **110**, 185-195.

Masse, I., Bordet, R., Deplanque, D., Al Khedr, A., Richard, F., Libersa, C. and Pasquier, F. (2005) Lipid lowering agents are associated with a slower cognitive decline in Alzheimer's disease. *J Neurol Neurosurg Psychiatry*, **76**, 1624-1629.

Mattson, M.P., Barger, S.W., Furukawa, K., Bruce, A.J., Wyss-Coray, T., Mark, R.J. and Mucke, L. (1997) Cellular signaling roles of TGF beta, TNF alpha and beta APP in brain injury responses and Alzheimer's disease. *Brain Res Brain Res Rev*, **23**, 47-61.

Mattson, M.P., Pedersen, W.A., Duan, W., Culmsee, C. and Camandola, S. (1999) Cellular and molecular mechanisms underlying perturbed energy metabolism and neuronal degeneration in Alzheimer's and Parkinson's diseases. *Ann N Y Acad Sci*, **893**, 154-175.

McLean, C.A., Cherny, R.A., Fraser, F.W., Fuller, S.J., Smith, M.J., Beyreuther, K., Bush, A.I. and Masters, C.L. (1999) Soluble pool of Abeta amyloid as a determinant of severity of neurodegeneration in Alzheimer's disease. *Ann Neurol*, **46**, 860-866.

Mega, M.S., Cummings, J.L., Fiorello, T. and Gornbein, J. (1996) The spectrum of behavioral changes in Alzheimer's disease. *Neurology*, **46**, 130-135.

Michaelis, E.K. (1998) Molecular biology of glutamate receptors in the central nervous system and their role in excitotoxicity, oxidative stress and aging. *Prog Neurobiol*, **54**, 369-415.

Michikawa, M., Fan, Q.W., Isobe, I. and Yanagisawa, K. (2000) Apolipoprotein E exhibits isoform-specific promotion of lipid efflux from astrocytes and neurons in culture. *J Neurochem*, **74**, 1008-1016.

Miles, L.A., Dahlberg, C.M., Levin, E.G. and Plow, E.F. (1989) Gangliosides interact directly with plasminogen and urokinase and may mediate binding of these fibrinolytic components to cells. *Biochemistry*, **28**, 9337-9343.

Miles, L.A., Dahlberg, C.M., Plescia, J., Felez, J., Kato, K. and Plow, E.F. (1991) Role of cell-surface lysines in plasminogen binding to cells: identification of alpha-enolase as a candidate plasminogen receptor. *Biochemistry*, **30**, 1682-1691.

Mirza, R., Hayasaka, S., Takagishi, Y., Kambe, F., Ohmori, S., Maki, K., Yamamoto, M., Murakami, K., Kaji, T., Zadworny, D., Murata, Y. and Seo, H. (2006) DHCR24 gene knockout mice demonstrate lethal dermopathy with differentiation and maturation defects in the epidermis. *J Invest Dermatol*, **126**, 638-647.

Molinuevo, J.L., Garcia-Gil, V. and Villar, A. (2004) Memantine: an antiglutamatergic option for dementia. *Am J Alzheimers Dis Other Demen*, **19**, 10-18.

Morgan, D., Diamond, D.M., Gottschall, P.E., Ugen, K.E., Dickey, C., Hardy, J., Duff, K., Jantzen, P., DiCarlo, G., Wilcock, D., Connor, K., Hatcher, J., Hope, C., Gordon, M. and Arendash, G.W. (2000) A beta peptide vaccination prevents memory loss in an animal model of Alzheimer's disease. *Nature*, **408**, 982-985.

Mousavi, S.A., Malerod, L., Berg, T. and Kjeken, R. (2004) Clathrin-dependent endocytosis. *Biochem J*, **377**, 1-16.

Mutka, A.L., Lusa, S., Linder, M.D., Jokitalo, E., Kopra, O., Jauhiainen, M. and Ikonen, E. (2004) Secretion of sterols and the NPC2 protein from primary astrocytes. *J Biol Chem*, **279**, 48654-48662.

Nemecz, G., Fontaine, R.N. and Schroeder, F. (1988) A fluorescence and radiolabel study of sterol exchange between membranes. *Biochim Biophys Acta*, **943**, 511-521.

Nicoll, J.A., Wilkinson, D., Holmes, C., Steart, P., Markham, H. and Weller, R.O. (2003) Neuropathology of human Alzheimer disease after immunization with amyloid-beta peptide: a case report. *Nat Med*, **9**, 448-452.

Ogeng'o, J.A., Cohen, D.L., Sayi, J.G., Matuja, W.B., Chande, H.M., Kitinya, J.N., Kimani, J.K., Friedland, R.P., Mori, H. and Kalaria, R.N. (1996) Cerebral amyloid beta protein deposits and other Alzheimer lesions in non-demented elderly east Africans. *Brain Pathol*, **6**, 101-107.

Ohyama, Y., Meaney, S., Heverin, M., Ekstrom, L., Brafman, A., Shafir, M., Andersson, U., Olin, M., Eggertsen, G., Diczfalusy, U., Feinstein, E. and Bjorkhem, I. (2006) Studies on the transcriptional regulation of cholesterol 24-hydroxylase (CYP46A1): marked insensitivity toward different regulatory axes. *J Biol Chem*, **281**, 3810-3820.

Olson, M.F., Ashworth, A. and Hall, A. (1995) An essential role for Rho, Rac, and Cdc42 GTPases in cell cycle progression through G1. *Science*, **269**, 1270-1272.

Opitz, J.M. (1999) RSH (so-called Smith-Lemli-Opitz) syndrome. *Curr Opin Pediatr*, **11**, 353-362.

Orgogozo, J.M., Gilman, S., Dartigues, J.F., Laurent, B., Puel, M., Kirby, L.C., Jouanny, P., Dubois, B., Eisner, L., Flitman, S., Michel, B.F., Boada, M., Frank, A. and Hock, C. (2003) Subacute meningoencephalitis in a subset of patients with AD after Abeta42 immunization. *Neurology*, **61**, 46-54.

Panini, S.R., Delate, T.A. and Sinensky, M. (1992) Post-transcriptional regulation of 3-hydroxy-3-methylglutaryl coenzyme A reductase by 24(S),25-oxidolanosterol. *J Biol Chem*, **267**, 12647-12654.

Panini, S.R., Sexton, R.C., Gupta, A.K., Parish, E.J., Chitrakorn, S. and Rudney, H. (1986) Regulation of 3-hydroxy-3-methylglutaryl coenzyme A reductase activity and cholesterol biosynthesis by oxylanosterols. *J Lipid Res*, **27**, 1190-1204.

Paresce, D.M., Ghosh, R.N. and Maxfield, F.R. (1996) Microglial cells internalize aggregates of the Alzheimer's disease amyloid beta-protein via a scavenger receptor. *Neuron*, **17**, 553-565.

Parkkinen, J. and Rauvala, H. (1991) Interactions of plasminogen and tissue plasminogen activator (t-PA) with amphoterin. Enhancement of t-PA-catalyzed plasminogen activation by amphoterin. *J Biol Chem*, **266**, 16730-16735.

Parvathy, S., Ehrlich, M., Pedrini, S., Diaz, N., Refolo, L., Buxbaum, J.D., Bogush, A., Petanceska, S. and Gandy, S. (2004) Atorvastatin-induced activation of Alzheimer's alpha secretase is resistant to standard inhibitors of protein phosphorylation-regulated ectodomain shedding. *J Neurochem*, **90**, 1005-1010.

Pedrini, S., Carter, T.L., Prendergast, G., Petanceska, S., Ehrlich, M.E. and Gandy, S. (2005) Modulation of statin-activated shedding of Alzheimer APP ectodomain by ROCK. *PLoS Med*, **2**, e18.

Peri, A., Danza, G. and Serio, M. (2005) Seladin-1 as a target of estrogen receptor activation in the brain: a new gene for a rather old story? *J Endocrinol Invest*, **28**, 285-293.

Plow, E.F., Herren, T., Redlitz, A., Miles, L.A. and Hoover-Plow, J.L. (1995) The cell biology of the plasminogen system. *Faseb J*, **9**, 939-945.

Porstmann, T., Griffiths, B., Chung, Y.L., Delpuech, O., Griffiths, J.R., Downward, J. and Schulze, A. (2005) PKB/Akt induces transcription of enzymes involved in cholesterol and fatty acid biosynthesis via activation of SREBP. *Oncogene*, **24**, 6465-6481.

Puglielli, L., Konopka, G., Pack-Chung, E., Ingano, L.A., Berezovska, O., Hyman, B.T., Chang, T.Y., Tanzi, R.E. and Kovacs, D.M. (2001) Acyl-coenzyme A: cholesterol acyltransferase modulates the generation of the amyloid beta-peptide. *Nat Cell Biol*, **3**, 905-912.

Puglielli, L., Tanzi, R.E. and Kovacs, D.M. (2003) Alzheimer's disease: the cholesterol connection. *Nat Neurosci*, **6**, 345-351.

Qiu, W.Q., Walsh, D.M., Ye, Z., Vekrellis, K., Zhang, J., Podlisny, M.B., Rosner, M.R., Safavi, A., Hersh, L.B. and Selkoe, D.J. (1998) Insulin-degrading enzyme regulates extracellular levels of amyloid beta-protein by degradation. *J Biol Chem*, **273**, 32730-32738.

Rajagopal, R., Chen, Z.Y., Lee, F.S. and Chao, M.V. (2004) Transactivation of Trk neurotrophin receptors by G-protein-coupled receptor ligands occurs on intracellular membranes. *J Neurosci*, **24**, 6650-6658.

Recktenwald, D.J. and McConnell, H.M. (1981) Phase equilibria in binary mixtures of phosphatidylcholine and cholesterol. *Biochemistry*, **20**, 4505-4510.

Refolo, L.M., Malester, B., LaFrancois, J., Bryant-Thomas, T., Wang, R., Tint, G.S., Sambamurti, K., Duff, K. and Pappolla, M.A. (2000) Hypercholesterolemia accelerates the Alzheimer's amyloid pathology in a transgenic mouse model. *Neurobiol Dis*, **7**, 321-331.

Refolo, L.M., Pappolla, M.A., LaFrancois, J., Malester, B., Schmidt, S.D., Thomas-Bryant, T., Tint, G.S., Wang, R., Mercken, M., Petanceska, S.S. and Duff, K.E. (2001) A cholesterol-lowering drug reduces beta-amyloid pathology in a transgenic mouse model of Alzheimer's disease. *Neurobiol Dis*, **8**, 890-899.

Reiman, E.M., Caselli, R.J., Chen, K., Alexander, G.E., Bandy, D. and Frost, J. (2001) Declining brain activity in cognitively normal apolipoprotein E epsilon 4 heterozygotes: A foundation for using positron emission tomography to efficiently test treatments to prevent Alzheimer's disease. *Proc Natl Acad Sci U S A*, **98**, 3334-3339.

Religa, D. and Winblad, B. (2003) Therapeutic strategies for Alzheimer's disease based on new molecular mechanisms. *Acta Neurobiol Exp (Wars)*, **63**, 393-396.

Remacle-Bonnet, M., Garrouste, F., Baillat, G., Andre, F., Marvaldi, J. and Pommier, G. (2005) Membrane rafts segregate pro- from anti-apoptotic insulin-like growth factor-I receptor signaling in colon carcinoma cells stimulated by members of the tumor necrosis factor superfamily. *Am J Pathol*, **167**, 761-773.

Riddell, D.R., Christie, G., Hussain, I. and Dingwall, C. (2001) Compartmentalization of beta-secretase (Asp2) into low-buoyant density, noncaveolar lipid rafts. *Curr Biol*, **11**, 1288-1293.

Rockwood, K., Graham, J.E. and Fay, S. (2002) Goal setting and attainment in Alzheimer's disease patients treated with donepezil. *J Neurol Neurosurg Psychiatry*, **73**, 500-507.

Rodal, S.K., Skretting, G., Garred, O., Vilhardt, F., van Deurs, B. and Sandvig, K. (1999) Extraction of cholesterol with methyl-beta-cyclodextrin perturbs formation of clathrin-coated endocytic vesicles. *Mol Biol Cell*, **10**, 961-974.

Rondi-Reig, L., Libbey, M., Eichenbaum, H. and Tonegawa, S. (2001) CA1-specific N-methyl-D-aspartate receptor knockout mice are deficient in solving a nonspatial transverse patterning task. *Proc Natl Acad Sci U S A*, **98**, 3543-3548.

Rudel, L.L., Lee, R.G. and Cockman, T.L. (2001) Acyl coenzyme A: cholesterol acyltransferase types 1 and 2: structure and function in atherosclerosis. *Curr Opin Lipidol*, **12**, 121-127.

Runz, H., Rietdorf, J., Tomic, I., de Bernard, M., Beyreuther, K., Pepperkok, R. and Hartmann, T. (2002) Inhibition of intracellular cholesterol transport alters presenilin localization and amyloid precursor protein processing in neuronal cells. *J Neurosci*, **22**, 1679-1689.

Sankaram, M.B. and Thompson, T.E. (1990) Interaction of cholesterol with various glycerophospholipids and sphingomyelin. *Biochemistry*, **29**, 10670-10675.

Sawamura, N., Gong, J.S., Chang, T.Y., Yanagisawa, K. and Michikawa, M. (2003) Promotion of tau phosphorylation by MAP kinase Erk1/2 is accompanied by reduced cholesterol level in detergent-insoluble membrane fraction in Niemann-Pick C1-deficient cells. *J Neurochem*, **84**, 1086-1096.

Sawamura, N., Gong, J.S., Garver, W.S., Heidenreich, R.A., Ninomiya, H., Ohno, K., Yanagisawa, K. and Michikawa, M. (2001) Site-specific phosphorylation of tau accompanied by activation of mitogen-activated protein kinase (MAPK) in brains of Niemann-Pick type C mice. *J Biol Chem*, **276**, 10314-10319.

Schenk, D., Barbour, R., Dunn, W., Gordon, G., Grajeda, H., Guido, T., Hu, K., Huang, J., Johnson-Wood, K., Khan, K., Kholodenko, D., Lee, M., Liao, Z., Lieberburg, I., Motter, R., Mutter, L., Soriano, F., Shopp, G., Vasquez, N., Vandevert, C., Walker, S., Wogulis, M., Yednock, T., Games, D. and Seubert, P. (1999) Immunization with amyloid-beta attenuates Alzheimer-disease-like pathology in the PDAPP mouse. *Nature*, **400**, 173-177.

Scheuner, D., Eckman, C., Jensen, M., Song, X., Citron, M., Suzuki, N., Bird, T.D., Hardy, J., Hutton, M., Kukull, W., Larson, E., Levy-Lahad, E., Viitanen, M., Peskind, E., Poorkaj, P., Schellenberg, G., Tanzi, R., Wasco, W., Lannfelt, L., Selkoe, D. and Younkin, S. (1996) Secreted amyloid beta-protein similar to that in the senile plaques of Alzheimer's disease is increased in vivo by the presenilin 1 and 2 and APP mutations linked to familial Alzheimer's disease. *Nat Med*, **2**, 864-870.

Schroeder, F., Morrison, W.J., Gorka, C. and Wood, W.G. (1988) Transbilayer effects of ethanol on fluidity of brain membrane leaflets. *Biochim Biophys Acta*, **946**, 85-94.

Selkoe, D.J. (2001) Alzheimer's disease: genes, proteins, and therapy. *Physiol Rev*, **81**, 741-766.

Sherrington, R., Rogaev, E.I., Liang, Y., Rogaeva, E.A., Levesque, G., Ikeda, M., Chi, H., Lin, C., Li, G., Holman, K. and et al. (1995) Cloning of a gene bearing missense mutations in early-onset familial Alzheimer's disease. *Nature*, **375**, 754-760.

Simons, K. and Ehehalt, R. (2002) Cholesterol, lipid rafts, and disease. *J Clin Invest*, **110**, 597-603.

Simons, K. and Ikonen, E. (1997) Functional rafts in cell membranes. *Nature*, **387**, 569-572.

Simons, K. and Toomre, D. (2000) Lipid rafts and signal transduction. *Nat Rev Mol Cell Biol*, **1**, 31-39.

Simons, M., Keller, P., De Strooper, B., Beyreuther, K., Dotti, C.G. and Simons, K. (1998) Cholesterol depletion inhibits the generation of beta-amyloid in hippocampal neurons. *Proc Natl Acad Sci U S A*, **95**, 6460-6464.

Simons, M., Schwarzler, F., Lutjohann, D., von Bergmann, K., Beyreuther, K., Dichgans, J., Wormstall, H., Hartmann, T. and Schulz, J.B. (2002) Treatment with simvastatin in normocholesterolemic patients with Alzheimer's disease: A 26-week randomized, placebo-controlled, double-blind trial. *Ann Neurol*, **52**, 346-350.

Singh, S.K. and Chakravarty, S. (2003) Antispermatogenic and antifertility effects of 20,25-diazacholesterol dihydrochloride in mice. *Reprod Toxicol*, **17**, 37-44.

Sjogren, M. and Blennow, K. (2005) The link between cholesterol and Alzheimer's disease. *World J Biol Psychiatry*, **6**, 85-97.

Sjogren, M., Gustafsson, K., Syversen, S., Olsson, A., Edman, A., Davidsson, P., Wallin, A. and Blennow, K. (2003) Treatment with simvastatin in patients with Alzheimer's disease lowers both alpha- and beta-cleaved amyloid precursor protein. *Dement Geriatr Cogn Disord*, **16**, 25-30.

Skovronsky, D.M., Doms, R.W. and Lee, V.M. (1998) Detection of a novel intraneuronal pool of insoluble amyloid beta protein that accumulates with time in culture. *J Cell Biol*, **141**, 1031-1039.

Snipes, G.J. and Suter, U. (1997) Cholesterol and myelin. *Subcell Biochem*, **28**, 173-204.

Song, B.L., Javitt, N.B. and DeBose-Boyd, R.A. (2005) Insig-mediated degradation of HMG CoA reductase stimulated by lanosterol, an intermediate in the synthesis of cholesterol. *Cell Metab*, **1**, 179-189.

Sparks, D.L., Hunsaker, J.C., 3rd, Scheff, S.W., Kryscio, R.J., Henson, J.L. and Markesbery, W.R. (1990) Cortical senile plaques in coronary artery disease, aging and Alzheimer's disease. *Neurobiol Aging*, **11**, 601-607.

Sparks, D.L., Liu, H., Scheff, S.W., Coyne, C.M. and Hunsaker, J.C., 3rd. (1993) Temporal sequence of plaque formation in the cerebral cortex of non-demented individuals. *J Neuropathol Exp Neurol*, **52**, 135-142.

Sparks, D.L., Scheff, S.W., Hunsaker, J.C., 3rd, Liu, H., Landers, T. and Gross, D.R. (1994) Induction of Alzheimer-like beta-amyloid immunoreactivity in the brains of rabbits with dietary cholesterol. *Exp Neurol*, **126**, 88-94.

Steiner, H. and Haass, C. (2000) Intramembrane proteolysis by presenilins. *Nat Rev Mol Cell Biol*, **1**, 217-224.

Stokin, G.B., Lillo, C., Falzone, T.L., Brusch, R.G., Rockenstein, E., Mount, S.L., Raman, R., Davies, P., Masliah, E., Williams, D.S. and Goldstein, L.S. (2005) Axonopathy and transport deficits early in the pathogenesis of Alzheimer's disease. *Science*, **307**, 1282-1288.

Stottrup, B.L. and Keller, S.L. (2006) Phase behavior of lipid monolayers containing DPPC and cholesterol analogs. *Biophys J*, **90**, 3176-3183.

Strittmatter, W.J. and Roses, A.D. (1995) Apolipoprotein E and Alzheimer disease. *Proc Natl Acad Sci U S A*, **92**, 4725-4727.

Strittmatter, W.J., Saunders, A.M., Schmechel, D., Pericak-Vance, M., Enghild, J., Salvesen, G.S. and Roses, A.D. (1993) Apolipoprotein E: high-avidity binding to beta-amyloid and increased frequency of type 4 allele in late-onset familial Alzheimer disease. *Proc Natl Acad Sci U S A*, **90**, 1977-1981.

Tanzi, R.E. (1999) A genetic dichotomy model for the inheritance of Alzheimer's disease and common age-related disorders. *J Clin Invest*, **104**, 1175-1179.

Terry, R.D. (1998) The cytoskeleton in Alzheimer disease. *J Neural Transm Suppl*, **53**, 141-145.

Terry, R.D., Masliah, E., Salmon, D.P., Butters, N., DeTeresa, R., Hill, R., Hansen, L.A. and Katzman, R. (1991) Physical basis of cognitive alterations in Alzheimer's disease: synapse loss is the major correlate of cognitive impairment. *Ann Neurol*, **30**, 572-580.

Vainio, S., Bykov, I., Hermansson, M., Jokitalo, E., Somerharju, P. and Ikonen, E. (2005) Defective insulin receptor activation and altered lipid rafts in Niemann-Pick type C disease hepatocytes. *Biochem J*, **391**, 465-472.

Vainio, S., Jansen, M., Koivusalo, M., Rog, T., Karttunen, M., Vattulainen, I. and Ikonen, E. (2006) Significance of sterol structural specificity. Desmosterol cannot replace cholesterol in lipid rafts. *J Biol Chem*, **281**, 348-355.

Vetrivel, K.S., Cheng, H., Lin, W., Sakurai, T., Li, T., Nukina, N., Wong, P.C., Xu, H. and Thinakaran, G. (2004) Association of gamma-secretase with lipid rafts in post-Golgi and endosome membranes. *J Biol Chem*, **279**, 44945-44954.

Vetrivel, K.S. and Thinakaran, G. (2006) Amyloidogenic processing of beta-amyloid precursor protein in intracellular compartments. *Neurology*, **66**, S69-73.

Wahrle, S., Das, P., Nyborg, A.C., McLendon, C., Shoji, M., Kawarabayashi, T., Younkin, L.H., Younkin, S.G. and Golde, T.E. (2002) Cholesterol-dependent gamma-secretase activity in buoyant cholesterol-rich membrane microdomains. *Neurobiol Dis*, **9**, 11-23.

Walker, E.S., Martinez, M., Brunkan, A.L. and Goate, A. (2005) Presenilin 2 familial Alzheimer's disease mutations result in partial loss of function and dramatic changes in Abeta 42/40 ratios. *J Neurochem*, **92**, 294-301.

Wang, J., Megha and London, E. (2004) Relationship between sterol/steroid structure and participation in ordered lipid domains (lipid rafts): implications for lipid raft structure and function. *Biochemistry*, **43**, 1010-1018.

Waterham, H.R., Koster, J., Romeijn, G.J., Hennekam, R.C., Vreken, P., Andersson, H.C., FitzPatrick, D.R., Kelley, R.I. and Wanders, R.J. (2001) Mutations in the 3beta-hydroxysterol Delta24-reductase gene cause desmosterolosis, an autosomal recessive disorder of cholesterol biosynthesis. *Am J Hum Genet*, **69**, 685-694.

Wechsler, A., Brafman, A., Shafir, M., Heverin, M., Gottlieb, H., Damari, G., Gozlan-Kelner, S., Spivak, I., Moshkin, O., Fridman, E., Becker, Y., Skaliter, R., Einat, P., Faerman, A., Bjorkhem, I. and Feinstein, E. (2003) Generation of viable cholesterol-free mice. *Science*, **302**, 2087.

Wolozin, B., Kellman, W., Ruosseau, P., Celesia, G.G. and Siegel, G. (2000) Decreased prevalence of Alzheimer disease associated with 3-hydroxy-3-methyglutaryl coenzyme A reductase inhibitors. *Arch Neurol*, **57**, 1439-1443.

Wood, W.G., Gorka, C. and Schroeder, F. (1989) Acute and chronic effects of ethanol on transbilayer membrane domains. *J Neurochem*, **52**, 1925-1930.

Wu, C., Miloslavskaya, I., Demontis, S., Maestro, R. and Galaktionov, K. (2004) Regulation of cellular response to oncogenic and oxidative stress by Seladin-1. *Nature*, **432**, 640-645.

Yaffe, K., Barrett-Connor, E., Lin, F. and Grady, D. (2002) Serum lipoprotein levels, statin use, and cognitive function in older women. *Arch Neurol*, **59**, 378-384.

Yang, D.S., Small, D.H., Seydel, U., Smith, J.D., Hallmayer, J., Gandy, S.E. and Martins, R.N. (1999) Apolipoprotein E promotes the binding and uptake of beta-amyloid into Chinese hamster ovary cells in an isoform-specific manner. *Neuroscience*, **90**, 1217-1226.

Yokoyama, C., Wang, X., Briggs, M.R., Admon, A., Wu, J., Hua, X., Goldstein, J.L. and Brown, M.S. (1993) SREBP-1, a basic-helix-loop-helix-leucine zipper protein that controls transcription of the low density lipoprotein receptor gene. *Cell*, **75**, 187-197.

Yu, W., Ko, M., Yanagisawa, K. and Michikawa, M. (2005) Neurodegeneration in heterozygous Niemann-Pick type C1 (NPC1) mouse: implication of heterozygous NPC1 mutations being a risk for tauopathy. *J Biol Chem*, **280**, 27296-27302.

Zerbinatti, C.V. and Bu, G. (2005) LRP and Alzheimer's disease. *Rev Neurosci*, **16**, 123-135.

ACKNOWLEDGEMENTS

Here I like to acknowledge the people who contributed in some way or another to the development and completion of this work

First of all I like to thank Prof. Dr. Roger M. Nitsch who offered me to accomplish my PhD thesis in his well-equipped department. I particularly thank him for his generosity and support, and for his valuable suggestions. I am indebted to Dr. M. Hasan Mohajeri who supervised my work and gave me the opportunity to follow my own ideas and interests in AD research.

Furthermore I am very grateful to Prof. Dr. Esther Stöckli and Prof. Dr. Alex Hajnal for accepting me as an external PhD student, for their participation in my ZNZ steering committee and for advising me during the whole process of this doctoral thesis. I am indebted to Prof. Markus Glatzel for accepting to be the external evaluator of my dissertation

Moreover I would like to acknowledge my collaborators Dr. Maria Dolores Ledesma for her brilliant ideas, her motivation and excellent technical support and Prof. Dr. Carlos Dotti for a very fruitful teamwork. I especially thank PD Dr. Dieter Lütjohann and Karin Thelen for their time and concentrated efforts doing the GC/MS analyses.

Sincere thanks are given to Arames Crameri, who introduced me to the field of AD research and who always was a fair and delightful team-player. I very much appreciated his sweeping enthusiasm for scientific issues, his altruistic help and excellent technical support, his generosity and his cheerful soul.

I thank all the people from FOR1 for an enjoyable atmosphere, and special thanks go to Fabienne Brunner for carefully reading this manuscript and Danielle Gretener for her professional help in many organizational and business issues, and both of them for many hours of inspiring and pleasurable discussions but even more for being supportive and honest friends.

And I want to dearly thank my parents for supporting me during almost one decade of university education, who patiently listended to my enjoyment, my hopes, my complains and my sorrows and who were always standing behind me.

CURRICULUM VITAE

Name	Katrin Kuehnle
Date of Birth	22.02.1977
Place of Birth	Friedrichshafen, Germany
Nationality	German

EDUCATION

2003-2006	PhD thesis in Neuroscience at the Division of Psychiatry Research and the Neuroscience Center Zürich, Switzerland. Project: Effects of DHCR24 depletion *in vivo* and *in vitro*
2001-2002	Diploma thesis in Cancer Research at CUSTOS Biotech GmBH, Berlin, Germany. Project: Differential Gene expression in liver metastases.
2001	Diploma, Final examinations: Molecular Biology and Genetics, Biochemistry, Immunology/Parasitology
1997-2001	Advanced studies of Biology, Humboldt-University Berlin, Germany
1996-1997	Basic studies of Biology, Eberhard-Karls University Tübingen, Germany
1987-1996	Gymnasium Markdorf, Baden-Württemberg, Germany

PROFESSIONAL EXPERIENCE

2001	Freelancer in medical journalism: writing for NETZEITUNG.DE
12/2000-04/2001	Schering, Pharmaceutical Company, Berlin. Industrial training at the Department of Microbiology: Biological Quality-Control of contrast media
04/2000-12/2000	Cornell University, New York. Training period at the Boyce Thompson Institute for plant research. Project: Localizing and sequencing and the nuclear gene *mcdI* from *Chlamydomonas reinhardtii*
02/2000-04/2000	Department of Crystallography, FU Berlin. Practical training. Project: Over-expression of *rcsA* and *rcsB* in *E. coli* and protein engineering
09/1999-02/2000	Max Planck Institute for Molecular Genetics, Berlin: Training period. Project: Role of acetyltransferase homologues in transcriptional repression and histone acetylation in *Saccharomyces cerevisiae*

LANGUAGES

German mother tongue
English fluent
French advanced
Latin A-level

PRESENTATIONS, TALKS and PUBLICATIONS

International Conference of Alzheimer's disease, poster, 2006 Madrid, Spain
APOPIS meeting, talk, 2006, Nice, France
2nd Brain Symposium, talk, 2006, Sils Maria, Switzerland
APOPIS meeting, 2005, Brussels, Belgium
AD/PD biannual conference, 2005, Sorrento, Italy
NCCR conference, poster, 2005, Ittingen, Switzerland
1st Brain Symposium, talk, 2005, Sils Maria, Switzerland
Center of Neuroscience Zurich Annual Meeting, poster, 2003-2005 Zurich, Switzerland
PhD Retreat, talk, 2003, Valens, Switzerland

Kuehnle K, Ledesma MD, Crameri A, Thelen KM, Brunner F, Kulic L, Lutjohann D, Nitsch RM, Mohajeri MH. Functional replacement of cholesterol by desmosterol: Age-dependent increase in desmosterol rescues DRM-related functions in cholesterol deficient $DHCR24^{-/-}$ mice. (in review October 2006)

Kuehnle K, Crameri A, Nitsch RM, Mohajeri MH. Dual role of DHCR24/seladin-1 in neuroprotection. (submitted October 2006)

Brunner F, Wollmer MA, **Kuehnle K**, Hoerndli F, Hock C, Nitsch RM, Papassotiropoulos A. A *SOAT1* haplotype modulates *SOAT1* mRNA expression and reduces the risk for sporadic Alzheimer's disease. (manuscript in preparation)

Crameri A, Biondi E, **Kuehnle K**, Lutjohann D, Thelen KM, Perga S, Dotti CG, Nitsch RM, Ledesma MD, Mohajeri MH. 2006. The role of seladin-1/DHCR24 in cholesterol biosynthesis, APP processing and Abeta generation in vivo. EMBO J. 25;25(2):432-43.

Bandapalli OR, Geheeb M, Kobelt D, **Kuehnle K**, Elezkurtaj S, Herrmann J, Gressner AM, Weiskirchen R, Beule D, Bluthgen N, Herzel H, Franke C, Brand K. 2006. Global analysis of host tissue gene expression in the invasive front of colorectal liver metastases. Int J Cancer. 1;118(1):74-89.

Murakami S, **Kuehnle K**, Stern DB. 2005. A spontaneous tRNA suppressor of a mutation in the Chlamydomonas reinhardtii nuclear MCD1 gene required for stability of the chloroplast petD mRNA. Nucleic Acids Res. 9;33(10):3372-80.

Gaugler MN, Tracy J, **Kuhnle K**, Crameri A, Nitsch RM, Mohajeri MH. 2005. Modulation of Alzheimer's pathology by cerebro-ventricular grafting of hybridoma cells expressing antibodies against Abeta in vivo. FEBS Lett. 31;579(3):753-6.

Mohajeri MH, **Kuehnle K**, Li H, Poirier R, Tracy J, Nitsch RM. 2004. Anti-amyloid activity of neprilysin in plaque-bearing mouse models of Alzheimer's disease. FEBS Lett. 26;562(1-3):16-21.

Mohajeri MH, Gaugler M N, Martinez J, Tracy J, Li H, Crameri A, **Kuehnle K,** Wollmer MA, Nitsch RM. 2004. Assessment of the Bioactivity of Antibodies against β-Amyloid Peptide in vitro and in vivo. Neurodegenerative Diseases 1:160-167.

The EMBO Journal (2006), 1–12 | © 2006 European Molecular Biology Organization | All Rights Reserved 0261-4189/06
www.embojournal.org

THE EMBO JOURNAL

The role of seladin-1/DHCR24 in cholesterol biosynthesis, APP processing and Aβ generation *in vivo*

Arames Crameri[1,5], Elisa Biondi[2,5], Katrin Kuehnle[1,5], Dieter Lütjohann[3], Karin M Thelen[3], Simona Perga[2], Carlos G Dotti[2,4], Roger M Nitsch[1], Maria Dolores Ledesma[2,4,*] and M Hasan Mohajeri[1,*]

[1]Division of Psychiatry Research, University of Zurich, Zurich, Switzerland, [2]Cavalieri Ottolenghi Scientific Institute, Università degli Studi di Torino, Orbassano, Italy, [3]Department of Clinical Pharmacology, University of Bonn, Germany and [4]Center for Human Genetics, Catholic University of Leuven and Flanders Interuniversitary Institute for Biotechnology (VIB4), Leuven, Belgium

The cholesterol-synthesizing enzyme seladin-1, encoded by the *Dhcr24* gene, is a flavin adenine dinucleotide-dependent oxidoreductase and regulates responses to oncogenic and oxidative stimuli. It has a role in neuroprotection and is downregulated in affected neurons in Alzheimer's disease (AD). Here we show that seladin-1-deficient mouse brains had reduced levels of cholesterol and disorganized cholesterol-rich detergent-resistant membrane domains (DRMs). This was associated with inefficient plasminogen binding and plasmin activation, the displacement of β-secretase (BACE) from DRMs to APP-containing membrane fractions, increased β-cleavage of APP and high levels of Aβ peptides. In contrast, overexpression of seladin-1 increased both cholesterol and the recruitment of DRM components into DRM fractions, induced plasmin activation and reduced both BACE processing of APP and Aβ formation. These results establish a role of seladin-1 in the formation of DRMs and suggest that seladin-1-dependent cholesterol synthesis is involved in lowering Aβ levels. Pharmacological enhancement of seladin-1 activity may be a novel Aβ-lowering approach for the treatment of AD.

The EMBO Journal advance online publication, 12 January 2006; doi:10.1038/sj.emboj.7600938

Subject Categories: neuroscience; molecular biology of disease

Keywords: Aβ; Alzheimer; cholesterol; neurodegeneration; therapy

*Corresponding authors. MD Ledesma, Cavalieri Ottolenghi Scientific Institute, Università degli Studi di Torino, AO San Luigi Gonzaga, Regione Gonzole 10, 10043 Orbassano, Turin, Italy.
Tel.: +39 011 670 5482; Fax: +39 011 670 5449;
E-mail: lola.ledesma@unito.it or MH Mohajeri, Division of Psychiatry Research, University of Zurich, August-Forel Strasse 1, 8008 Zurich, Switzerland. Tel.: +41 44 634 8872; Fax: +41 44 634 8874;
E-mail: mohajeri@bli.unizh.ch
[5]These authors contributed equally to this work

Received: 20 July 2005; accepted: 6 December 2005

Introduction

Accumulation of amyloid-β peptides (Aβ) in the CNS is an invariant feature of the pathology of Alzheimer's disease (AD), the most common form of dementia. Aβ peptides are derived from proteolytic cleavage of the amyloid precursor protein (APP), with the β-secretase (BACE) cleaving at the N-terminus and γ-secretase at the C-terminus of Aβ peptides. Genetic studies of familial AD cases have led to the identification of alterations in genes associated with the disease that result in increased production of Aβ peptide or to C-terminal extended forms that aggregate more readily (Capell *et al*, 1998; Hardy and Selkoe, 2002). These observations, together with studies on Aβ toxicity (Small *et al*, 2001), support the view of a key role of Aβ in AD pathophysiology (Huang *et al*, 1999; Chen *et al*, 2000; Janus *et al*, 2000; Morgan *et al*, 2000; Mucke *et al*, 2000; Small *et al*, 2001; Casas *et al*, 2004; Schmitz *et al*, 2004). Thus, concentrated effort has been focused on the identification of modifying factors (Corder *et al*, 1993) and regulatory mechanisms of the proteases that control APP cleavage and are involved in Aβ production, as well as on proteases with the capacity to degrade the peptide (Selkoe, 2001).

Seladin-1, encoded by a single gene (*Dhcr24*) on chromosome 1, is an evolutionarily conserved gene with homologies to a family of flavin adenine dinucleotide-dependent oxidoreductases (Greeve *et al*, 2000). It catalyzes the reduction of the Δ24 double bond of sterol intermediates of cholesterol metabolic pathway (Waterham *et al*, 2001). As an exemplar, seladin-1 reduces the Δ24 double bond of desmosterol, the immediate precursor of cholesterol, to form cholesterol (Waterham *et al*, 2001). Functional deficiency in the *Dhcr24* gene causes, in humans, desmosterolosis, a severe autosomal recessive disorder characterized by gross developmental abnormalities and elevated desmosterol levels in plasma (Waterham *et al*, 2001). Moreover, seladin-1 is a key regulator of Ras-induced senescence, and cellular responses to oncogenic and oxidative stimuli (Wu *et al*, 2004). Greeve *et al* (2000) have previously shown the protective activity of seladin-1 against oxidative and Aβ-mediated toxicity and that seladin-1 levels are lower in affected neurons of AD brain.

The cholesterol synthesizing activity of seladin-1 suggests a possible role in the formation of the cholesterol-rich detergent-resistant membrane domains (DRMs or rafts), but this activity has not been studied to date. DRMs are operationally defined as membrane domains resistant to solubilization by nonionic detergent at 4°C (Ciana *et al*, 2005). The *in vivo* counterpart of the DRMs is under intense investigation. Experimental evidence has revealed the disorganization of DRMs in AD brains, possibly because of low cholesterol content (Ledesma *et al*, 2003a). In a recent study, it has been described that DRMs participate in the segregation of APP from BACE, therefore reducing APP β-cleavage and Aβ

production in cultured primary neurons and CHO cells, respectively (Abad-Rodriguez *et al*, 2004). Furthermore, disruption of DRMs results in diminished activity of the Aβ-degrading enzyme plasmin, because of decreased membrane plasminogen binding to the plasma membrane (Ledesma *et al*, 2000, 2003a, b). Altogether, these data support a possible link between AD and brain cholesterol loss. In contrast, the use of statins to reduce cholesterol led to the reduction of Aβ production, favoring the view of high cholesterol as a risk factor for AD (Simons *et al*, 1998; Fassbender *et al*, 2001).

To determine the role of seladin-1 in APP processing and Aβ production, we analyzed seladin-1-deficient mice and we overexpressed seladin-1 in cultured human neuroblastoma cells. We provide here evidence for a key role of seladin-1 in the regulation of brain cholesterol levels, DRM formation, plasmin activation, APP processing and Aβ levels *in vivo* and *in vitro*.

Results

Seladin-1 influences the membrane and cellular cholesterol levels in mouse brains and in cultured human neuroblastoma cells

To determine to which extent the levels of brain cholesterol depend on seladin-1, we first analyzed the effects of genetic seladin-1 depletion on steady-state cholesterol levels *in vivo*. The analysis of seladin-1 mRNA levels in the brain of wild-type mice, heterozygous mice with depletion of one (heterozygous) or knockout mice with depletion of both (homozygous) seladin-1 alleles (Wechsler *et al*, 2003) revealed a gene-dose-dependent reduction in the heterozygous mice compared to their wild-type littermates ($43.8 \pm 3.3\%$, $P = 0.009$). There was no seladin-1 mRNA expression detectable in the homozygous mice (Figure 1A). The brains of seladin-1 heterozygous mice exhibited an average reduction of 29% in membrane ($P = 0.02$; Figure 1B) and 15% in total cellular cholesterol ($P = 0.042$; Figure 1C) compared to wild-type brains. Furthermore, cholesterol amount was undetectable in the homozygous mouse brains (Figure 1B and C). To characterize the effect of seladin-1 expression on cholesterol metabolism, we analyzed the effects of seladin-1 depletion on the levels of the cholesterol precursor, desmosterol, and of the major degradation product of cholesterol in the brain, 24OH-cholesterol. Desmosterol was 5.7-fold ($P = 0.012$) and 50-fold ($P = 0.00006$) increased in heterozygous and homozygous mouse brains, respectively (Figure 1D), indicating that desmosterol accumulates upon seladin-1 deficiency. Moreover, decreased seladin-1 expression led to a significant reduction in the catabolic product 24OH-cholesterol in heterozygous ($24.6 \pm 4.3\%$, $P = 0.017$) and knockout ($97.6 \pm 0.47\%$, $P = 0.0004$) compared to control brains. Altogether, these results unveil for the first time the key role of seladin-1 in the regulation of brain cholesterol metabolism. Consistent with an essential role of cholesterol in vertebrate cell viability, homozygous mice did not survive beyond the first month.

Having demonstrated the consequences of seladin-1 deficiency in cholesterol metabolism, we next tested whether increasing seladin-1 levels would cause the opposite effects. To this aim, we generated human neuroblastoma SH-SY5Y cells constitutively expressing seladin-1. Analysis of seladin-1 mRNA revealed a significant increase ($684 \pm 121\%$, $P = 0.0001$) in the seladin-1-overexpressing cells (Figure 1E). Significant increases of 1.9-fold in membrane cholesterol ($P = 0.003$; Figure 1F) and 1.7-fold in total cellular cholesterol ($P = 0.001$; Figure 1G) were found in seladin-1-overexpressing cells when compared to the control cultures, confirming the bioactivity of the transgene. Consistent with the *in vivo* data, desmosterol levels were dramatically reduced in cells overexpressing seladin-1 ($43 \pm 5.2\%$, $P = 0.001$) (Figure 1H), whereas 24OH-cholesterol amounts were increased ($172 \pm 2.3\%$, $P = 0.00001$) when compared to control cultures.

Seladin-1 contributes to the specific recruitment of DRM proteins and lipids into DRMs

Given the above results and that cholesterol is a main component of DRMs and affects DRM functions (Simons *et al*, 1998; Simons and Toomre, 2000), we first tested whether changes in seladin-1 expression alter these membrane domains *in vivo*. Therefore, DRM protein and lipid composition was analyzed in the brains of wild-type and seladin-1 heterozygous mice that, in contrast to the seladin-1 homozygous mice, develop normally and survive to adulthood without major health problems but present a moderate, still significant, reduction of cholesterol (see above). DRMs were isolated upon cold-detergent extraction of total brain extracts and gradient centrifugation. In the seladin-1 heterozygous brains, significantly lower protein levels were found in the light fractions 4–6 of the gradient, which correspond to detergent-resistant membranes (Figure 2A). To determine whether this reduction of protein content was the consequence of general or DRM-specific protein loss, the flotation profiles of the DRM markers flotillin 1 and the cellular prion protein (PrP^c) as well as of the non-DRM marker transferrin receptor (TfR) were analyzed. In agreement with a DRM-specific shortage, reduction of brain seladin-1 levels resulted in the displacement of DRM markers, flotillin 1 (Figure 2B and C) and PrP^c (Figure 2D and E), away from the DRM fractions. Thus, while in wild-type mice $20.2 \pm 1.45\%$ of total protein, $12.3 \pm 1.21\%$ of total flotillin 1 and $40.5 \pm 4.68\%$ of total PrP^c were present in DRM fractions 4–6, these percentages decreased to 13.8 ± 1.56, 5.1 ± 2.19 and $12.5 \pm 5.32\%$, respectively, in seladin-1 heterozygous mouse brains. All the differences found were statistically significant ($P < 0.03$). In contrast, no change was observed in the flotation profile of the non-DRM protein TfR (Figure 2F and G).

Conversely, significantly higher protein levels were found in the light fractions 4–6 of the seladin-1-overexpressing cell extracts compared to control cells (31.6 ± 2.02 and $22.2 \pm 2.02\%$, respectively, $P = 0.01$; Figure 2H). Consistent with a recruitment of DRM-specific proteins and not to a general protein contribution, flotillin 1 (Figure 2I and J) and PrP^c (Figure 2K and L) were enriched in fractions 4–6 of seladin-1-overexpressing cell gradients when compared to control cells, whereas TfR remained always in detergent-soluble heavy fractions (8–10) (Figure 2M and N). Quantitative analysis showed that, $4.8 \pm 1.15\%$ of total flotillin 1 and $10.4 \pm 1.73\%$ of total PrP^c float to DRMs in control cells, which increased to 18.7 ± 2.66 and $30.5 \pm 2.89\%$, respectively, in seladin-1-overexpressing cells ($P = 0.004$ and 0.001).

The analysis of the distribution of several lipids in the flotation gradient fractions revealed that the presence of

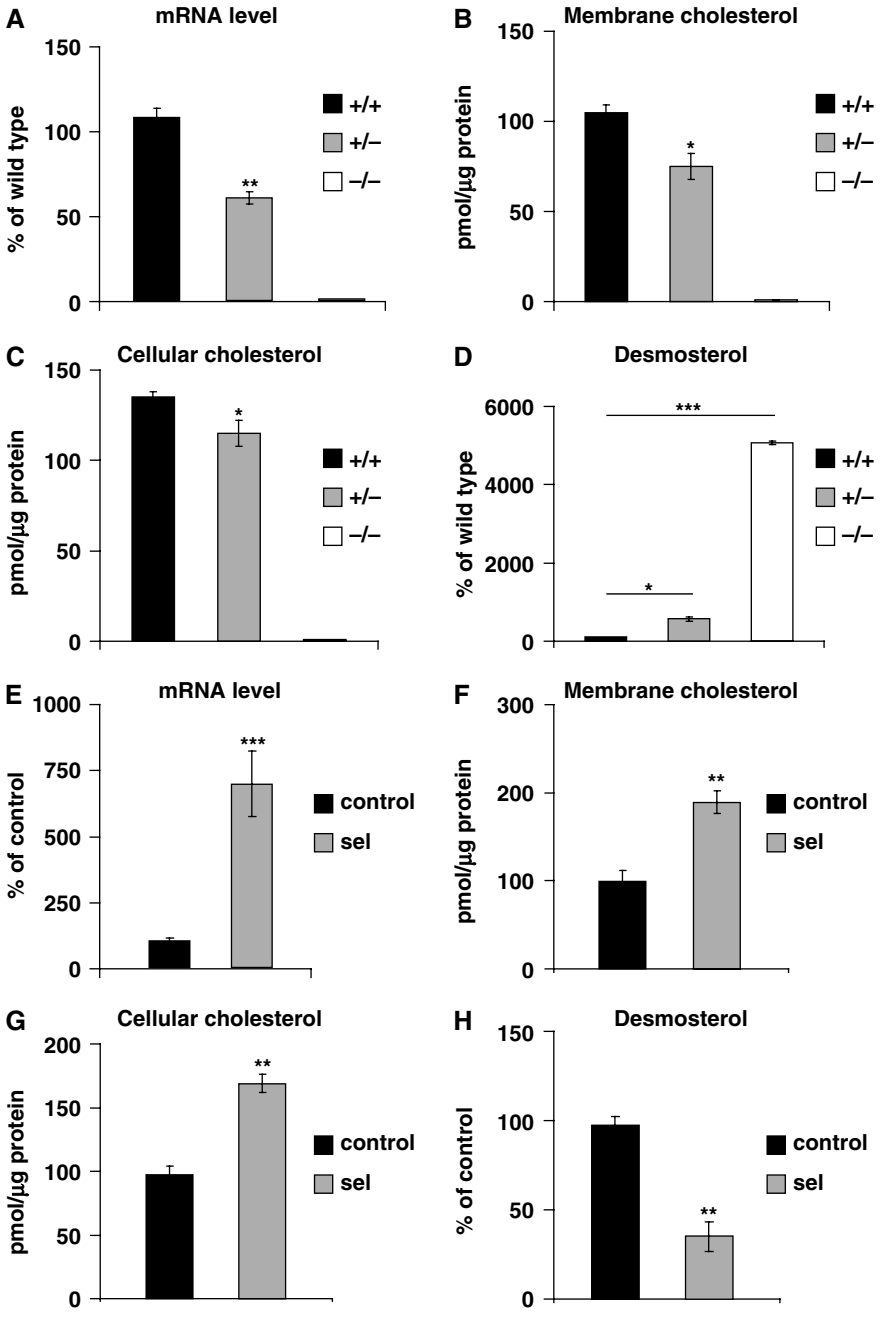

Figure 1 The level of cholesterol is dependent on seladin-1 expression *in vivo* and *in vitro*. Seladin-1 mRNA expression level was 44% lower in heterozygous (+/−) compared to wild-type mouse brains (+/+), whereas no seladin-1 mRNA was detectable in the brains of seladin-1 knockout mice (−/−) (**A**). In brain extracts of seladin-1 heterozygous (+/−) mice, membrane cholesterol (**B**) and cellular cholesterol (**C**) were significantly reduced by 29 and 15%, respectively, compared to wild-type (+/+) littermates. In knockout (−/−) mice, membrane and cellular cholesterol were undetectable (B, C). Desmosterol was 5.7- and 50-fold increased in heterozygous (+/−) and in knockout (−/−) brains, respectively, when compared to wild-type littermates (**D**). In seladin-1-overexpressing SH-SY5Y human neuroblastoma cells, seladin-1 mRNA expression level was 680% higher compared to control cells (**E**), and membrane cholesterol (**F**) and cellular cholesterol (**G**) were significantly increased by 1.9- and 1.7-fold, respectively. Desmosterol was significantly lower (two-fold) in seladin-1-overexpressing cells compared to control cultures (**H**). Values in panels A–D and E–H are expressed as a percentage change in the corresponding values of wild-type mouse brains or control cells, respectively, that were considered as 100%. The graphs show the average and standard error from three different mouse brains for each condition, and from three independent seladin-1-overexpressing and control SH-SY5Y cultures. Statistical significance is indicated by asterisks: $*P<0.05$, $**P<0.009$, $***P<0.0002$.

cholesterol, sphingomyelin and the ganglioside GM1 was also modulated by seladin-1 levels, whereas no changes in the amounts of desmosterol and total phospholipids were detected in the DRM fractions *in vivo* and *in vitro* (Supplementary Figures 1 and 2).

Altogether, these results indicate that seladin-1 is required for the specific recruitment of DRM proteins and lipids into detergent-insoluble membrane domains and that its deficiency results in DRM disorganization, evident by displacement of DRM-specific lipids and proteins.

Seladin-1 affects DRM-dependent plasminogen binding and activation

Given the influence of seladin-1 on DRM composition, we reasoned that changes in its expression would also affect DRM-dependent functions. Plasminogen binding to the membrane leads to the activation of the Aβ-degrading enzyme plasmin in DRMs (Ledesma *et al*, 2003a). Therefore, we first investigated whether changes in seladin-1 expression

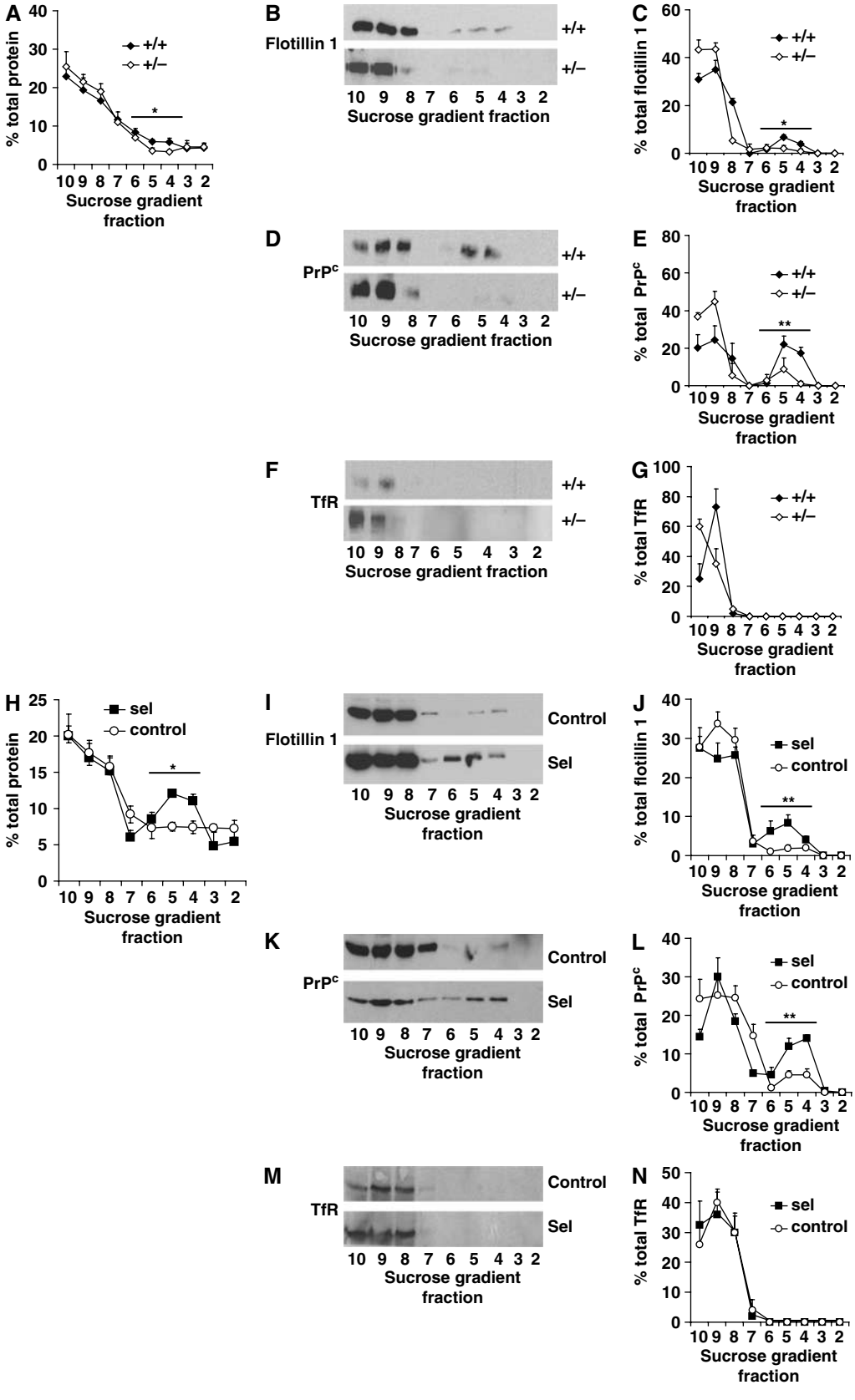

affect plasminogen binding and plasmin activity *in vivo*. Endogenous plasmin activity was reduced in heterozygous brains when compared to controls (Figure 3A). To analyze plasminogen binding, exogenous plasminogen was added to isolated membranes and plasmin activity was measured. Seladin-1 deficiency resulted in reduced plasmin activity, indicating a diminished ability of heterozygous seladin-1 brain membranes to bind plasminogen (Figure 3B). Accordingly, the amount of endogenous plasminogen bound to the membrane was clearly reduced in seladin-1 heterozygous mouse brains (42.9±10.9% of that in wild-type brains, $P=0.005$; Figure 3C and E), whereas the endogenous levels of total plasminogen were similar in all mouse brains (Figure 3D and F). Endogenous plasmin activity was also measured in membranes derived from control and seladin-1-overexpressing cells. The latter exhibited a clear increase in plasmin activity (Figure 3G). Furthermore, plasmin activity upon addition of exogenous plasminogen was also higher in seladin-1-overexpressing cells than in control cells, indicating an increased ability of seladin-1-overexpressing cell-derived membranes to bind plasminogen (Figure 3H). This was further confirmed by Western blot analysis showing that while there were no significant differences on the endogenous levels of total plasminogen in control and seladin-1-overexpressing cells (Figure 3J and L), the amount of plasminogen bound to the membrane was clearly increased in the latter (247±14.7%, $P=0.004$; Figure 3I and K).

Seladin-1 alters BACE1–APP membrane compartmentalization, APP β-cleavage and Aβ generation in vitro and in vivo

DRMs segregate a major pool of the APP-β-secretase BACE1 from its non-DRM substrate APP, restricting APP β-cleavage and Aβ production in cultured primary neurons and CHO cells, respectively (Abad-Rodriguez *et al*, 2004). Hence, we determined whether low levels of seladin-1, leading to decreased cholesterol concentrations and DRM alterations, affect BACE1–APP membrane segregation and their functional interaction *in vivo*. The flotation profiles revealed that BACE1 was displaced from light fractions 4–6 to APP-containing heavy fractions in seladin-1 heterozygous mouse brains compared to wild-type brains. The percentages of total BACE1 in DRM fractions 4–6 in wild-type and heterozygous seladin-1 mice were 36.4±3.58 and 9.7±1.97%, respectively ($P=0.003$; Figure 4A and B). In contrast, no changes in the flotation profile of APP, as well as in its concentration, were detected between the genotypes (Figure 4C and D). To test if the changes in membrane compartmentalization had a functional consequence, we measured the levels of APP β-cleavage. The amount of the APP β-C-terminal fragment (β-CTF) was significantly increased (201±16%, $P=0.04$) in seladin-1 heterozygous mouse brains (Figure 4E and F and Supplementary Figure 4A).

To assess whether high levels of seladin-1 would reverse the effects observed upon its deficiency, the flotation profiles of BACE1 and APP were also analyzed in seladin-1-overexpressing and control cells. While APP always remained in the heavy fractions 9–10 (Figure 4I and J), more BACE1 was recruited in the light fractions upon seladin-1 overexpression (Figure 4G and H). Quantitative analysis revealed that 54.4±9.8% of BACE1 is in the APP-containing fractions 9–10 in the control cells, whereas the percentage significantly diminishes to 35.6±4.3% in seladin-1-overexpressing cells ($P=0.04$; Figure 4H and J). Consistent with the enhanced membrane segregation of BACE1 from APP, the generation of APP β-CTF was significantly reduced (34±11%, $P=0.04$) in seladin-1-overexpressing cells (Figure 4K and L). Taken together, the above observations reveal an important role of seladin-1 in the regulation of BACE1–APP interaction and thus in APP β-cleavage.

Finally, we determined whether these alterations affect the levels of Aβ, utilizing ELISA systems that measure specifically murine and human Aβ peptides. In concert with higher amyloidogenic APP processing, $A\beta_{40}$ was significantly increased (152±16%, $P=0.027$; Figure 5A) in total brain extracts of heterozygous mice. Because the endogenous mouse $A\beta_{42}$ levels are extremely low in young wild-type mice, as previously reported (Refolo *et al*, 2001), the $A\beta_{42}$ measurements were below the detection level. We therefore analyzed age-matched wild-type and seladin-1 heterozygous mice cross bred to the Tg2576 SwAPP mouse line (SwAPP/seladin-1). The SwAPP mice overexpress human APP carrying the Swedish mutations under the regulatory sequence of the neuronal Prp promoter. These mutations located at the N-terminus of the Aβ peptide lead to increased β-cleavage and therefore elevated levels of $A\beta_{40}$ and $A\beta_{42}$ (Hsiao *et al*, 1995). In accordance with the murine ELISA data, $A\beta_{40}$ was significantly increased in heterozygous SwAPP/seladin-1 mouse brains (270±31%, $P=0.024$; Figure 5B). In these mice, $A\beta_{42}$ levels also revealed a significant increase compared to the SwAPP littermates (159±0.3%, $P=0.015$; Figure 5C), whereas the ratio of $A\beta_{40}$ to $A\beta_{42}$ did not significantly differ between the genotype groups (136±31%; Figure 5D), suggesting that the changes in Aβ levels were not due to a change in the γ-secretase activity. These data demonstrate that the elevation of Aβ concentrations in the seladin-1-deficient mice is caused by enhanced β-cleavage of APP *in vivo*.

Figure 2 Seladin-1 modulates DRM protein composition. Homogenates from wild-type (+/+) and seladin-1 heterozygous (+/−) mouse brains and from control and seladin-1-overexpressing SH-SY5Y cells were extracted and centrifuged in a sucrose gradient. Fractions were collected and numbered from the lightest to the heaviest (2 to 10). The amount of protein in each gradient fraction is expressed as a percentage of the total protein along the gradient (**A, H**). Representative Western blots of the gradient fractions using antibodies against the DRM marker proteins flotillin 1 (**B, I**) and PrP^c (**D, K**), and the non-DRM protein TfR (**F, M**) are shown. Graphs on the right show the distribution of flotillin 1 (**C, J**), PrP^c (**E, L**) and TfR (**G, N**) in each fraction as a percentage of the total amount of the respective proteins along the entire gradient. Seladin-1 deficiency in mouse brains led to a significant decrease of the protein amount in fractions 4–6 corresponding to DRMs (A) and resulted in significantly lower amounts of DRM markers in these fractions (B–E), whereas the distribution of TfR did not differ between wild-type (+/+) and heterozygous (+/−) mouse brains (F, G). In contrast, overexpression of seladin-1 in SH-SY5Y cells led to an increased amount of protein in fractions 4–6 compared to control cells (H) and to significantly higher levels of the DRM markers flotillin 1 (I, J) and PrP^c (K, L), whereas the distribution of the non-DRM protein TfR remained unchanged (M, N). The graphs show the average and standard error from three different mouse brains for each condition and from three independent seladin-1-overexpressing and control SH-SY5Y cultures. Asterisks show statistical significance of the difference in the total amount of respective proteins in the DRM fractions 4–6. $*P<0.02$, $**P<0.008$.

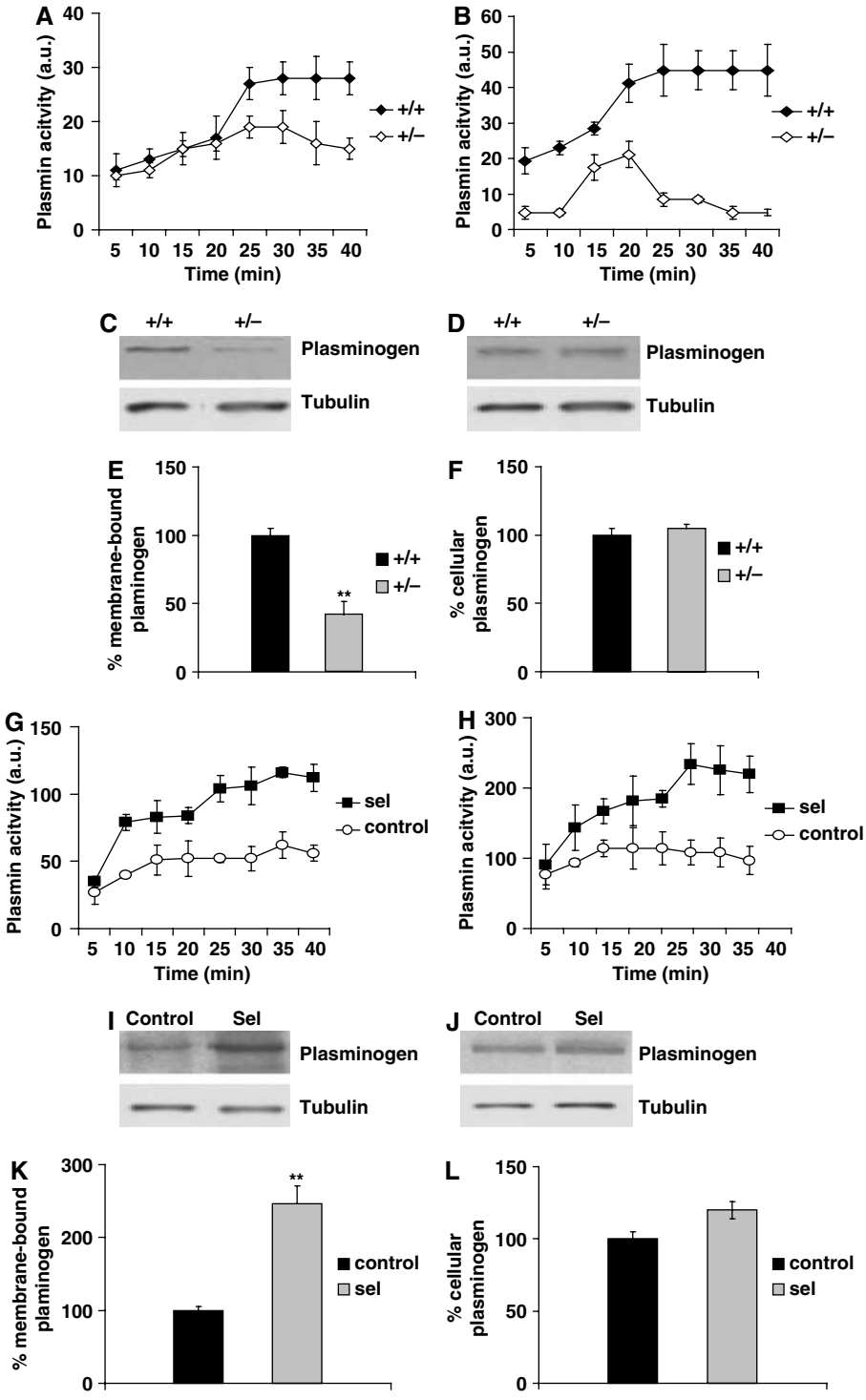

Figure 3 Plasminogen binding and plasmin activation depend on seladin-1 levels. Plasmin activity (expressed in arbitrary units) was measured at the indicated times in membranes isolated from wild-type (+/+) and seladin-1 heterozygous (+/−) mouse brains. The ability to bind plasminogen was monitored by measuring plasmin activity after the addition of exogenous plasminogen to the membrane fractions. Both endogenous plasmin activity (**A**) and the ability to bind plasminogen (**B**) were clearly reduced in the heterozygous mouse brains. Membrane-bound plasminogen was significantly decreased in heterozygous (+/−) brains (**C, E**). Endogenous levels of cellular plasminogen, however, were not altered in wild-type (+/+) and heterozygous mouse brains (**D, F**). The amount of tubulin is shown as a loading control in all Western blots (C, D, I, J). In contrast, seladin-1 overexpression *in vitro* resulted in increased endogenous plasmin activity (**G**). Moreover, when exogenous plasminogen was added to isolated membranes, plasmin activity was higher in membrane fractions isolated from seladin-1-overexpressing cells (**H**). Membrane-bound plasminogen was significantly elevated in these cells (**I, K**). Cellular plasminogen levels did not differ between overexpressing and control cells (**J, L**). Data in all the graphs correspond to mean value and standard error from three different mouse brains for each condition and from three independent seladin-1-overexpressing and control SH-SY5Y cultures. $^{**}P<0.006$.

In contrast, the generation of both $A\beta_{40}$ and $A\beta_{42}$ was reduced to 78.5 ± 4.8 and $71.48 \pm 6.7\%$ ($P = 0.001$ and 0.003, respectively; Figure 5E and F) in seladin-1-overexpressing compared to control cells, whereas the ratio of $A\beta_{40}$ to $A\beta_{42}$ revealed no significant difference (Figure 5G). LDH and MTT assays confirmed that there was no interference with the viability of cells in both cultures, ruling out the potential effect of the transgene expression on cell survival. In the LDH and MTT assays, 102 ± 3.2 and $98 \pm 1.8\%$ viable cells were found in seladin-1-overexpressing cultures, respectively, when the corresponding levels of control cells were set as 100%. Altogether, these data confirm the crucial role of seladin-1 protein and cholesterol levels in modulating Aβ generation.

Discussion

The results of this study show that cholesterol levels are modulated by modifying the expression of the cholesterol-synthesizing enzyme, seladin-1. Our approach is different from previous work that relied on pharmacological inhibition of early steps of cholesterol synthesis or on using lipid-extracting drugs in cultured cells and *in vivo* that has led to controversial results (Simons *et al*, 1998; Sparks *et al*, 2000, 2002; Fassbender *et al*, 2001; Kirsch *et al*, 2003; Park *et al*, 2003; Abad-Rodriguez *et al*, 2004). We show that seladin-1 deficiency results in lower membrane cholesterol levels in mouse brains and, as a consequence, in altered DRMs. This in turn contributes to reduced membrane binding of plasminogen and plasmin activation and to increased APP β-cleavage and Aβ production *in vivo*. Importantly, the overexpression of seladin-1 caused the opposite biochemical changes as observed for seladin-1 deficiency.

In our colony, seladin-1 homozygous mice were born to published frequency (Wechsler *et al*, 2003). These mice, however, were extremely weak, half of the size of littermates and most of them (90%) died before reaching the age of 3 weeks (Supplementary Figure 4). Therefore, to study the effects of a moderate cholesterol reduction, we analyzed the seladin-1 heterozygous mice that develop normally and have no problem of health, fertility or longevity. Neuropathological and immunohistochemical examinations of these mice revealed no detectable differences between wild-type and heterozygous mice concerning morphology, cellular distribution and viability of the brain cells (unpublished data). Considering that cholesterol is an essential component of vertebrate cell membranes and exhibits essential biological roles, it is striking that seladin-1 knockout mice survive beyond birth. The question arises as to which mechanism/s enable the seladin-1 knockout mice to reach embryonic maturation and postnatal development, even if short. With mice, in contrast to humans, cholesterol passes the placenta. Therefore, one reasonable answer is that circulating cholesterol, contributed from the heterozygous mother, suffices for early development. In this scenario, soon after birth seladin-1 knockout mice are compromised due to the deficiency to synthesize cholesterol. Alternatively, embryonic development and the short postnatal survival in the seladin-1 knockout mice may depend on the substitution of cholesterol by desmosterol. In agreement with this possibility, one study indicated that desmosterol could replace cholesterol without deleterious effects in fibroblasts (Rothblat *et al*, 1970). Although this last scenario would imply a non-essential role of cholesterol in early developmental processes, it also indicates an essential requirement of cholesterol for full maturation. Indeed, seladin-1 heterozygous mice, which show a 29% reduction of brain membrane cholesterol, exhibit alterations in DRM composition and DRM-dependent functions. Moreover, although changes in seladin-1 expression also affect the amount of desmosterol in mouse brains, the distribution of this lipid in DRMs was not altered. In addition, experimental increase of desmosterol levels in cultured cells did not affect DRM-related functions analyzed in this work, whereas moderate reduction of cholesterol changed these parameters (Supplementary Figures 2 and 3). These results strongly support our conclusion that the reduction of cholesterol but not the increase of desmosterol levels mediates the seladin-1-induced alterations in DRMs observed *in vivo*. Altogether, our data reveal that proper brain maturation requires the maintenance of a certain steady-state level of brain cholesterol and that a modest reduction of cholesterol in brain could have deleterious consequences.

Seladin-1 can exert antiapoptotic function, and apoptosis may lead to elevated Aβ levels in the brains of AD patients and mouse models (Gervais *et al*, 1999; Mohajeri *et al*, 2002). We found, however, no apoptotic cell death in the heterozygous and wild-type mouse brains. Moreover, the viability of seladin-1-overexpressing and control cultures did not differ at any time points. Taken together, these data provide the evidence that the effects described in this work are not a consequence of the antiapoptotic function of seladin-1.

The finding that low expression of seladin-1 paralleled a reduction in brain membrane cholesterol offers a new perspective on the role that this protein might play in AD pathology. Because seladin-1 is downregulated in vulnerable areas of brains in AD patients (Greeve *et al*, 2000), it is reasonable to think that low levels of seladin-1, promoted by yet to be identified causes, are responsible for the membrane cholesterol reduction found in such brains (Ledesma *et al*, 2003a). This would consequently lead to Aβ accumulation via a combination of inefficient Aβ degradation (due to low plasmin activity) and increased APP amyloidogenic cleavage. Iivonen *et al* (2002), in contrast, could not find an association between reduced seladin-1 transcription levels in AD brains and Aβ content. The fact that cholesterol levels were not measured in this study together with the low number of samples analyzed precludes drawing a definitive conclusion. Indeed, cholesterol loss has been observed in a significant number but not in all AD brains (Ledesma *et al*, 2003a). Altogether, these data suggest that compensatory mechanisms to the effects of seladin-1 deficiency on cholesterol levels might exist that would differ among AD patients. Moreover, alternative mechanisms (i.e. mutations in APP or presenilins) would be responsible for Aβ accumulation in certain AD cases. Further research, including large-scale studies, is required to clarify these matters.

Seladin-1 also participates in the Ras/p53 pathway by binding to p53 leading to p53 accumulation (Wu *et al*, 2004). Although the domain of seladin-1 involved in cholesterol synthesis is apparently not required for binding to p53, Ras signaling is modulated in a cholesterol- and DRM-dependent manner (Prior *et al*, 2003; Parton and Hancock, 2004). These examples suggest that altered seladin-1 levels could contribute to disease conditions through both cholesterol-

dependent and -independent modulation of cell survival/death pathways.

In conclusion, our data provide the evidence for a role of seladin-1 in providing enough cholesterol to generate and maintain proper DRM composition and function (Simons and Toomre, 2000). In this regard, the alterations produced by seladin-1 deficiency, such as increased APP amyloidogenic cleavage, Aβ peptide accumulation and decreased plasmin

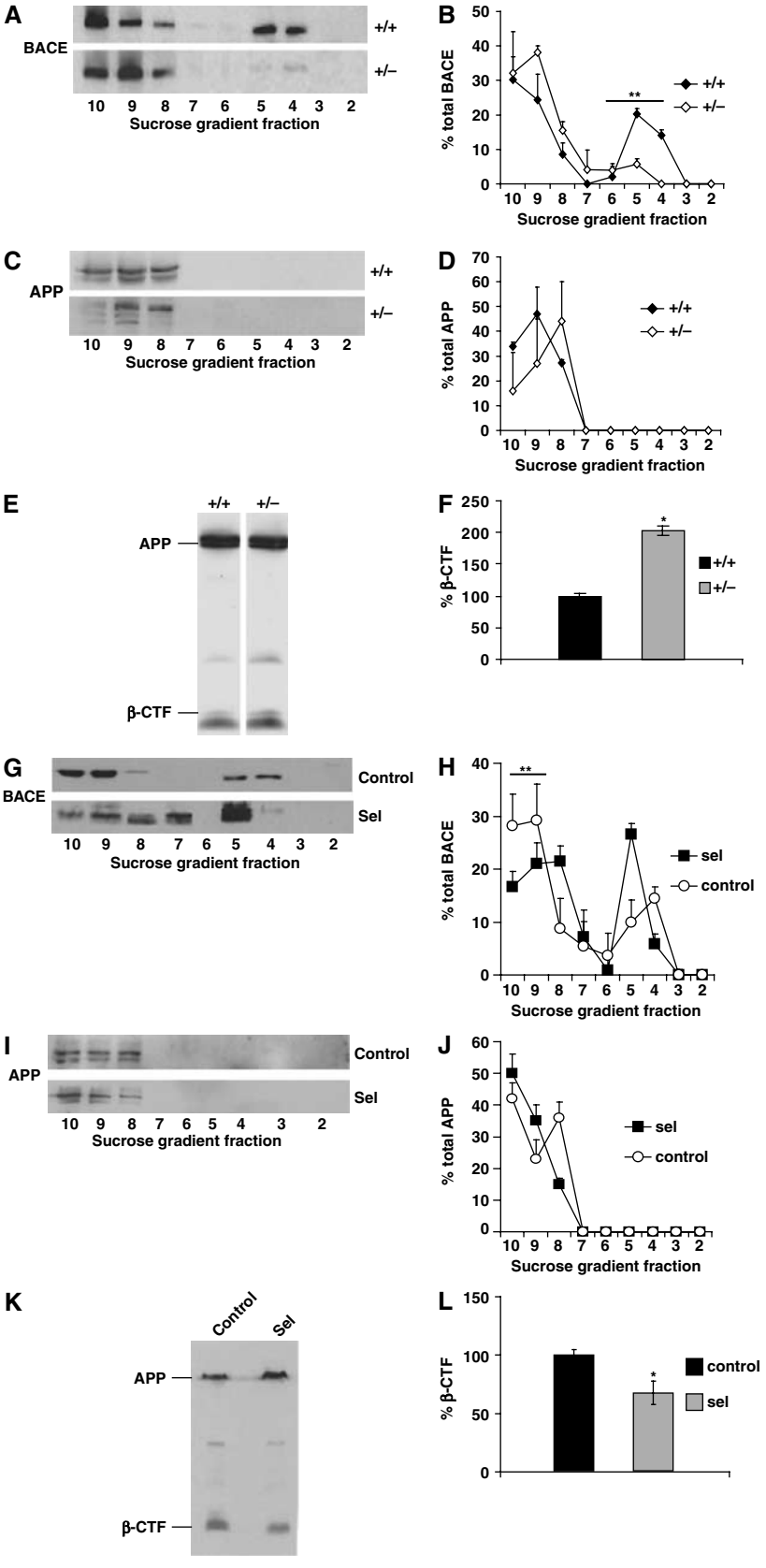

levels, could explain both amyloid build-up and cytopathology in AD *in vivo*. Our study demonstrates the consequences of cholesterol loss in brain cells *in vivo* and provides groundwork to better understanding of the roles of cholesterol in health and disease.

Materials and methods

Cell culture

The open reading frame of human seladin-1 (KIAA0018;DHCR24) (Swiss-Prot: Q15392) was cloned in pcDNA3 expression plasmid (Invitrogen). A hemagglutinin tag was added in-frame to the C-terminus of the protein. The expression was controlled by the CMV promoter. SH-SY5Y cells were cultured in DMEM NUT-F12 medium (Invitrogen) containing 10% fetal calf serum (FCS), 5% horse serum (HS) and 5000 U/ml penicillin and 5000 μg/ml streptomycin. Transfections were performed using Lipofectamine 2000 (Invitrogen). Stably transfected cultures were established by addition of 125 μM G418 (Invitrogen) to the medium. SH-SY5Y cells stably expressing the EGFP protein under the control of the same promoter were used as controls.

Cell viability assays

Before harvesting the cells for quantification of Aβ levels, the viability of the seladin-1-overexpressing and SH-SY5Y control cultures was determined using the MTT (Sigma) and the LDH assay (Sigma) according to the manufacturers' instructions.

Mice

Heterozygous breeding pairs with target depletion of one seladin-1 allele were received from Dr E Feinstein (Quark Biotech Inc.). Seladin-1-deficient mice were bred and genotyped as previously described (Wechsler *et al*, 2003). In addition, seladin-1 heterozygous mice were bred to SwAPP transgenic mice overexpressing human APP harboring the Swedish double mutation (Hsiao *et al*, 1995) (SwAPP/seladin-1). All animal experiments and husbandry were performed compliant with national guidelines. All mice were analyzed at 3 weeks of age.

Antibodies, Western blots and quantification

Monoclonal anti-flotillin 1 (clone 18; Transduction Laboratories), monoclonal anti-PrP^c POM-1 (kindly provided by Dr A Aguzzi, University of Zurich), monoclonal anti-TfR (clone CD-71; Santa Cruz Biotechnology Inc.), polyclonal anti-human plasminogen (Biogenesis), monoclonal anti-N-terminal APP (clone 22C11; Roche), polyclonal chicken anti-BACE1 (raised against Fc-Asp 2-fusion protein, kindly provided by Dr C Dingwall, GlaxoSmithKline), polyclonal anti-C-terminal APP (Sigma) and monoclonal 6E10 (Signet) antibodies were used for Western blot analysis. Monoclonal anti-tubulin (Calbiochem) was used as an internal loading control and for normalization of densitometric analysis of the immunoreactive bands. All antibodies were diluted in 5% fat-free milk in 35 mM Tris–HCl (pH 7.4) and 140 mM NaCl (TBS buffer). For Western blotting, 15% polyacrylamide–SDS gels and Novex 10–20% Tricine gels (Invitrogen) were used. Proteins were transferred to a nitrocellulose membrane (0.45 μm pore; Bio-Rad). Species-specific peroxidase-conjugated secondary antibodies and the ECL detection method (Amersham) were subsequently used. Quantification of immunoreactive bands was carried out by densitometry of the scanned autoradiograms under conditions of non-saturated signal using the NIH-image software.

Aβ measurement

Hemi-brains from 3-week-old mice with the depletion of one seladin-1 allele (heterozygous) and wild-type littermates ($n=4$ for each) as well as their littermates carrying the SwAPP transgene were homogenized in a buffer containing 100 mM Tris and 150 mM NaCl (pH 7.4) and proteinase inhibitors (Roche). These total extracts were analyzed by a modified sandwich ELISA that detects specifically either $A\beta_{40}$ or $A\beta_{42}$ (Takeda, Japan) according to the provider's protocol. Aβ was captured with a specific anti-Aβ antibody (BNT77). Aβ species ending in residue 40 or 42 were measured using horse radish peroxidase (HRP)-coupled monoclonal antibodies specific for $A\beta_{40}$ (HRP-conjugated BA27) and $A\beta_{42}$ (HRP-conjugated BC05) sequence. Seladin-1-overexpressing SH-SY5Y and control cells were cultured in a minimum volume of serum-free OPTIMEM medium (Invitrogen) for 30 h and homogenized in their supernatant by 10 passages through a 22-gauge syringe on ice. $A\beta_{40}$ and $A\beta_{42}$ levels were analyzed by ELISA as described above.

Quantitative RT–PCR

Total RNA from cells and brain tissue was extracted using TRIzol reagent (Invitrogen) following the manufacturer's instruction. Primers specific to human seladin-1 transgene, 5′-CCGTCCGAAAA CTCAG-3′ and 5′-GCGGTGGTAGTAGTGT-3′, and to murine seladin-1, 5′-CATCGTCCCACAAGTATG-3′ and 5′-CTCTACGTCGTCCGTCA-3′, were designed using the program *LC probe design software* (Roche). Seladin-1 mRNA was quantified in three independent cell cultures and mouse brains ($n=5$ for each group). The housekeeping genes phosphoglucokinase and porphobilinogen deaminase were used as reference genes. These two genes were selected based on our unpublished results showing a constant expression of these genes in various experimental conditions *in vitro* and *in vivo*, respectively. Light Cycler quantitative real-time PCR was performed with an RNA SYBR Green kit (Roche Diagnostics).

Total and membrane extract preparation

SH-SY5Y cells or mouse brains were homogenized in phosphate buffer saline containing 9% sucrose and protease inhibitors (CLAP: pepstatin, antipain, chymostatin, each at a final concentration of 25 μg/ml) using 10 strokes in a dounce homogenizer and 10 passages through a 22-gauge syringe on ice. The samples were centrifuged for 10 min at 4°C and 700 *g* and the supernatants considered as total extracts. A further centrifugation of the supernatant was performed at 100 000 *g* for 1 h at 4°C to pellet the membrane fraction. Protein concentration was quantified by the BCA method (Bio-Rad).

Detergent extraction and DRM isolation

Total SH-SY5Y cell or mouse brain extracts were incubated for 1 h at 4°C in 1% Triton X-100, 25 mM MES pH 7.0, 5 mM DTT, 2 mM EDTA and CLAP. The extracts were mixed with 90% sucrose prepared in MBS buffer (25 mM MES pH 7.0, 150 mM NaCl and CLAP) to reach a final concentration of 60% and over-layered in an SW40 centrifugation tube with a step gradient of 35 and 5% sucrose in MBS. After centrifugation at 100 000 *g* for 18 h at 4°C, 11 fractions

Figure 4 Seladin-1 alters BACE1–APP membrane segregation and APP β-cleavage. APP and BACE1 distribution along the sucrose gradient fractions of seladin-1 wild-type (+/+) and heterozygous (+/−) mouse brains (**A–D**) and from control cells and seladin-1-overexpressing SH-SY5Y (**G–J**) was analyzed by Western blot using specific antibodies. Left pictures show representative examples. Graphs on the right indicate the amount of BACE1 (B, H) and APP (D, J) in each fraction as a percentage of total BACE1 and APP, respectively. In seladin-1 heterozygous (+/−) mouse brains, BACE1 was displaced from fractions 4–6 (DRM fractions) to APP-containing heavy fractions 8–10 (A, B), whereas the APP flotation profile did not change between the groups and APP remained in the heavy fractions (C, D). In contrast, seladin-1 overexpression resulted in a significant decrease of BACE1 in the APP-containing fractions (G, H). There was no change in APP distribution in seladin-1-overexpressing compared to control cells (I, J). APP β-cleavage was analyzed by Western blot of cellular extracts containing an equal amount of protein prepared from wild-type (+/+) and heterozygous (+/−) mouse brains (**E**) and from control and seladin-1-overexpressing SH-SY5Y cells (**K**). Levels of APP β-CTF (see also Supplementary Figure 4A) were normalized to the amount of full-length APP (**F, L**). Seladin-1 deficiency revealed a significant two-fold increase in the amount of β-CTF in heterozygous (+/−) mouse brains (F). In concert to the *in vivo* data, overexpression of seladin-1 in SH-SY5Y cells led to a significant decrease (34%) of APP β-CTF (L). The ratio of β-CTF to APP in wild-type (+/+) mouse brain (F) and in control SH-SY5Y cells (L) was considered as 100%. Data in all the graphs correspond to mean value and standard error from three different mouse brains for each condition and from three independent seladin-1-overexpressing and control SH-SY5Y cultures. $*P<0.05$, $**P<0.004$.

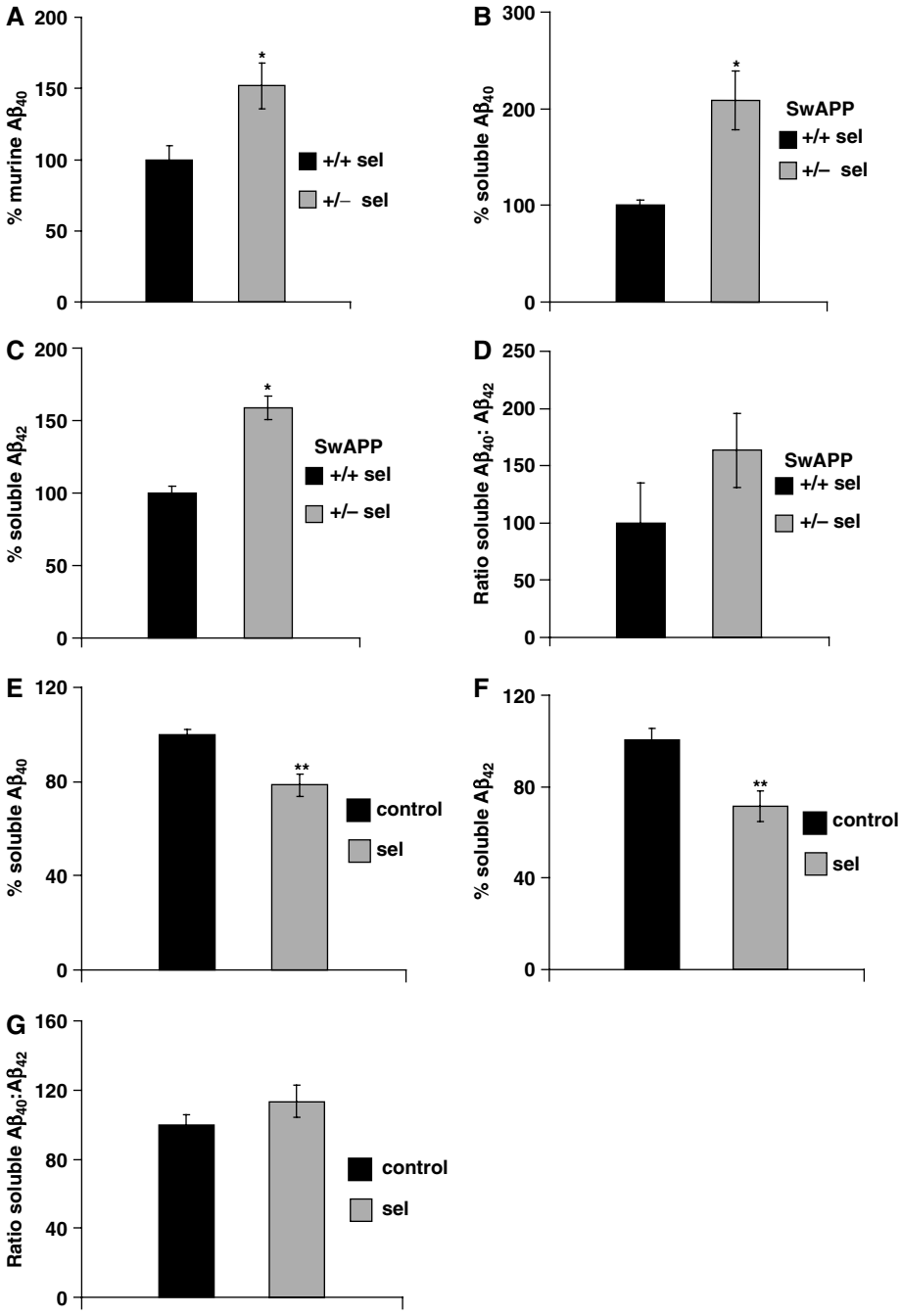

Figure 5 Seladin-1 affects Aβ generation *in vivo* and *in vitro*. Measurement of murine $A\beta_{40}$ levels in wild-type (+/+ sel) and seladin-1 heterozygous (+/− sel) mouse brains without overexpression of the APP transgene revealed a significant increase of the murine $A\beta_{40}$ peptide in the latter ($n=4$) (**A**). $A\beta_{40}$ levels of wild-type mouse brains were considered as 100%. $^{*}P=0.027$. Quantification of $A\beta_{40}$ and $A\beta_{42}$ in the brains of seladin-1 wild-type and heterozygous mice with the simultaneous overexpression of SwAPP confirmed that seladin-1 deficiency leads to higher Aβ steady-state levels. Brain $A\beta_{40}$ levels showed a significant 2.7-fold increase ($^{*}P=0.024$) in heterozygous (SwAPP/+/− sel) mouse brains compared to seladin-1 wild-type littermates expressing solely the SwAPP transgene (SwAPP/+/+ sel) (**B**). Levels of soluble $A\beta_{42}$ were significantly increased by 1.6-fold ($^{*}P=0.015$) in heterozygous (SwAPP/+/− sel) mouse brains (**C**). The ratio of $A\beta_{40}$ to $A\beta_{42}$ levels revealed no significant differences between the two genotypes (**D**). In seladin-1-overexpressing SH-SY5Y cultures, $A\beta_{40}$ (**E**) and $A\beta_{42}$ (**F**) were significantly decreased when compared to control cultures ($n=10$ for each, $^{**}P=0.001$ and 0.003, for $A\beta_{40}$ and $A\beta_{42}$, respectively), whereas the ratio of $A\beta_{40}$ to $A\beta_{42}$ levels did not show significant differences between the two groups (**G**).

were collected from the top of each tube. Fractions 4–6 were identified as the DRM fraction by the presence of the DRM markers flotillin 1, PrP^{c} and GM1 in the control samples.

Lipid analysis

Lipids were extracted from membrane pellets as described (Bligh and Dyer, 1959). Cholesterol, sphingomyelin or desmosterol was subsequently analyzed by thin-layer chromatography (TLC) on silica gel 60 HPTLC plates using a two-solvent system (hydrophilic running solvent: chloroform/acetone/acetic acid/methanol/water (50:20:10:10:5); and hydrophobic solvent: hexane/ethyl acetate (5:2)). The ganglioside GM1 was analyzed by slot-blot using cholera toxin subunit B linked to a peroxidase (Sigma). Quantification was carried out by densitometry of the scanned TLCs or

autoradiograms under conditions of non-saturated signal using the NIH-image software. Phospholipids were determined using the Phospholipid B kit (WAKO) according to the manufactures' protocol.

Sterol analysis

Confluent cells (80%) were cultured in FCS/HS free DMEM NUT-F12 medium without phenol red during 24 h, washed once with ice-cold PBS containing 2 mg/ml BSA (Sigma) and twice with PBS. The sterols were extracted twice from confluent cells grown in a tissue culture dish (diameter 10 cm) using 4 ml hexan/isopropanol (3:2) containing 1 μg epicoprostanol as an internal standard. Similarly, sterols were extracted from fontal brain regions expanding from interaural regions 6 to 4 and from each fraction of the flotation gradient. Gas chromatography–mass spectrometry was performed to determine the total levels of the extracted sterols as described (Lutjohann *et al*, 2002).

As an alternative method, we also measured cholesterol in total and membrane extracts containing equal amounts of protein (40 μg) using the Ecoline 25 cholesterol kit (Merck). The optical density was measured at 500 nm. Pure cholesterol solutions (Sigma) were used as standards. The amounts of all sterols are normalized to the corresponding protein amounts (brains) or the number of cultured cells.

Desmosterol addition and cholesterol reduction in SH-SY5Y cells

Desmosterol and methyl-β-cyclodextrin (Sigma) were complexed as described previously for cholesterol by Klein *et al* (1995). These complexes containing 0.3 mM desmosterol were added to the medium of SH-S5Y5 cells at a final 1:10 dilution together with 2 μg/ml free desmosterol and incubated for 1 h at 37°C. In certain experiments, before the addition of desmosterol complexes, the cells were incubated for 48 h with 0.4 μM mevilonin (Sigma) and 1 mM methyl-β-cyclodextrin to extract 30% cholesterol as described by Abad-Rodriguez *et al* (2004). The incorporation of desmosterol was monitored by TLC using pure desmosterol (Sigma) as standard. Cholesterol reduction was monitored by the Ecoline 25 kit as described above. Cell viability after these treatments was not affected (Estus *et al*, 1997).

Plasminogen binding and plasmin activity

A 200 μg portion of freshly prepared membrane extracts from SH-SY5Y cells or mouse brains was resuspended in Hank's balanced saline solution and 0.1% ovalbumin (Sigma) and was placed in a 96-multiwell plate in the presence of 2 mM chromogenic peptide to measure endogenous plasmin activity. In parallel experiments, plasminogen binding to cellular membranes was determined by addition of 2 μM human plasminogen to the same extracts. Plasmin enzymatic activity was assayed using the chromogenic substrate S-2251 (Chromogenix) specific for this protease. Absorbance was measured at 37°C and 405 nm in an ultramicroplate reader Elx808iu (BioteK, Instruments Inc.) every 5 min.

Quantification of APP C-terminal fragments

Equal amounts of total extracts (40 μg) from either SH-SY5Y cells or mouse brains were submitted to 15% PAGE–SDS, transferred to nitrocellulose and blotted with either 6E10 or the anti-APP C-terminal antibody to detect full-length APP and its C-terminal fragments, respectively. Quantification was carried out by densitometry of the scanned autoradiograms using the NIH-image software. The amount of the C-terminal fragments was normalized to the amount of full-length APP in each lane.

Statistical analysis

Data were collected by investigators blinded to the experimental setup and were statistically analyzed by non-parametric Mann–Whitney *U*-test. In all graphs, mean ± s.e. (standard error of the mean) are shown. *P*-values <0.05 were considered to be statistically significant.

Supplementary data

Supplementary data are available at *The EMBO Journal* Online.

Acknowledgements

We thank Dr E Feinstein (Quark Biotech Inc.) for providing the seladin-1-deficient mice and Takeda Pharmaceutical Company Limited for providing antibodies against Aβ for their quantification by ELISA. This work was supported by grants from the Swiss National Science Foundation, the University of Zurich, NCCR, SAMW, Hermann Klaus, Hartmann Müller and the Novartis Foundations to MHM, Regione Piemonte to MDL and by EU contract LSHM-CT-2003-503330 (APOPIS) to RN and CGD.

References

Abad-Rodriguez J, Ledesma MD, Craessaerts K, Perga S, Medina M, Delacourte A, Dingwall C, De Strooper B, Dotti CG (2004) Neuronal membrane cholesterol loss enhances amyloid peptide generation. *J Cell Biol* **167:** 953–960

Bligh EG, Dyer WJ (1959) A rapid method of total lipid extraction and purification. *Can J Biochem Physiol* **37:** 911–917

Capell A, Grunberg J, Pesold B, Diehlmann A, Citron M, Nixon R, Beyreuther K, Selkoe DJ, Haass C (1998) The proteolytic fragments of the Alzheimer's disease-associated presenilin-1 form heterodimers and occur as a 100–150-kDa molecular mass complex. *J Biol Chem* **273:** 3205–3211

Casas C, Sergeant N, Itier JM, Blanchard V, Wirths O, van der Kolk N, Vingtdeux V, van de Steeg E, Ret G, Canton T, Drobecq H, Clark A, Bonici B, Delacourte A, Benavides J, Schmitz C, Tremp G, Bayer TA, Benoit P, Pradier L (2004) Massive CA1/2 neuronal loss with intraneuronal and N-terminal truncated Abeta42 accumulation in a novel Alzheimer transgenic model. *Am J Pathol* **165:** 1289–1300

Chen G, Chen KS, Knox J, Inglis J, Bernard A, Martin SJ, Justice A, McConlogue L, Games D, Freedman SB, Morris RG (2000) A learning deficit related to age and beta-amyloid plaques in a mouse model of Alzheimer's disease. *Nature* **408:** 975–979

Ciana A, Balduini C, Minetti G (2005) Detergent-resistant membranes in human erythrocytes and their connection to the membrane-skeleton. *J Biosci* **30:** 317–328

Corder EH, Saunders AM, Strittmatter WJ, Schmechel DE, Gaskell PC, Small GW, Roses AD, Haines JL, Pericak-Vance MA (1993) Gene dose of apolipoprotein E type 4 allele and the risk of Alzheimer's disease in late onset families. *Science* **261:** 921–923

Estus S, Tucker HM, van Rooyen C, Wright S, Brigham EF, Wogulis M, Rydel RE (1997) Aggregated amyloid-beta protein induces cortical neuronal apoptosis and concomitant 'apoptotic' pattern of gene induction. *J Neurosci* **17:** 7736–7745

Fassbender K, Simons M, Bergmann C, Stroick M, Lutjohann D, Keller P, Runz H, Kuhl S, Bertsch T, von Bergmann K, Hennerici M, Beyreuther K, Hartmann T (2001) Simvastatin strongly reduces levels of Alzheimer's disease beta-amyloid peptides Abeta 42 and Abeta 40 *in vitro* and *in vivo*. *Proc Natl Acad Sci USA* **98:** 5856–5861

Gervais FG, Xu D, Robertson GS, Vaillancourt JP, Zhu Y, Huang J, LeBlanc A, Smith D, Rigby M, Shearman MS, Clarke EE, Zheng H, Van Der Ploeg LH, Ruffolo SC, Thornberry NA, Xanthoudakis S, Zamboni RJ, Roy S, Nicholson DW (1999) Involvement of caspases in proteolytic cleavage of Alzheimer's amyloid-beta precursor protein and amyloidogenic A beta peptide formation. *Cell* **97:** 395–406

Greeve I, Hermans-Borgmeyer I, Brellinger C, Kasper D, Gomez-Isla T, Behl C, Levkau B, Nitsch RM (2000) The human DIMINUTO/DWARF1 homolog seladin-1 confers resistance to Alzheimer's disease-associated neurodegeneration and oxidative stress. *J Neurosci* **20:** 7345–7352

Hardy J, Selkoe DJ (2002) The amyloid hypothesis of Alzheimer's disease: progress and problems on the road to therapeutics. *Science* **297:** 353–356

Hsiao KK, Borchelt DR, Olson K, Johannsdottir R, Kitt C, Yunis W, Xu S, Eckman C, Younkin S, Price D, Iadecola C, Clark HB, Carlson G (1995) Age-related CNS disorder and early death in transgenic FVB/N mice overexpressing Alzheimer amyloid precursor proteins. *Neuron* **15:** 1203–1218

Huang X, Cuajungco MP, Atwood CS, Hartshorn MA, Tyndall JD, Hanson GR, Stokes KC, Leopold M, Multhaup G, Goldstein LE, Scarpa RC, Saunders AJ, Lim J, Moir RD, Glabe C, Bowden EF, Masters CL, Fairlie DP, Tanzi RE, Bush AI (1999) Cu(II) potentiation of alzheimer abeta neurotoxicity. Correlation with cell-free hydrogen peroxide production and metal reduction. *J Biol Chem* **274:** 37111–37116

Iivonen S, Hiltunen M, Alafuzoff I, Mannermaa A, Kerokoski P, Puolivali J, Salminen A, Helisalmi S, Soininen H (2002) Seladin-1 transcription is linked to neuronal degeneration in Alzheimer's disease. *Neuroscience* **113:** 301–310

Janus C, Pearson J, McLaurin J, Mathews PM, Jiang Y, Schmidt SD, Chishti MA, Horne P, Heslin D, French J, Mount HT, Nixon RA, Mercken M, Bergeron C, Fraser PE, St George-Hyslop P, Westaway D (2000) A beta peptide immunization reduces behavioural impairment and plaques in a model of Alzheimer's disease. *Nature* **408:** 979–982

Kirsch C, Eckert GP, Mueller WE (2003) Statin effects on cholesterol micro-domains in brain plasma membranes. *Biochem Pharmacol* **65:** 843–856

Klein U, Gimpl G, Fahrenholz F (1995) Alteration of the myometrial plasma membrane cholesterol content with beta-cyclodextrin modulates the binding affinity of the oxytocin receptor. *Biochemistry* **34:** 13784–13793

Ledesma MD, Abad-Rodriguez J, Galvan C, Biondi E, Navarro P, Delacourte A, Dingwal C, Dotti CG (2003a) Raft disorganization leads to reduced plasmin activity in Alzheimer's disease brains. *EMBO Rep* **4:** 1190–1196

Ledesma MD, Da Silva JS, Crassaerts K, Delacourte A, De Strooper B (2000) Brain plasmin enhances APP alpha-cleavage and Abeta degradation and is reduced in Alzheimer's disease brains. *EMBO Rep* **1:** 530–535

Ledesma MD, Da Silva JS, Schevchenko A, Wilm M, Dotti CG (2003b) Proteomic characterisation of neuronal sphingolipid–cholesterol microdomains: role in plasminogen activation. *Brain Res* **987:** 107–116

Lutjohann D, Brzezinka A, Barth E, Abramowski D, Staufenbiel M, von Bergmann K, Beyreuther K, Multhaup G, Bayer TA (2002) Profile of cholesterol-related sterols in aged amyloid precursor protein transgenic mouse brain. *J Lipid Res* **43:** 1078–1085

Mohajeri MH, Saini K, Schultz JG, Wollmer MA, Hock C, Nitsch RM (2002) Passive immunization against beta-amyloid peptide protects central nervous system (CNS) neurons from increased vulnerability associated with an Alzheimer's disease-causing mutation. *J Biol Chem* **277:** 33012–33017

Morgan D, Diamond DM, Gottschall PE, Ugen KE, Dickey C, Hardy J, Duff K, Jantzen P, DiCarlo G, Wilcock D, Connor K, Hatcher J, Hope C, Gordon M, Arendash GW (2000) A beta peptide vaccination prevents memory loss in an animal model of Alzheimer's disease. *Nature* **408:** 982–985

Mucke L, Masliah E, Yu GQ, Mallory M, Rockenstein EM, Tatsuno G, Hu K, Kholodenko D, Johnson-Wood K, McConlogue L (2000) High-level neuronal expression of abeta 1–42 in wild-type human amyloid protein precursor transgenic mice: synaptotoxicity without plaque formation. *J Neurosci* **20:** 4050–4058

Park IH, Hwang EM, Hong HS, Boo JH, Oh SS, Lee J, Jung MW, Bang OY, Kim SU, Mook-Jung I (2003) Lovastatin enhances Abeta production and senile plaque deposition in female Tg2576 mice. *Neurobiol Aging* **24:** 637–643

Parton RG, Hancock JF (2004) Lipid rafts and plasma membrane microorganization: insights from Ras. *Trends Cell Biol* **14:** 141–147

Prior IA, Muncke C, Parton RG, Hancock JF (2003) Direct visualization of Ras proteins in spatially distinct cell surface microdomains. *J Cell Biol* **160:** 165–170

Refolo LM, Pappolla MA, LaFrancois J, Malester B, Schmidt SD, Thomas-Bryant T, Tint GS, Wang R, Mercken M, Petanceska SS, Duff KE (2001) A cholesterol-lowering drug reduces beta-amyloid pathology in a transgenic mouse model of Alzheimer's disease. *Neurobiol Dis* **8:** 890–899

Rothblat GH, Burns CH, Conner RL, Landrey JR (1970) Desmosterol as the major sterol in L-cell mouse fibroblasts grown in sterol-free culture medium. *Science* **169:** 880–882

Schmitz C, Rutten BP, Pielen A, Schafer S, Wirths O, Tremp G, Czech C, Blanchard V, Multhaup G, Rezaie P, Korr H, Steinbusch HW, Pradier L, Bayer TA (2004) Hippocampal neuron loss exceeds amyloid plaque load in a transgenic mouse model of Alzheimer's disease. *Am J Pathol* **164:** 1495–1502

Selkoe DJ (2001) Clearing the brain's amyloid cobwebs. *Neuron* **32:** 177–180

Simons K, Toomre D (2000) Lipid rafts and signal transduction. *Nat Rev Mol Cell Biol* **1:** 31–39

Simons M, Keller P, De Strooper B, Beyreuther K, Dotti CG, Simons K (1998) Cholesterol depletion inhibits the generation of beta-amyloid in hippocampal neurons. *Proc Natl Acad Sci USA* **95:** 6460–6464

Small DH, Mok SS, Bornstein JC (2001) Alzheimer's disease and Abeta toxicity: from top to bottom. *Nat Rev Neurosci* **2:** 595–598

Sparks DL, Martin TA, Gross DR, Hunsaker III JC (2000) Link between heart disease, cholesterol, and Alzheimer's disease: a review. *Microsc Res Tech* **50:** 287–290

Sparks DL, Martins R, Martin T (2002) Cholesterol and cognition: rationale for the AD cholesterol-lowering treatment trial and sex-related differences in beta-amyloid accumulation in the brains of spontaneously hypercholesterolemic Watanabe rabbits. *Ann NY Acad Sci* **977:** 356–366

Waterham HR, Koster J, Romeijn GJ, Hennekam RC, Vreken P, Andersson HC, FitzPatrick DR, Kelley RI, Wanders RJ (2001) Mutations in the 3beta-hydroxysterol Delta24-reductase gene cause desmosterolosis, an autosomal recessive disorder of cholesterol biosynthesis. *Am J Hum Genet* **69:** 685–694

Wechsler A, Brafman A, Shafir M, Heverin M, Gottlieb H, Damari G, Gozlan-Kelner S, Spivak I, Moshkin O, Fridman E, Becker Y, Skaliter R, Einat P, Faerman A, Bjorkhem I, Feinstein E (2003) Generation of viable cholesterol-free mice. *Science* **302:** 2087

Wu C, Miloslavskaya I, Demontis S, Maestro R, Galaktionov K (2004) Regulation of cellular response to oncogenic and oxidative stress by Seladin-1. *Nature* **432:** 640–645

